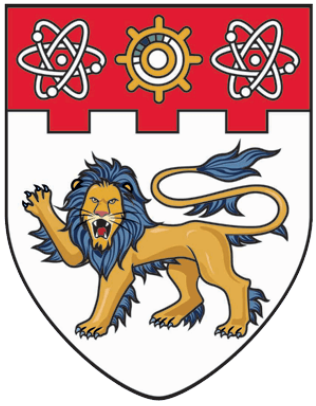

NANYANG TECHNOLOGICAL UNIVERSITY

SINGAPORE

DEVELOPING A ZEBRAFISH MODEL OF EPIDERMOLYSIS BULLOSA

ABRAHA GEBREGZIABHER KAHSAY

SCHOOL OF BIOLOGICAL SCIENCES

2019

DEVELOPING A ZEBRAFISH MODEL OF EPIDERMOLYSIS BULLOSA

ABRAHA GEBREGZIABHER KAHSAY

School of Biological Sciences

A thesis submitted to Nanyang Technological University in partial fulfilment of the requirement for the degree of Doctor of Philosophy

2019

STATEMENT OF ORIGINALITY

I hereby certify that the work embodied in this thesis is the result of original research done by me except where otherwise stated in this thesis. The thesis work has not been submitted for a degree or professional qualification to any other university or institution. I declare that this thesis is written by myself and is free of plagiarism and of sufficient grammatical clarity to be examined. I confirm that the investigations were conducted in accord with the ethics policies and integrity standards of Nanyang Technological University and that the research data are presented honestly and without prejudice.

12/04/2019 

Abraha Gebregziabher KAHSAY

SUPERVISOR DECLARATION STATEMENT

I have reviewed the content and presentation style of this thesis and declare it of sufficient grammatical clarity to be examined. To the best of my knowledge, the thesis is free of plagiarism and the research and writing are those of the candidate's except as acknowledged in the Author Attribution Statement. I confirm that the investigations were conducted in accord with the ethics policies and integrity standards of Nanyang Technological University and that the research data are presented honestly and without prejudice.

12/04/2019 **Thomas James CARNEY**

AUTHORSHIP ATTRIBUTION STATEMENT

This thesis **does not** contain any materials from papers published in peer-reviewed journals or from papers accepted at conferences in which I am listed as an author.

12/04/2019  **Abraha Gebregziabher KAHSAY**

ACKNOWLEDGEMENTS

Praise to the Almighty God for everything he has done for me. The office of Agency for Science, Technology and Research (A*STAR) Scholarship of Singapore and Nanyang Technological University are highly acknowledged for the financial assistance and giving me the opportunity to pursue my PhD.

I would like to thank my supervisor, Dr.Thomas James Carney, who has been wonderful mentor and helpful over the past 4 years. He has got talent to bring someone to cross the space between the knowledge levels and bring closer some insights into mysteries of science; his guidance has been most educational and interesting.

The contribution of my co-supervisor, Prof.Philip Ingham, and my Thesis Advisory Committee (TAC) members, (Prof.Artur Schmidtchen, Prof.Maurice Van Steensel and Prof.Tan Suet Mien), was also indispensable of which their questions, comments and suggestions helped me a lot to advance my research work where they deserve a huge credit.

Many thanks to all members of TJC and PWI lab, past and present with who I have been very privileged to work with. I gratefully acknowledge all staffs of the IMCB fish facility, histopathology facility and IMB-IMCB joint EM suite.

Last but not least, many thanks to my family and friends for all their love, encouragements and support throughout the journey.

TABLE OF CONTENTS

LIST OF TABLES

LIST OF FIGURES

LIST OF THE ABBREVIATIONS AND ACRONYMS

ABCC6	ATP Binding Cassette, Subfamily C, Member 6
AVA	Agri Food and Veterinary Authority
BCIP	Bromo chloro indolyl phosphate
BLAST	Basic Local Alignment Search Tool
BMP	Bone Morphogenetic Protein
BMZ	Basement Membrane Zone
BP	Bullous Pemphigoid
BPAG1	Bullous Pemphigoid Antigen1
Cas9	CRISPR Associated Protein 9
CCD	Charged Coupled Device
CD	Cluster of Differentiation
COL7A1	Collagen 7 A1 gene
COLVII	Type VII Collagen
CRISPR	Clustered regularly interspaced short palindromic repeats
DAPI	Diamidino phenylindole
DEB	Dystrophic Epidermolysis Bullosa
DEJ	Dermal Epidermal Junction
DIG	Digoxigenin
DMSO	Dimethyl Sulfoxide
dpf	Days Post Fertilization
EB	Epidermolysis Bullosa
EBL	Epidermal Basal Layer
EBS –MP	Epidermolysis Bullosa Simplex-Mottled Pigmentation

EBS	Epidermolysis Bullosa Simplex
EBS-DM	Epidermolysis Bullosa Dowling Meara
EBS-K	Epidermolysis Bullosa Simplex Koebner
EBS-WC	Epidermolysis Bullosa Simplex Weber Cockayne
ECM	Extra Cellular Matrix
EGFP	Enhanced Green fluorescent protein
EGFR	Epidermal Growth Factor Receptor
EMT	Epithelial Mesenchymal Transition
EpCAM	Epithelial Cell Adhesion Molecule
EVL	Enveloping Layer
FN3	Fibronectin type III Domain
FREM1	FRAS1 Related Extracellular Matrix Protein 1
gRNA	guide RNA
hpf	hours post fertilization
IF	Intermediate Filaments
IRF6	Interferon Regulatory Factors 6
ITGA3	Integrin Alpha 3
JEB	Junctional Epidermolysis Bullosa
kDa	Kilodalton
KIND1	Kindler 1
KRT	Keratin
krtt1c19e	Keratin type I Chromosome 19 e gene
LAMA5	Laminin Alpha 5
LGL1	Lethal Giant Larvae
LSM	Laser Scanning Microscope

MeOH	Methanol
MMPs	Matrix Metalloproteinases
MO	Morpholino
NBT	Nitroblue tetrazolium
OCT	Optical Cutting Temperature
PBS	Phosphate Buff ered Saline
PBT	Phosphate Buffered Triton
PCR	Polymerase Chain Reaction
pEGFPC1	Enhanced Green fluorescent protein tagged plasmid at its C terminus
PFA	Paraformaldehyde
PLEC1	Plectin 1
PTU	Phenyl thiourea
RT-PCR	Reverse transcription Polymerase chain reaction
SgRNA	Single Guide Ribonucleic Acid
SMART	Simple Modular Architecture Research Tool
SPINT1	Serine Protease Inhibitor, Kunitz Type I
SWATH MS	Sequential Window Acquisition of all Theoretical Fragment Ion Spectra Mass Spectrometry
TEM	Transmission Electron Microscopy
Tol2	Transposase mRNA
VWA	Von Willebrand Factor Type A Domain
ZFIN	Zebrafish Information Network
ZiFiT	Zinc Finger Targeter

ABSTRACT

Skin forms the physical boundary between internal and external environment being the first line of defense against insults. It is composed of variety of cells expressing specific molecules that maintain the normal structural integrity and function. One family of molecules includes keratins which are cytoskeletal complex proteins that form intermediate filaments in the epithelial cells. However, the entire organization and function of keratin networks can be disrupted because of single mutation in one of these molecules, leading to the inherited skin disease, epidermolysis bullosa simplex, an inherited skin disorder characterized by the formation of blisters. Zebrafish has not been extensively used to model human skin diseases to date. Hence, the main target of this work is establishing robust models of heritable skin diseases in zebrafish, focusing mostly on basal keratinocytes bullosa diseases to understand their molecular pathomechanism *in vivo*. Here we have generated transgenic lines overexpressing mutant forms of zebrafish Krtt1c19e and human KRT14 proteins, which are associated with generation of epidermolysis bullosa simplex in humans. Confocal analysis of immunostained zebrafish larvae expressing these mutant forms of KRT14 and Krtt1c19e showed subtle differences in keratin distribution in basal cells, but which produce keratin aggregates and dramatic alterations in keratin architecture upon heat and cold stress, suggesting that mutant keratins are affecting proper keratin dimerization process. We also found that there is cell adhesion disruption and keratinocytes detachment in the epidermolysis bullosa simplex zebrafish model via live imaging of basal

keratinocytes. In addition, using the CRISPR/Cas9 system, we generated *col7a1* null zebrafish to establish a dystrophic epidermolysis bullosa zebrafish model. As of yet, no blistering has been observed under normal condition and proteomics analysis was carried out to check the status of the protein in the *col7a1* double knockout fish. We found upregulation of three collagens; Col28a2a, Col6a2 and Col14a1b. Overall, this study provides new insights into understanding cellular and molecular defects *in vivo* and establishes a platform for testing human epidermolysis bullosa simplex patient genetic lesions and development of therapeutic screens.

CHAPTER 1. INTRODUCTION

1. HUMAN SKIN

Skin, the largest organ of the human body, serves as a protective barrier from different environmental aggressors by creating a physical boundary between the internal and external environment. It constantly faces external challenges and serves the first line of defense to combat the insults (Kanitakis, 2002; Proksch, Brandner, & Jensen, 2008).

Human skin consists of three layers; the epidermis, the dermis and the hypodermis. The epidermis, outer layer of the skin, is a stratified squamous epithelium sits above the basement membrane zone (BMZ). It prevents the body from harmful microorganism causing infections and dehydration via retaining body fluids (Candi, Schmidt, & Melino, 2005; Fuchs & Raghavan, 2002). The dermis, the middle layer, is composed of collagens and elastins, and is relatively acellular. The dermis lies on the hypodermis, innermost layer, mainly consists of adipocytes and loose connective tissue (Metcalfe & Ferguson, 2007).

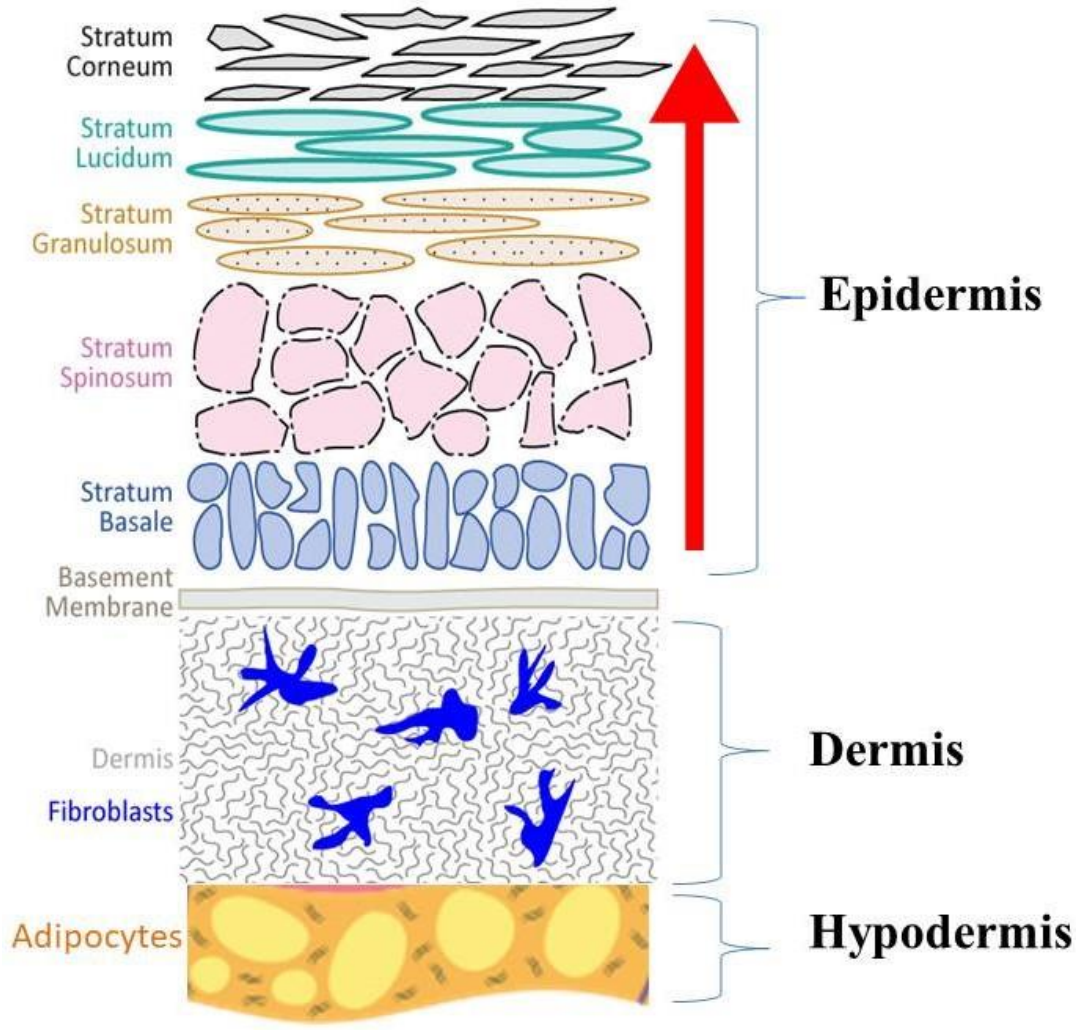

Figure 1: Layers of human skin

Schematic representation of human skin indicating stratified epithelium (epidermis) consisting of distinct strata from stratum basale to stratum corneum. The upper most layer is a lipid rich water barrier consisting of dead corneocytes. The red arrow showing direction of differentiation whereby cells progress from the basal zone outwards towards the surface. The extracellular basement membrane where the basal stratum sits on, the dermis with fibroblasts, collagens and elastins, and the hypodermis with adipocytes are shown (Source: Sketched by Thomas J. Carney).

1.1. Epidermis

The epidermis is a stratified squamous epithelium which progressively differentiates from the basal layer towards the superficial direction. The epidermis is composed of five layers such as basal layer, spinous layer, granular layer, stratum lucidum and stratum corneum (Figure 1) (James, Berger, & Elston, 2006).

The epidermis is composed primarily of cell derived from basal layer called keratinocytes and other cell populations found in the superficial layer such as Merkel cells, Langerhans' cells and melanocytes (Candi et al., 2005; Fuchs & Raghavan, 2002). Cells in the epidermis are continually dividing and give rise to new skin cells. The epidermis is a dynamic tissue where the basal cells proliferates and differentiates to renew the subsequent layer of the epidermis (Haake, Scott, & Holbrook, 2001).

1.1.1. Keratinocytes

Keratinocytes are the most abundant cell type which accounts for about 95% of the cells type found in the superficial layer of the skin (J. McGrath, Eady, & Pope, 2004). Keratinocytes found in the basal layer are called basal cells or basal keratinocytes. From this niche, they differentiate and migrate towards the outermost layer of the epidermis where they undergo cornification (James et al., 2006) in which keratinocytes start terminal differentiation. In this process keratinocytes maintain their integrity via keratin intermediate filaments and linked

to each other by desmosome junctions. Epidermal differentiation complex expression in the cells of the granular layer generates different proteins such as profilaggrin, keratohyalin, Involucrin and loricrin which are involved in keratinization process(Candi et al., 2005; Maestrini et al., 1996). Moreover, many lipids are synthesized in lamellar granules and form a water proof layer in the cornified layer. The transition of granular to cornified layer is characterized by a series of morphological changes. This final step involves a combination of proteins formed by transglutaminases which is important to cross link proteins and form a cornified envelop close to the cell surface(Candi et al., 2005). Finally, keratins are the only kind of proteins present in the cornified cells, providing mechanical strength(Y. Pan et al., 2016).

In the epidermis, keratinocytes are responsible to form tight junction to maintain their integrity at different stages of differentiation. Tight junctions play important role to maintain skin integrity by sealing the intracellular space between epithelial cells. Those tight junctions connecting keratinocytes are composed of junctional adhesion molecule, occluding and claudins (Bazzoni & Dejana, 2001; Furuse et al., 2002).

1.1.2.Basement membrane zone

The basement membrane zone is a porous interface between the epidermis and the underlying dermis that allows exchange of extracellular matrix (ECM) components and serves as a bridge in the dermal-epidermal junction (DEJ). The components of

the BMZ are produced by the epidermis and dermis of the skin (Kierszenbaum & Tres, 2015).

The BMZ consists of two layers, basal lamina which can further be divided into lamina lucida and lamina densa, and reticular connective tissue (Paulsson, 1992). The outermost BMZ is formed by the plasma membrane of basal keratinocytes and their attachments (Figure 2). The protein complexes that connect basal keratinocytes to the lamina lucida of DEJ are composed of integrins, laminins, fibronectin, nidogen and bullous pemphigoid antigens which are components of hemidesmosomes. Components of the lamina lucida are linked to the underlying lamina densa which contains collagen IV, V and crosslinking elements. The DEJ is attached to the underlying dermis via anchoring fibrils, collagen VII (Haschek, Rousseaux, Wallig, Bolon, & Ochoa, 2013) (See section 1.4.2 and 1.6).

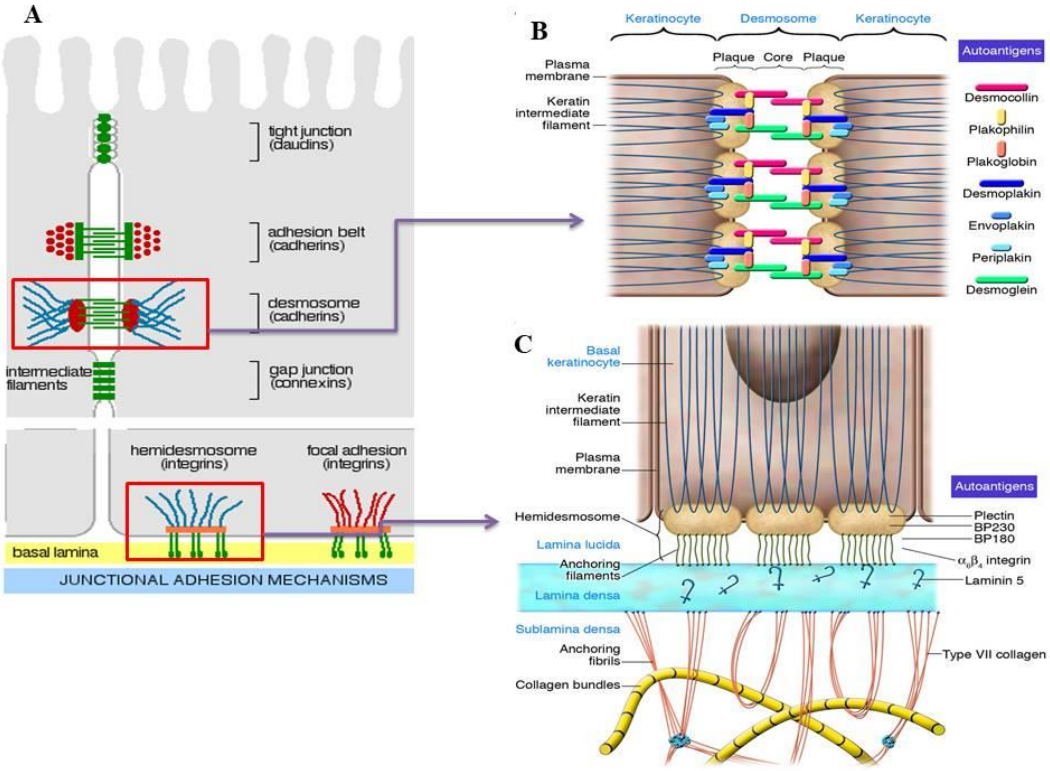

Figure 2: Dermo-epidermal junctional adhesion of the skin

(A) Junctional adhesion mechanisms of the skin illustrating cell to cell and cell to matrix adhesion, (B) Desmosomes, protein complexes which connects keratin intermediate filaments of keratinocytes to the neighboring cell, (C) keratin filaments of basal keratinocytes to the extracellular matrix proteins via hemidesmosomes (Hertl, Eming, & Veldman, 2006).

1.2. Dermis

The dermis, the middle layer, is composed of collagens, fibronectin, fibrillin and elastin which make the skin to be strong and flexible (Figure 1). The dermis is vascularized; relatively acellular, innervated, and contains hair follicles, sweat and sebaceous glands.

The two main layers of the dermis are the papillary layer (stratum papillare) and the reticular layer (stratum reticulare). The superficial layer forms conic projections alternating with epidermal rete ridges, which enables the dermis and epidermis for better adhesion by increasing the contact surface area between the layers. This layer consists of loose bundles of collagen and thin elastic fibres which stretch perpendicular to the dermal-epidermal junction (James et al., 2006).

The three types of cells in the dermis are fibroblasts, adipocyte and macrophages among which fibroblasts are the main cell types which are responsible for the production and secretion of procollagen and elastic fibers (Marks & Miller, 2017).

1.3. Hypodermis

Hypodermis, the subcutaneous tissue, is the lowermost layer right below the dermis. It is composed of loose connective tissue and contains cell types such as fibroblasts, macrophages and adipocytes, the main type of cells being adipocytes which accounts for 50% of the population of the cell types found in the layer. The role of hypodermis is to connect the dermis with the muscle and bones via septa, a connective tissue. It contains blood vessel and nerves (González, 2013).

1.4. Cell Adhesion Mechanisms

1.4.1. Cell-cell adhesion mechanism

To maintain the normal function and integrity of the skin, layers and cells of the epidermis are connected to each other by adhesion mechanisms. Keratinocytes are connected to each other by four main cell-cell junctional adhesion mechanisms includes the cadherin mediated adherens junctions and desmosomes, tight junctions and gap junctions (Figure 2).

Adherens junctions connect actin microfilaments of a cell to the neighboring cells via E-cadherin in the epithelium, whereas desmosomes associate with the keratin intermediate filaments of keratinocytes and give mechanical flexibility (Perez-Moreno, Jamora, & Fuchs, 2003; Vasioukhin & Fuchs, 2001; Yonemura, Itoh, Nagafuchi, & Tsukita, 1995). Gap junctions are important components of cell to cell adhesion which allows molecules ions and signals to pass via controlled gate between neighboring cells (Matter & Balda, 2003; Steed, Balda, & Matter, 2010).

The integrity of the epidermis is mainly dependent on desmosomes protein complexes that connect the keratin intermediate filaments of neighboring keratinocytes which includes desmogleins, desmocollins, desmoplakin, plakophilin, plakoglobin, periplakin and envoplakin (J. McGrath et al., 2004).

1.4.2. Cell-matrix adhesion mechanism

The main groups of cell adhesion molecules that primarily mediate cell-matrix adhesions are integrins. They are heterodimers of α and β subunits which comprise 24 members that are transmembrane cell adhesion receptors connecting the basal cells to the ECM. In addition to their adhesion functions, integrins play an important role in signal transductions (Alberts et al., 2002).

At the DEJ, basal keratinocytes adhere to the underlying BM through two types of integrin dependent junctions called hemidesmosomes and focal adhesions. Both are found on the basal cell membrane facing the basement membrane, and both utilize integrins, receptors for ECM. Hemidesmosomes link to keratin intermediate filaments of the basal keratinocytes and focal adhesion associate to actin microfilaments (Figure 2 & 3). Hemidesmosomes are multiprotein complexes which connects the basal keratinocytes to the ECM (Walko, Castañón, & Wiche, 2015).

The main components of hemidesmosome protein complexes are plectin and integrin α6β4 which connect to the keratin intermediate filaments and laminin 332, respectively (Figure 3) and maintain mechanical stability of the protein complexes. Tetraspanin (CD151), BP 230 and BP 180 (bullous pemphigoid antigens 230 and 180) are other components of hemidesmosomes (Jones, Hopkinson, & Goldfinger, 1998).

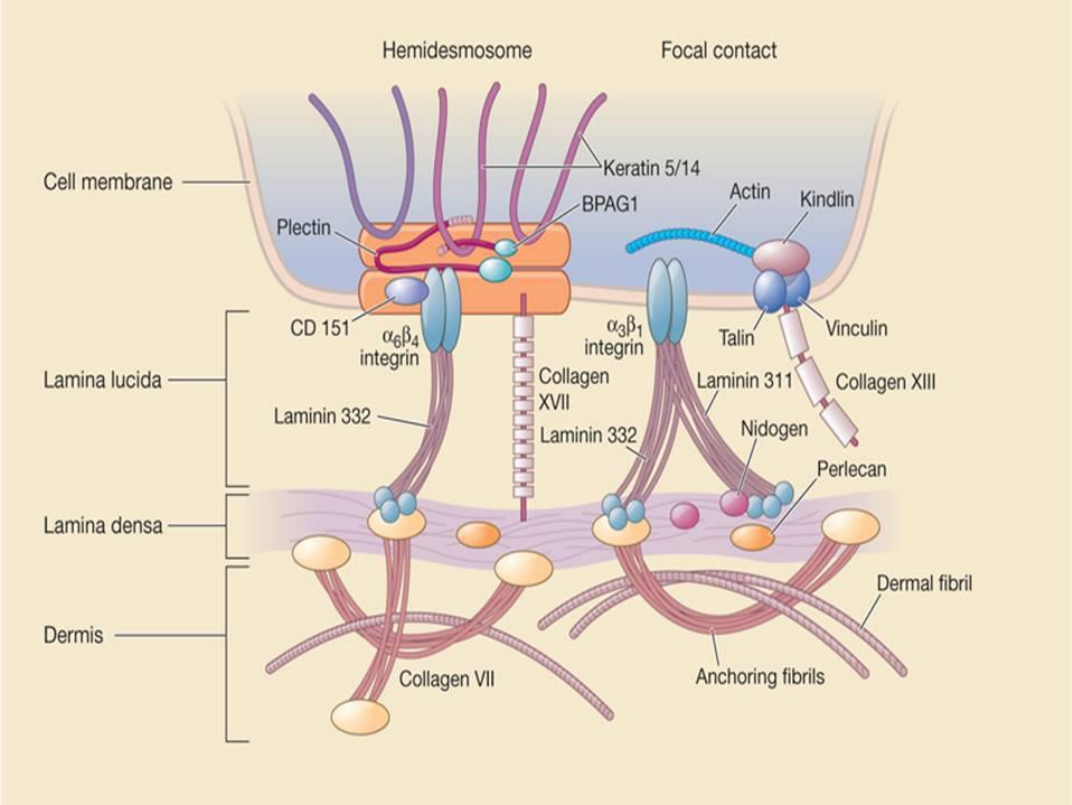

Figure 3: Cell-matrix adhesion of the skin

Illustration showing components of hemidesmosomes comprises plectin, integrin α6β4, CD151, laminin 332, BPAG1 and collagen XVII, focal adhesion components which contains nidogen, laminin 311, integrin α3β1 and perlecan (Bruckner-Tuderman & Aimee, 2008).

Focal adhesions are integrin containing protein complexes that associate intracellular actin microfilaments and the ECM components in different cells types. They are large, dynamic structures through which the cytoskeleton of a cell connects to the extracellular matrix. Components of focal adhesions include integrin α3β1, talin, vinculin, α-actinin and Kindlin1 (Wozniak, Modzelewska, Kwong, & Keely, 2004).

1.5. Intermediate Filament

Intermediate filaments (IF) are cytoskeletal protein of cells. The main role of IF is to provide mechanical support for the cell and maintain its normal structure and function. IF are found in the cytoplasm (keratin intermediate filaments) and the nucleus (lamins). The diameter of their filament is about 8-12nm which is intermediate between the actin microfilament (4-6nm) and the microtubules (25nm) in diameter. Based on their DNA and amino acid sequences, intermediate filaments protein family is subdivided into six subfamilies. In the human genome, intermediate filaments are encoded by 70 different genes associated with 119 discrete clinical disorders (http://www.interfil.org/intro.php). Keratin intermediate filaments, type I (acidic) and type II (basic) are found in the epithelial cells and are obligate heterodimers.

In contrast, the type III intermediate filaments are found in muscle, mesenchyme, glial cells and neurons consists of desmin, vimentin, glial fibrillary acidic protein, and peripherin, respectively and form homodimers. The type IV intermediate filaments include neurofilaments, nestin and α-internexin that are mainly expressed in neural cells. Type V intermediate filaments constituted of nuclear lamins, considered to stand apart from the other due to its nuclear localization signal in its primary sequence, and its ubiquitous expression pattern. Type VI intermediate filaments includes proteins phakinin and filensin, the two eye lens intermediate filaments (Eriksson et al., 2009; Fuchs & Weber, 1994).

All Intermediate filament share common three domain structures, a central coiled-coil α-helical conserved domain flanked by amino terminal head (N-terminal) domain and a carboxyl terminal tail (C-terminal) domains which are non helical and vary in different IF proteins (Herrmann, Strelkov, Burkhard, & Aebi, 2009).

1.5.1. Keratin intermediate filaments

The largest group of IF family is keratin genes where they encompass 54 different functional genes out of 70 genes in the human genome coding for IF proteins. The most abundant proteins in the epithelial cells are keratins and account for 75% of all IF genes in vertebrates, being found in the epithelia of the body. They are critical for cellular integrity, cell signaling , protein targeting, apoptosis and protection against stress (Ku & Omary, 2006; Owens & Lane, 2003; Pallari & Eriksson, 2006; X. Pan, Hobbs, & Coulombe, 2013; D. Toivola, Strnad, Habtezion, & Omary, 2010; D. M. Toivola, Tao, Habtezion, Liao, & Omary, 2005).

On the basis of biochemical properties, keratins are divided into type I and type II which are acidic and basic, respectively (Coulombe & Omary, 2002). In humans, there are 28 type I and 26 type II keratins. The members of the type I keratins are KRT9 to KRT20, KRT23 to KRT28 and KRT31 to KRT40 that are partners of the type II keratins including KRT1 to KRT8 and KRT71 to KRT86. 27 type I keratins are located on chromosome 17q21.2 and type II keratins on chromosome 12q13 as clusters (Schweizer et al., 2006).

Keratins have a conserved molecular structure, a central α-helical rod domain (Figure 4) of which the coiled-coil α helical domain plays an important role in facilitating filament formation (Lupas, 1996).

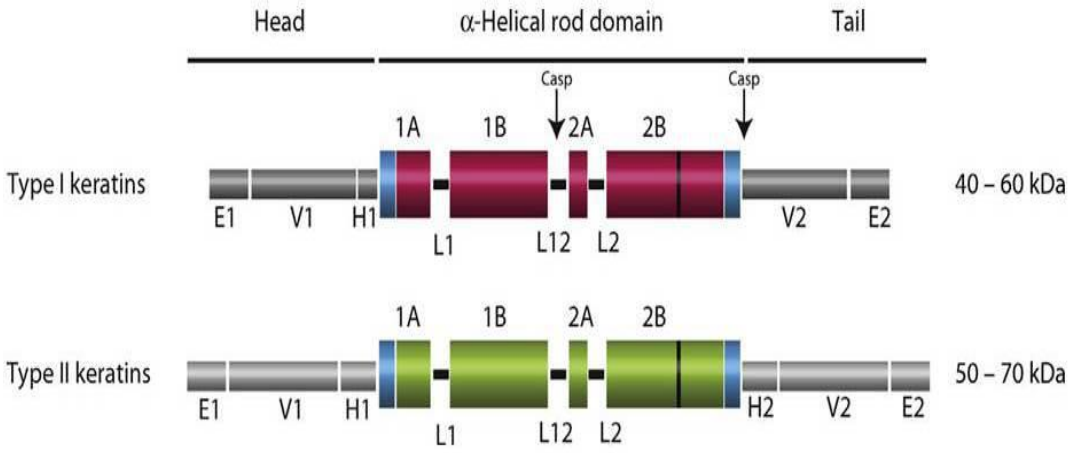

Figure 4: Structural domain of keratin intermediate filaments:

Diagram demonstrating α-helical rod domain, head and tail domains, subdomains, linker segments which separates the subdomains and molecular size of type I and type II keratin proteins

About 310 amino acids form the coiled-coil α-helical domain where it has four (1A,2A,1B and 2B) helical segments and three (L1,L2 and L12) linkers which are in between the segments (Figure 4) (North, Steinert, & Parry, 1994; Weber, Plessmann, Dodemont, & Kossmagk- Stephan, 1988). Helix initiation and termination regions of keratins located at 1A and 2B helical segments that are highly conserved domains of which are essential for keratin assembly. In addition to the coiled-coil α-helical domain, keratins also contains variable, head and tail domains which are non helical (Herrmann et al., 2009).

Majority of keratins also contain subdomains in their head and tail region where end (E1), homologous (H) and variable (V1) and H2, V2 and E2 in their head region, respectively (Figure 3). These head and tail domains have diff erent function in which they are responsible for the diff erence within and between keratin groups and can serve a substrate for post translational modifications which in turn regulate functional properties and structural organizations of keratins.

The helix initiation and termination regions located at 1A and 2B helical segments are known as mutational "hot spots" and give rise to more severe phenotypes in most genetic diseases as compared to those mutations found in head and tail domains (Corden & McLean, 1996; Coulombe, Kerns, & Fuchs, 2009) as these highly conserved regions are essential for keratin assembly.

Keratin intermediate filaments assemble into obligate heterodimers in a parallel pathway by winding their α-helical rod domain and dimers assemble into tetramers in an anti-parallel orientation. A number of tetramers arrange end to end to make a protofilaments and finally form a long and non polar intermediate filament (Herrmann & Aebi, 2004) as shown in figure 5.

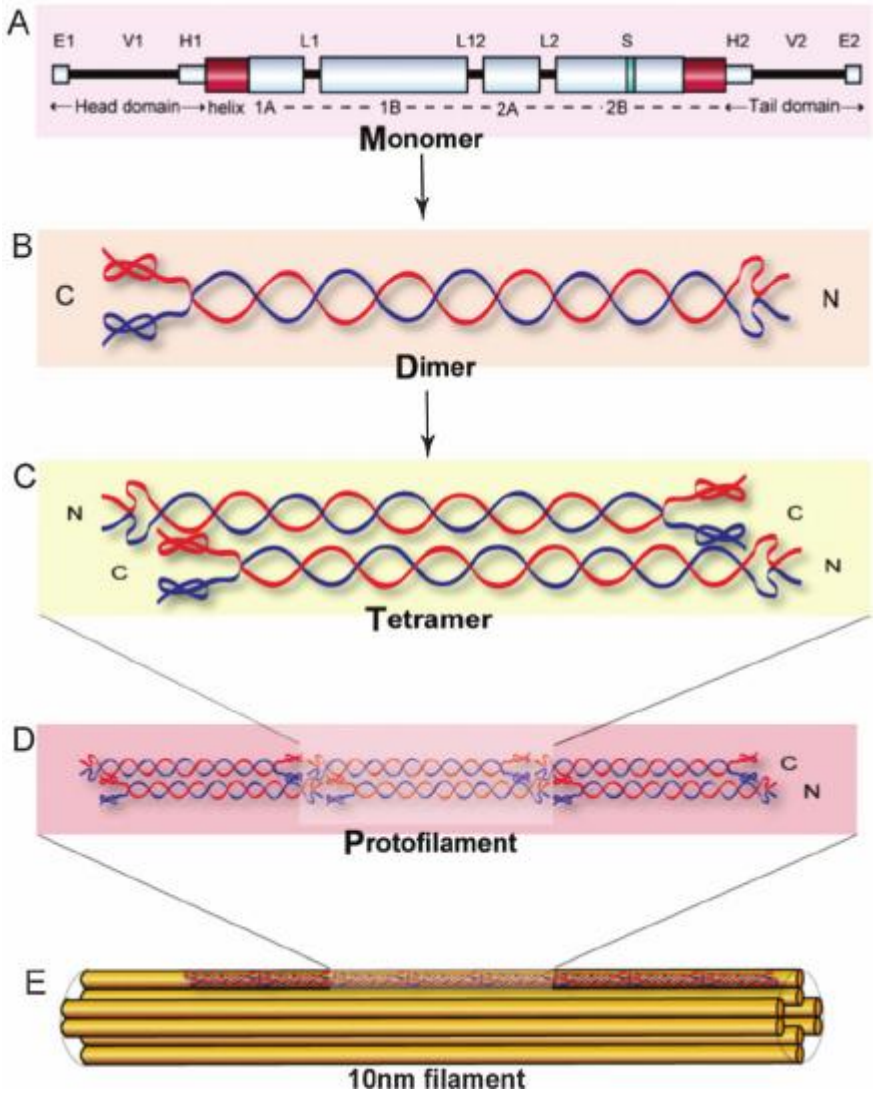

Figure 5: Keratin intermediate filament assembly

Diagram showing alignment and polymerization process of keratin IF. (A) Keratin domains, (B) Type I and type II keratins align in a parallel orientation to form parallel dimers, (C) Two dimers then associate to make tetramers in an anti-parallel orientation. (D) The lateral and longitudinal aggregations of tetramers form protofilaments which eventually make up (E) intermediate filaments (Banerjee, Wu, Yu, Qi, & Li, 2014).

Keratin intermediate filament expression varies within different type of epithelial cells and is dependent on cell and tissue type, and developmental stage, state of differentiation and disease conditions. Keratins are divided into two clusters based on their expression pattern in which those keratins expressed in the simple epithelia are called the “S” type keratins and those keratins expressed in the stratified epithelium of the epidermis are the “E” type keratins (Coulombe & Lee, 2012).

Generally, the differential expression of keratin IF proteins describe the type of epithelium in the body. For example, KRT8 and KRT18 are the main components of keratin IF of the simple epithelium. They are expressed in a single layered epithelium and are called primary simple epithelial keratins. Other keratins expressed in the simple epithelia are KRT7 (gland ducts and internal epithelia), KRT19 (mammary glands) and KRT20 (gastro intestinal, endocrine and urethral epithelium) (B. L. Bader, Magin, Hatzfeld, & Franke, 1986; BARTEK, TAYLOR-PAPADIMITRIOU, MILLER, & MILLIS, 1985; Moll, Löwe, Laufer, & Franke, 1992; Smith et al., 2002).

In the basal layer of the epidermis the basal keratinocytes express pair of keratin IF, KRT5 and KRT14 as their major keratins (Sun et al., 1983) and keratinocytes found at the spinous and granular layers predominantly express KRT1 and KRT10. Other suprabasal keratins include KRT2 and KRT9 believed to have delayed expression to support KRT1 and KRT10 at sites of high mechanical strain (Candi et al., 2005; Fuchs & Green, 1980; Simpson, Patel, & Green, 2011). The expression

profile and level of keratin intermediate filament is affected by stress conditions such as tissue injury and disease.

The epidermis keratinocytes express KRT6, KRT16 and KRT17 instead of KRT1 and KRT10 in the suprabasal cells during epidermal injury(Jiang et al., 1993; Weiss, Eichner, & Sun, 1984). Keratinocytes are the main components of the epidermis responsible to repair the layer through epithelialization process after injury (Pastar et al., 2014). Keratinocytes change their morphology from cuboidal and become flat during re-epithelialization process. This change in morphology helps them to extend lamellipodia in a polarized mode and migrate to the wound site. Keratinocytes secret collagenases and proteases such as matrix metalloproteinases (MMPs) to cleave and dissolve damaged part of the ECM. When keratinocytes migrate from their sedentary state during wound healing process it is called epithelial mesenchymal transition (EMT) (Holmbeck & Szabova, 2006; Leopold, Vincent, & Wang, 2012).

Keratinocytes proliferate to generate new keratinocytes and replace the lost cells at a much faster rate than the normal tissue to close the wound edge. The migration of keratinocytes towards the wound edge is continuous till the cells meet in the middle and after they meet, migration is prevented by contact inhibition. Finally, keratinocytes start to retain their original shape to cuboidal, establish cell-cell adhesion mechanisms and secrete new basement membrane proteins (Gurtner, Werner, Barrandon, & Longaker, 2008; Martin, 1997).

The change in behavior of keratinocytes is associated with dramatic changes in keratin intermediate filaments expression and this could indicate keratins are key regulators of the epithelial growth and regeneration.

1.5.2. Keratins and inherited skin disorders

The link between keratin mutations and inherited skin blistering disorders is vital to determine the significance of keratin intermediate filaments and their associated protein components. The first skin blistering disorder identified is EBS which occurs because of keratin mutations (Bonifas, Rothman, & Epstein, 1991) and this started to define the link between keratins and skin disorders. A number of keratin mutations associated with skin fragility disorders have been found where most of the mutation autosomal dominant (Szeverenyi et al., 2008).

There is a wide range of disease phenotype depending on where the mutant keratins are expressed in the skin. For example, defects in KRT5 or KRT14, keratin IF result in EBS (Bonifas et al., 1991; Pfendner, Sadowski, & Uitto, 2005). Whilst mutations in KRT1 and/or KRT10, keratins expressed in the suprabasal cells, result in a disease condition called bullous congenital epidermolytic hyperkeratosis (Cheng et al., 1992; Virtanen et al., 2001). Ichthyosis and palmoplantar keratoderma are associated with the mutations of KRT2 and KRT9, respectively, keratin filaments expressed in the upper spinous layer of the epidermis(Reis et al., 1994; Rothnagel et al., 1994). White-sponge nevus is an autosomal dominant condition of the oral mucosa is due to mutations in oral mucosal keratins, KRT4 and KRT13 (Richard, De Laurenzi, Didona, Bale, & Compton, 1995; E. Rugg et

al., 1995). Pachyonychia congenita is a rare genodermatosis due to mutations in KRT6, KRT16 and KRT17 (Agarwal et al., 2013; Bowden et al., 1995). Since basal layer of the epidermis primarily express KRT5 and KRT14, mutations in these genes are linked with skin blistering disorder called epidermolysis bullosa simplex. This will be discussed in section 1.7.1.

1.6. Type VII Collagen

Whilst basal keratinocytes adhere to the BM through integrins, the BM itself anchors to the dermis through anchoring fibrils. This is mediated by collagen VII. Collagen VII (also called Type VII collagen, COLVII, Col7) is a protein that in human is coded by *COL7A1* gene, found in chromosome 3p21.3 which consists of 118 exons (A. M. Christiano et al., 1994; Greenspan, 1993; Ryynänen et al., 1991). Collagen VII is main structural constituent of the anchoring fibrils of the skin that connects the basement membrane with the underline dermis (Burgeson et al., 1985).

Basal keratinocytes and fibroblasts are the source of collagen VII and primarily synthesized and secreted as procollagens with a molecular weight of 300kDa. The procollagen polypeptide first form a triple helical trimer of 900kDa and then undergo a complex polymerization process (Ryynänen et al., 1991).

Individual collagen VII monomers are composed of three identical alpha chains. These monomers form antiparallel dimers which polymerizes into anchoring fibrils

(Lunstrum, Sakai, Keene, Morris, & Burgeson, 1986; Sakai, Keene, Morris, & Burgeson, 1986). The procollagen of collagen VII associate via their C-terminal and the collagenous domains fold into triple helix (Figure 6).

The triple helix of collagen VII form anti-parallel dimers after being secreted into the extracellular space and dimerization process is stabilized by disulfide bonds after proteolytic cleavage of C-terminus. Then, dimers associate laterally to form anchoring fibrils (Figure 6). These anchoring fibrils are key structural proteins that connect the BM to the dermis (Varki, Sadowski, Uitto, & Pfendner, 2007).

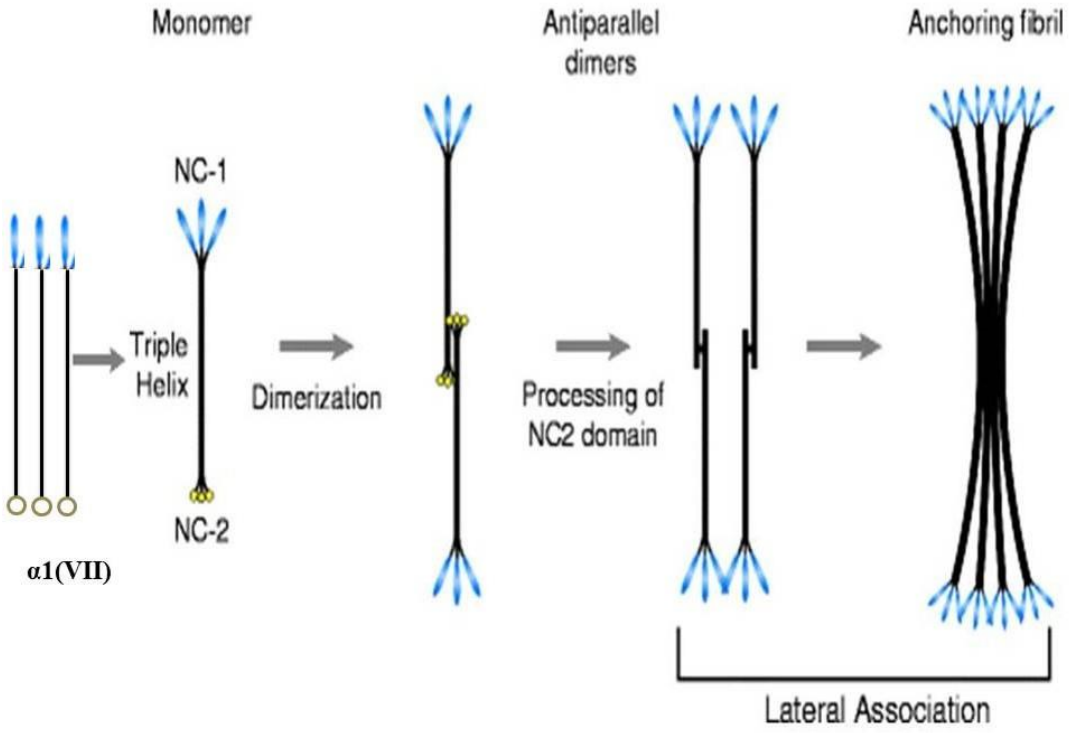

Figure 6: Type VII collage assembly

Diagram displaying polymerization of anchoring fibrils: Three identical α1 (VII) procollagens forming triple helix in a parallel manner which is called a monomer and two monomers associate to form anti-parallel dimers. Then the dimers laterally associate to become anchoring fibrils (Birk & Brückner, 2011).

Collagen VII is a large collagen with non collagenous domains, N-terminal (NC1) and C-terminal (NC2), and a central α-helical collagenous domain(Lunstrum et al., 1986). The non-collagenous domain (NC1) associate to the ECM proteins such as laminin 332, laminin 311 and type IV collagen and with type I,III,V collagen fibers in the dermis (Marks & Miller, 2017; Villone et al., 2008), and stabilizing the dermal-epidermal junction.

Fibronectin type III (FN3) repeats are the most common and the largest subdomains of fibronectin. They are involved in cell morphology, cell adhesion, cell migration and embryonic differentiation. Furthermore, von Willebrand factor (vWF) type A (VWA) domains of collagen VII protein are involved in multiprotein complex formation and many biological activities including cell signal transduction, cell migration and adhesion. In human, mutations in *COL7A1* gene which encodes for collagen VII including VWA or FN3 domains cause skin blistering disorder, epidermolysis bullosa (Chamcheu et al., 2009; Colombatti, Bonaldo, & Doliana, 1993; Petersen et al., 1983). This will be discussed in section 1.7.3.

1.7. Epidermolysis Bullosa

Epidermolysis bullosa is a group of hereditary mechanobollus diseases of animals and human characterized by blister formation and erosion of the skin in response to minor mechanical trauma (J.-D. Fine et al., 2008). In severe form of EB, blisters and

erosions are not limited to the epidermis where the symptoms can also arise in other part of the body like digestive tract, upper airway, bladder and genitals.

Epidermolysis bullosa was first discovered by Koebner in 1886 (J.-D. Fine et al., 2008). Recent advances have helped to the documentation of different mutations in variety of genes, which are responsible for the genetic heterogeneity of EB (Castiglia & Zambruno, 2010; J.-D. Fine et al., 2008; Sawamura, Nakano, & Matsuzaki, 2010).

Mutations of structural proteins which anchor the basement membrane to the epidermis results in blister formation where the skin becomes fragile. Minor mechanical trauma and frictional movement are aggravating factors for the abnormality. The type of mutation and mode of inheritance determines the severity of clinical manifestations which is highly variable among individuals. Mutations in about 20 genes are identified as a cause of EB that encompasses mutations in keratin intermediate filaments, desmosome and hemidesmosome complexes, components of the focal adhesions, and dermo-epidermal anchoring complexes are causative of the disease (J. D. Fine, 2010).

There are about 500,000 international epidermolysis bullosa cases in the world with the incidence rate of 1 per 17,000 live births (Pohla-Gubo, Cepeda-Valdes, & Hintner, 2010). Males and females are equally affected without discrimination. Epidermolysis bullosa is not always apparent following birth and parents can be carriers of the disease without showing clinical manifestations. It is suspected when newborns show blisters and/or erosions in the skin and mucus membrane. Milder

case of epidermolysis bullosa may become apparent following physical activities (Grando et al., 2003).

Once suspected, EB can be diagnosed easily by dermatologists. Taking skin biopsy and observing under a microscope helps to identify where the separating of the skin happens and this helps to define the subtype. Advanced microscopy with high resolution/magnification power is mostly used as it detects the structural abnormalities of skin. Molecular techniques are contributing to identify genes which are defective in epidermolysis bullosa victims (patients and their family members) (Pulkkinen & Uitto, 1999).

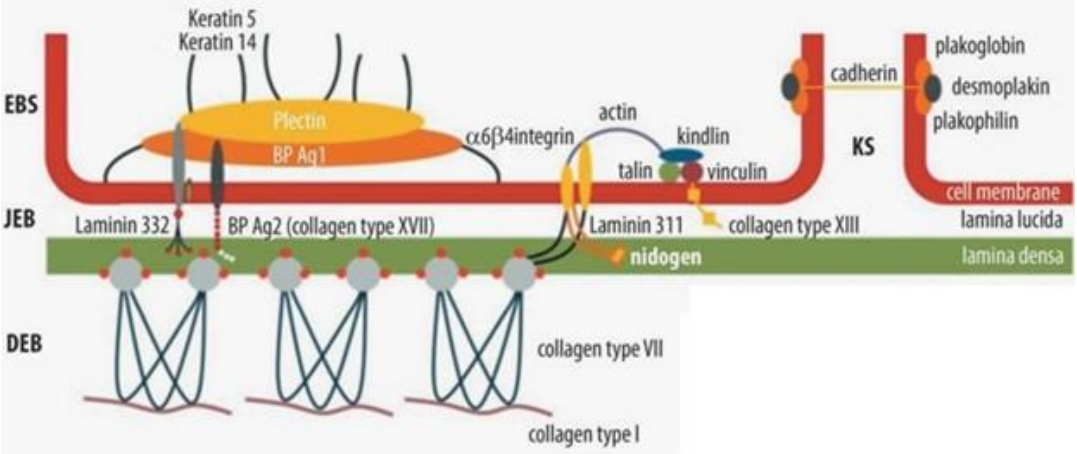

Figure 7: Types and key proteins involved in the pathogenesis of EB

Schematic illustration of the four main types of EB and the different structural proteins responsible for the occurrence of the genetic disease condition. Epidermolysis bullosa simplex (EBS), Junctional epidermolysis bullosa (JEB), dystrophic epidermolysis bullosa (DEB) and Kindler syndrome (KS) (Boeira et al., 2013).

Currently, there are four main types of epidermolysis bullosa, defined by site of cleavage (Figure 7 and Table 2). Epidermolysis bullosa simplex, where cleavage

occurs within the epidermis, junctional epidermolysis bullosa, where cleavage occurs in the lamina lucida, dystrophic epidermolysis bullosa, where cleavage occurs just beneath the lamina densa. The fourth type, Kindler syndrome is caused due to mutations in Kindlin1 and characterized by multiple cleave sites in the epidermis (J.-D. Fine et al., 2008).

1.7.1. Epidermolysis bullosa simplex

Epidermolysis bullosa simplex (EBS) is the most common type of EB and covers about 75 to 85% of all cases and resulted mostly from mutations of keratins (KRT5 and KRT14) and plectin (PLEC1) genes. Rupturing of the epidermal basal keratinocytes leads to a fluid filled blistering of the epidermis (Figure 9). Its occurrence is mostly related to dominant genetic mutations of KRT5 and KRT14 proteins (Lane et al., 1992). EBS severity ranges from mild to severe which is dependent on the nature and location of mutation in the responsible genes/proteins (P. A. Coulombe, M. E. Hutton, A. Letal, et al., 1991) (Figure 8).

However, there are other genetic modifiers not yet identified and environmental factors such as climate changes and life style, apparently influence the severity of EBS phenotypes as there are different subtypes associated with the same mutation (Covello, 1998; E. L. Rugg et al., 2007). Blistering phenotype of all EBS progressively increase as environmental temperature rises. Hot weather especially when associated with humidity can aggravate skin blisters and temperature regulation is important as preventive measures of EBS. Dressing style such as

sticky dressing is also another factor that worsens disease phenotypes by increasing frictions and leading to skin blisters in EBS patients(Atherton & Denyer, 2003; Boeira et al., 2013; Clark, 2003).

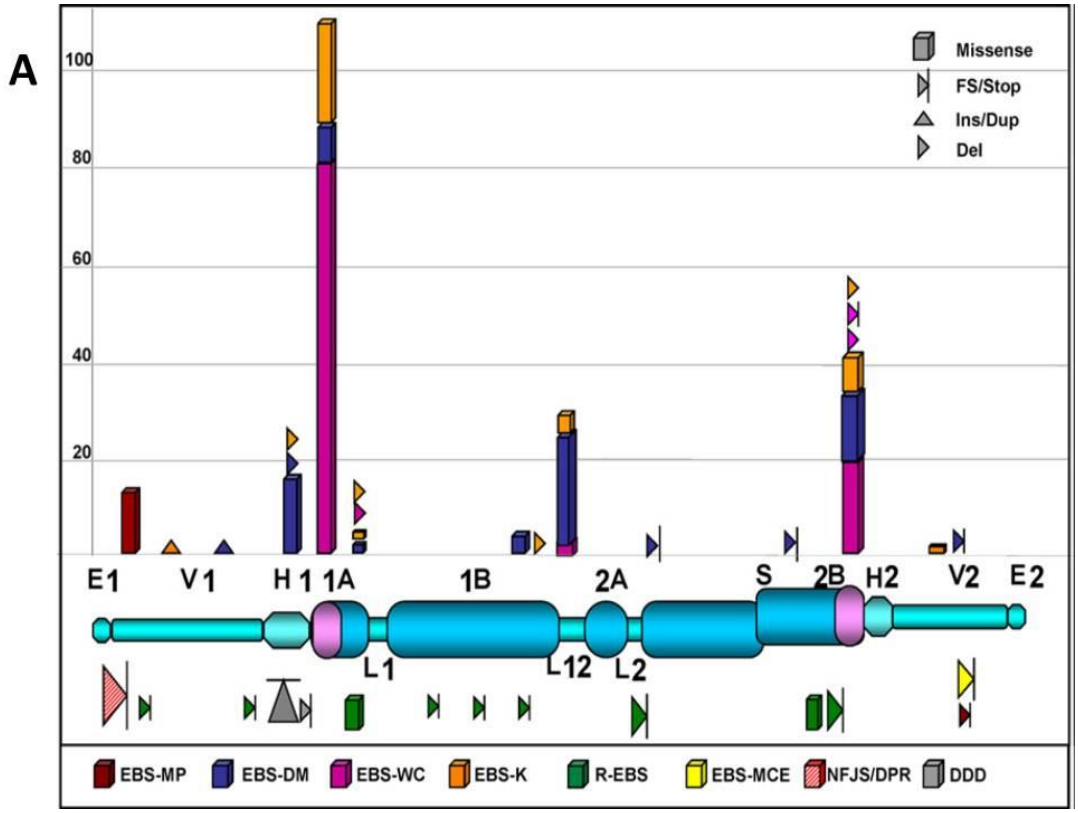

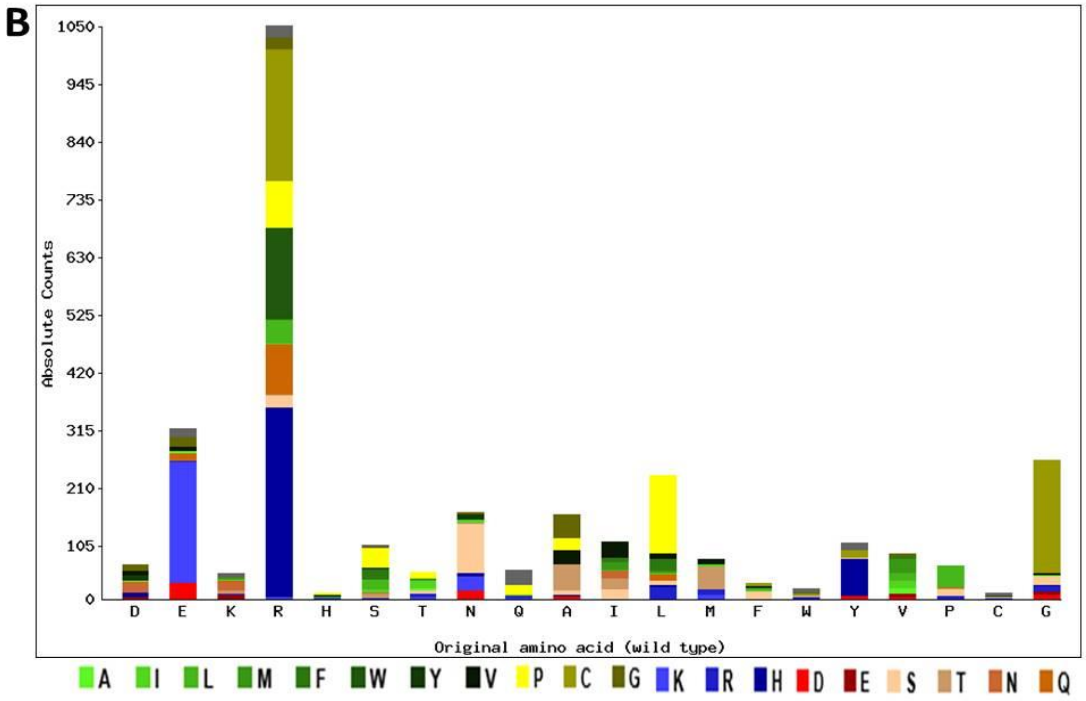

Figure 8: Common mutation sites in keratin protein domains and different subtypes of EBS

(A) Diagram displaying keratin 14 protein domains and the sites of mutation causing different subtype of EBS and other keratinization diseases. X-axis represents domains of keratin 14 protein and Y-axis represents relative frequency of mutations. EBS with mottled pigmentation (EBS-MP), EBS Dowling-Meara (EBS-DM), EBS Weber-Cockayne (EBS-WC), EBS Koebner (EBS-K), Recessive EBS(R-EBS), EBS with migratory circinate erythema, Naegeli_Franceschetti-Jadassohn syndrome/dermatopathia pigmentosa reticularis (NFJS/DPR) and Dowling-Degos disease (DDD) (Uitto, Richard, & McGrath, 2007), (B) Common sites of dominant mutations showing amino acid substitutions of human KRT14 where the X-axis indicates the original amino acids along the protein domain and the Y-axis displays the number of amino acid changes identified in EBS patients (http://www.interfil.org/statistics.php).

Most of the severe forms of EBS are due to point mutations in the helix initiation (1A domain) or termination (2B domain) domain of either KRT14 or KRT5. In contrast, mutations in the non-helical head, tail, and linker domains of KRT5/KRT14 usually give rise to mild form of EBS (Uitto & Richard, 2004).

The severe form of EBS, EBS-Dowling Meara, which is caused by KRT14 mutations that are found in the conserved boundary region of the central α-helical rod domain and the commonly mutated amino acid in KRT14 is arginine amino acid at position 125(Arg125) which is found at the helix initiation motif of the KRT14 and causes severe form of EBS-DM in humans (Figure 8 A & B) (Szeverenyi et al., 2008)

Table 1: Example of sequence variants associated with epidermolysis bullosa simplex Dowling-Meara type (EBS-DM)

cDNA Variant	Protein Variant	Protein Variant Types	Disease Name	Reference
c.373C>T	p.Arg125Cys	Substitution	EBS-DM	(Tsuruta et al., 2011)
c.374G>C	p.Arg125Pro	Substitution	EBS-DM	(Morley et al., 2003) (Bchetnia et al., 2012)
c.373C>A	p.Arg125Ser	Substitution	EBS-DM	(Bchetnia et al., 2012
c.374G>A	p.Arg125His	Substitution	EBS-DM	(Müller et al., 2006)
c.374G>T	p.Arg125Leu	Substitution	EBS-DM	(Ołdak et al., 2010)

Many patients with EBS-DM have been found of which 70% of them were associated with the substitution of arginine residue of the codon 125 (p.Arg125). As shown in the table 1, the highly conserved helix initiation domain is a

mutational hotspot where the amino acid arginine can be substituted by different amino acid residues and give rise to similar EBS-DM phenotypes, the most severe subtype of epidermolysis bullosa simplex (Table 1) irrespective of the substituted amino acid.

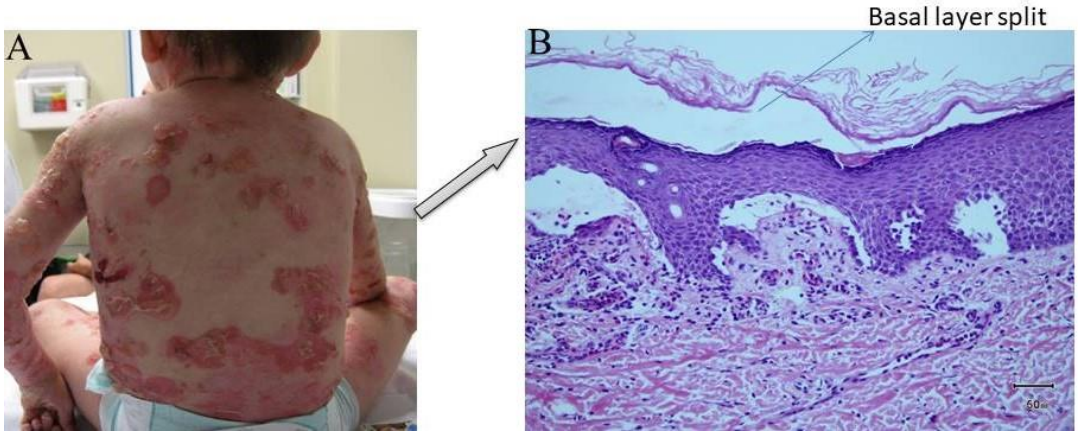

Figure 9: Epidermolysis bullosa simplex phenotype

(A)EBS patient with vesicles and bullosa all over the body, (B) separation of the lower epidermis at the basal layer caused by cytolysis of basal keratinocytes (Alikhan, Farshidi, & Shwayder, 2009)

Based on the site of mutations in KRT14/KRT5, clinical extent and severity, there are three main subtypes of EBS namely EBS-Dowling Meara, EBS Waber-Cockyne and EBS Koebner.

1.7.1.1. EBS Dowling-Meara

The most severe subtype of EBS usually manifested at birth with blistering, erosions and erythema is EBS Dowling-Meara (EBS-DM) due to pathogenic defects which comprises heterogeneous missense mutation is in the conserved

domains of KRT14/KRT5. The phenotypes of EBS-DM spontaneously progress gradually with age and give rise to diseases like oral ulcers, palmoplantar keratoderma and nail dystrophy in adult hood.

In EBS-DM patients, most of the keratin mutations are dominant. However, few patients have been found with recessive mutations in KRT14. Additionally, KRT14 knockout also results in severe form of EBS-DM while in some cases a mild phenotype have been observed (Pfendner et al., 2005; Uitto et al., 2007).

EBS-DM is diagnosed using immunohistochemistry and/or electron microscopy, by detecting an intra epidermal cleavage of the stratum basale. Moreover, patients with this subtype typically shows a number of aggregates in the basal keratinocytes of the epidermis resulting from non-filamentous keratin proteins (Ishida-Yamamoto et al., 1991).

1.7.1.2. EBS Koebner

Epidermolysis bullosa simplex Koebner (EBS-K) is generalized form of EBS characterized by mild blistering elsewhere at birth usually in response to minor mechanical trauma and occurs more regularly during hot and humid weather. Mostly affected areas of the body are the extremities such as hands and feet due to high chance getting mechanical trauma. Mutations in helical and non-helical KRT5/KRT14 domains may cause this subtype of EBS(Chen, Bonlfas, Matsumura, Blumenfeld, & Epstein Jr, 1993).

1.7.1.3. EBS Weber-Cockayne

Waber-Cockayne EBS is considered as the least severe subtype of EBS in which blister are limited to the hands and feet. Blistering phenotypes in patients with EBS-WC starts to manifest in early childhood unlike the other EBS subtypes where blistering starts at birth. Mutations causing EBS-WC are found elsewhere in the helical and non-helical domain of KRT14/KRT5 proteins. Individuals with EBS_WC usually suffer from thickening of the skin on the hands and feet, palmoplantar keratoderma(Chan et al., 1994).

1.7.2. Junctional epidermolysis bullosa

Junctional epidermolysis bullosa (JEB) is a less common type of EB which covers about 5% of all types. Mostly, JEB is inherited by autosomal recessive manner. Diagnosis of JEB is based on tissue cleavage of lamina Lucida within dermo-epidermal junction membrane zone due to hemidosmosomal protein defects (J- D Fine, Johnson, Weiner, & Suchindran, 2004).

Generalized JEB which is characterized by serious hemorrhagic blisters in areas exposed to heat, trauma or friction. Three JEB subtypes are identified. The first subtype Herlitz is a severe form in which patients die at a postnatal period. The second subtype, non Herlitz is milder subtype where patients aff ected survive to adulthood carrying skin fragility disorders throughout their life time and the third, pyloric atresia subtypes which is due to ITGA6 or ITGB4 mutations (McMillan,

Akiyama, & Shimizu, 2003). The most important causes of the first two subtypes of junctional epidermolysis bullosa are mutation of genes such as laminin 332 and collagen XVII (J-D Fine et al., 2004). Laminin 332 is the main component of anchoring filaments involved in cell-matrix adhesion by interacting with α6β4 and α3β1 integrins and anchoring fibrils, collagen VII. A transmembrane protein, collagen XVII is also a component of hemidesmosomes which the intracellular domain interacts with plectin, BP230 and β4 integrins and to laminin with its extracellular domain to stabilize dermal-epidermal adhesions. Recently, It has been reported that successive treatment of JEB in 7 years old boy who lost most of his skin because of mutation in LAMB3 (beta chain of Laminin 332) by taking skin cells from non blistering area of the body, grow mutation free epidermal grafts and able to replace 80 % of the lost skin by healthy new epidermis (Hirsch et al., 2017) .

1.7.3. Dystrophic epidermolysis bullosa

The most severe form of EB is the dystrophic form, where tissue separation is arises in the dermal layer of the affected patient. The dermal fibroblasts and basal keratinocytes produce important macromolecules to keep dermal-epidermal junction integrity among which collagen VII is central as it forms the anchoring fibrils connecting the BM to dermis (Burgeson & Christiano, 1997).

Loss of function of collagen VII leads to skin fragility where the connection between the dermis and epidermis become weak. This leads to the formation of

severe blister beneath the lamina densa, characteristics feature of DEB (Shinkuma, 2015).

Dystrophic epidermolysis bullosa occurs in the form of autosomal dominant or autosomal recessive mode of inheritance. Mutation in *COL7A1* results in all forms DEB. Dominant DEB and recessive DEB are the two known types of DEB of which dominant DEB is characterized by reduction in expression of collagen VII leading to mild blisters, mostly beginning at birth and its severity decreases with age. Generally, it has a good prognosis (J.-D. Fine et al., 2014). Recessive DEB shows a more severe phenotype characterized by severe skin, blistering and wounds (Hamada et al., 2009). Complete absence or very low expression of collagen VII is seen in recessive DEB. (Bruckner-Tuderman, 2010; J.-D. Fine et al., 2014).

Extra cutaneous manifestations such as gastro intestinal tract, genitourinary tract, kidney and heart are common feature of recessive DEB, and patients with this subtype have high probability of developing glomerulonephritis, renal amyloidosis, IgA nephropathy, cardiomyopathy and aggressive squamous cell carcinoma which is the biggest cause of mortality in patients (J.-D. Fine et al., 2008).

1.7.4. Kindler syndrome

Kindler syndrome is very rare, recessively inherited form of epidermolysis bullosa which has been added recently to the classification EB. It is characterized by mixed level cleavage where the skin separation can be in intraepidermal and/or sub

epidermal and it has a general distribution even to other organs. In addition to cutaneous complications, Kindler syndrome involves esophagitis, colitis and urethral strictures (J.-D. Fine et al., 2008). Previous reports have also shown that squamous cell carcinoma patients have developed Kindler syndrome (J. D. Fine, 2010).

Kindler syndrome is autosomal recessive, due to mutations in Kindlin-1 a gene which encodes kindlin1 protein (Jobard et al., 2003). The main role of kindlin-1 in healthy skin is to associate the actin cytoskeleton via focal adhesion complexes with the ECM components (Ussar et al., 2008). In contrast, when kindlin-1 expression is reduced, results in a severe disruption of epidermal basal layer which leads to kindler syndrome (Lai-Cheong, Ussar, Arita, Hart, & McGrath, 2008).

Table 2: Current classification of Epidermolysis bullosa

Main types of EB	Mode of inheritance	Subtypes of EB	Proteins involved
EBS			
Sub-basal	Ar	Lethal acantholytic EB	Desmoplakin
Basal	Ar	Plakophilin Deficiency	Plakophilin-1
	AD	Superficial EBS (EBS-S)	?
	AD	Localized EBS (EBS-loc)[a]	K5, K14
	AD	EBS Dowling-Meara (EBS-DM)	K5, K14
	AD	Other generalized EBS (EBS, gen-nonDM; EBS, gen-NDM)[b]	K5, K14
	AD	EBS with mottled pigmentation (EBS-MP)	K5
	AD	EBS of Ogna (EBS-Og)	Plectin
	AD	EBS with circinate migratory erythema (EBS-Migr)	K5
	Ar	EBS with muscular dystrophy (EBS-MD)	Plectin
	Ar	EBS with pyloric atresia (EBS-PA)	Plectin, integrin α6β4
	Ar	Autosomal recessive EBS (EBS-AR)	K14
	Ar	Autosomal recessive EBS (new subtype)	BPAG1-e
Herlitz (JEB-H)	Ar	-	Laminin-332
Other EBJ (EBJ-O)	Ar	JEB non-Herlitz type, generalized (JEB-nH gen)	Laminin-332, collagen type XVII
		JEB non-Herlitz type, localized (JEB-nH loc)	Collagen type XVII
		JEB with pyloric atresia (JEB-PA)	α6β4 integrin
		JEB reverse (JEB-I)	Laminin-332
		Late-onset JEB (JEB-Lo)	?
		LOC Syndrome	Laminin-332 α3 chain
DEB			
DDEB	AD	Generalized DDEB (ddeb-gen)	Collagen type VII
RDEB	Ar	Acral DDEB (ddeb-ac)	
		Pretibial DDEB (ddeb-Pt)	
		DDEB pruriginosa (ddeb-Pr)	
		DDEB -nails only (ddeb-na)	
		DDEB of the newborn (ddeb-BDN)	
		Severe generalized RDEB (RDEB-GS)[c]	Collagen type XVII
		Other generalized RDEB (RDEB-O)	
		Inverse RDEB (RDEB-I)	
		Pretibial RDEB (RDEB-Pt)	
		RDEB pruriginosa (RDEB-Pr)	
		Centripetal RDEB (RDEB-Ce)	
		RDEB of the newborn (RDEB-BDN)	
Kindler Syndrome	Ar	-	Kindlin-1

AD, autosomal dominant, AR autosomal recessive, DEB, dystrophic epidermolysis bullosa; DDEB / ddeb, dominant dystrophic epidermolysis bullosa; RDEB, recessive dystrophic epidermolysis bullosa; EBS, epidermolysis bullosa simplex; JEB, junctional epidermolysis bullosa.
Formerly called Weber-Cockayne EBS;
[b] Includes EB formerly called Köebner EBS;
[c] Fr formerly RDEB called Hallopeau Siemens.
Translated from the original published in *Clinics in Dermatology*, 2012,30(1):70-7, Intong LR & Murrell DF, Inherited Epidermolysis Bullosa: new diagnostic criteria and classification, Copyright 2012, with permission from Elsevier.[4]

(Source: (Uitto, 2012))

Even though treatment options for EB are not available, researchers are trying to use gene therapy, protein replacement therapy (collagen VII, laminin 332), and

cellular therapy which have shown promise. Still it is likely that several approaches should be combined to bring about a cure for the diff erent EB types (Uitto, 2012).

Different animal models have been developed to understand the cellular and molecular pathomechanism of human diseases to render approaches to develop and test new therapeutic drugs (Lieschke & Currie, 2007). The preferred animal model for a long period has been the mouse because of its similarities to humans. In some cases, development of the mouse model is not feasible because of high cost of development, relatively long lifespan, limited litter size and absence of the corresponding genes in the mouse genome.

These limitations have urged scientists to search for alternative animal models with a short lifespan, low cost to manage and availability of analogous genes with the human genome. And, the zebrafish has emerged as a useful model for human diseases. Why zebrafish and advantage over the other animal models will be discussed in detail below.

1.8. Zebrafish as an Animal Model

The zebrafish (Danio rerio) is a tropical small freshwater vertebrate native to the Himalayan region, first developed by George Streisinger in 1970s as an animal model (Stahl, 1985; Westerfield, 1995). The name zebrafish is given because of the five horizontal pigmented stripes. In recent years, the zebrafish has become an important model organism to explore biological processes *in vivo*.

Zebrafish is easy and cost effective to maintain. Females produce hundreds of embryos at weekly bases. Thus, enough number of transparent embryos can be collected and used for research all seasons under appropriate conditions (Laale, 1977). During development all major organs of zebrafish embryos can be seen within 36 hours of fertilization and at five days post fertilization, organogenesis of major organs is completed(Scholz et al., 2008).

The average maturation time is 3 to 4 months at 28°C and the adult zebrafish length varies from 3 to 5cm. Adult females can be identified easily from male fish by their swollen bellies. Males are slender and have an orange and reddish tint along the body (Westerfield, 1995).

Zebrafish embryos develop externally and are readily available for observation and manipulation right after fertilization. For many diseases, it is difficult to examine disease progression in other animal models without surgery and postmortem examination but in zebrafish, transparency enables observation of development and allows real-time imaging of internal organs (Charles B Kimmel, William W Ballard, Seth R Kimmel, Bonnie Ullmann, & Thomas F Schilling, 1995; Lele &

Krone, 1996). Due to these characteristics, the zebrafish has become a major model in developmental biology (Dooley & Zon, 2000; Lieschke & Currie, 2007). The application of zebrafish skin to study inherited skin diseases will be discussed here under section 1.8.1.

1.8.1. Application of zebrafish skin

Zebrafish have certain similarity to humans in genetics and skin development. About 70% of human genes have a zebrafish counterpart, and 84% of the genes that cause human diseases have a zebrafish orthologue (Vilella et al., 2008). Similar to humans, zebrafish skin has three compartments; the epidermis, dermis and hypodermis (figure 10). Due to its aquatic environment the epidermis has to protect the fish from physical damage, osmotic pressure stress and infectious organisms(Hawkes, 1974).

The epidermis of zebrafish embryo consists of two layers namely; the epidermal basal layer (EBL) and the enveloping layer (EVL). These two surface and inner layers are the simple epithelium of the zebrafish embryo (Kimmel, Warga, & Schilling, 1990; M'Boneko & Merker, 1988).

Enveloping layer is morphologically and functionally similar to the periderm of the mammalian embryo. EVL is generated during blastula period from the surface blastoderm. Its role is to protect the embryo from external damages and is essential for blastoderm morphogenesis through a tight connection with yolk syncytial layer (YSL) and the deep cells (Slanchev et al., 2009). The expression of EVL specific

genes is dependent on the two main transcription factors, Oct4 and IRF6 (Lachnit, Kur, & Driever, 2008; Sabel et al., 2009). Protrusion and migration of EVL cells requires epithelial cell adhesion molecules (EpCAM) (Slanchev et al., 2009).

After the formation of the three germ layers namely, ectoderm, mesoderm and endoderm, the EBL is generated during gastrulation (Heisenberg & Tada, 2002) and it covers the whole embryo at the end of gastrulation (Cherdantseva & Cherdantsev, 2003; Little & Mullins, 2006). Bone morphogenetic protein (BMP) is a signaling molecule conserved between mammals and fish, and a key regulator of EBL cells specification. The dorsally expressed BMP is also important to induce the expression of transcription factor ΔNp63, which is crucial for the development of epidermal ectoderm (H. Lee & Kimelman, 2002). ΔNp63 is the predominant isoform of p63, specifically expressed in cells of epithelial origin. ΔNp63 is specifically expressed in the non- neural ectoderm, a marker of proliferating epithelial cells and important epidermal cell proliferation (Aberdam et al., 2007; Bakkers, Hild, Kramer, Furutani-Seiki, & Hammerschmidt, 2002; H. Lee & Kimelman, 2002).

The adult fish epidermis is a multi-layer composed of basal layer, intermediate layer and superficial layer separated from the underlying dermis by BMZ (Le Guellec, Morvan-Dubois, & Sire, 2003). Unlike the terrestrial vertebrate's epidermis which is covered by an outer layer of keratinized dead cells, zebrafish skin surface is composed of living cells wreathed with microridges which helps to

prevent the fish from infections and osmotic shocks (Concha, Molina, Oyarzún, Villanueva, & Amthauer, 2003; Fishelson, 1984; Hawkes, 1974; Le Guellec et al., 2003).

In zebrafish epidermis, all cells are active metabolically and replaced when dead (Glover, Bucking, & Wood, 2013). The EBL is composed of single cell types, basal keratinocytes and its main function is to connect the epidermis to the basement membrane through hemidesmosome protein complexes. The epidermis of the adult fish is derived from basal keratinocytes and basal cells originally derived from epidermal progenitors within non-neural ectoderm as in the mouse (R. T. Lee, Asharani, & Carney, 2014).

The intermediate stratum is composed of a number of cells such as goblet cells that produce mucus as anti-bacterial and antifungal substances; club cells, produce alarm substances; and sensory cells (Pfeiffer, 1977; Whitear, 1986). Most of the cells found in the intermediate stratum remain undifferentiated and used to replace dead cells (Quilhac & Sire, 1999).

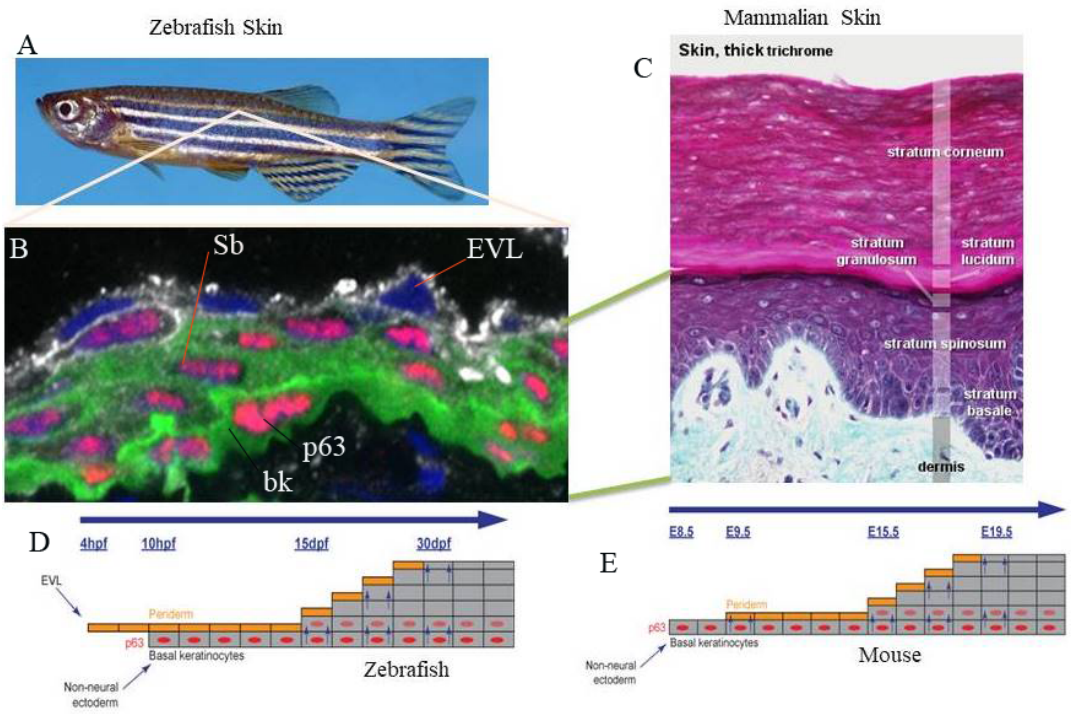

Figure 10: Comparison between zebrafish vs mammalian skin

Diagram displaying the similarities between zebrafish and mammalian epidermis, (A) Adult zebrafish, (B) Immunostained section of adult zebrafish skin showing expression of ΔNp63 which is a specific marker of basal keratinocytes (bk) and suprabasal cells (Sb) and the superficial enveloping layer cells (EVL), (C) mammalian skin where the stratum basale and spinosum are similar to the zebrafish epidermis, (D & E) zebrafish and mouse stratification mechanism where in both cases the basal keratinocytes are originally from non-neural ectoderm and expressed ΔNp63.

The dermis of teleost species can be divided in to two; the stratum laxum and the stratum compactum. Stratum laxum is a superficial region, highly vascularized and composed of a loose collagenous matrix with abundant fibroblasts, pigment cells, nerves and scales(Sire, 1989). Stratum compactum is a deep region of the dermis characterized by a dense collagen matrix with scattered fibrocytes. This layer is

penetrated with anchoring fibrils. The deep layer of the dermis is separated from the muscle cells by the hypodermis which is composed of adipocytes (fat storage cells), loosely organized collagen, chromatophores (xantophores, iridophores and melanophores), and vasculature(Le Guellec et al., 2003).

Zebrafish skin is advantageous to study skin development and pathology because it mimics human skin diseases which have been shown by many research findings. The anatomical and cytological similarities in the basal and suprabasal layers of the skin (Le Guellec et al., 2003; Sonawane et al., 2005) and genetic similarities (Amsterdam et al., 1999; Van Eeden et al., 1996) involved in epidermal development between zebrafish and human skin enables the zebrafish skin to be a good system to study inherited skin diseases.

1.8.2. Zebrafish models of human genetic skin diseases

It is feasible that the zebrafish model is becoming widely recognized as its convenient and cost effective model system that can be used to explore the pathomechanism of human genetic skin diseases (Q. Li & Uitto, 2014). Several zebrafish models have been developed to mimic the feature of heritable skin diseases. As an example of a blistering phenotype expected in zebrafish skin, antisnese morpholino knockdown of Fras1 exhibited embryonic fin blistering (Figure 11C) (Carney et al., 2010) which recaptulates human Fraser Syndrome. Mutations in *fras1*, *frem1* and *frem2* genes, zebrafish orthologues of human FRAS1, FREM1 and FREM2 mimics the epidermal blistering of distal appendages seen in Fraser Syndrome (Carney et al., 2010), which is a recessive multisystem

disorder characterized by embryonic epidermal blistering, cryptophlalmos, syndactyly, renal defects and a range of other developmental abnormalities(McGregor et al., 2003).

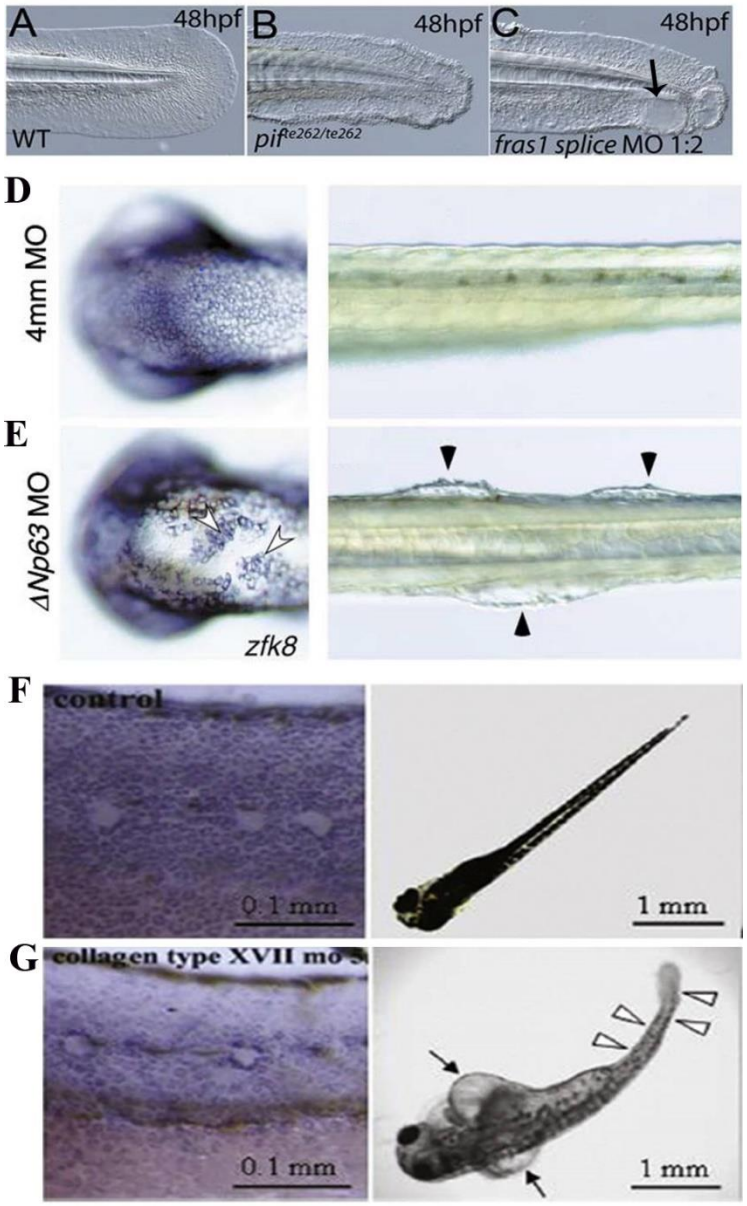

Figure 11: Skin blistering in zebrafish mutants and morphants

(A) Uninjected control of 48hpf zebrafish larva fin, (B) *pif* $^{te262/te262}$ mutant of 48hpf zebrafish larva fin, (C) *fras1* morphant showing fin blistering (black arrow) due to knockdown of Fras1 at 48hpf (Carney et al., 2010), (D) 4mm (mismatch) MO injected

control, (E) At 48hpf ΔNp63 morphants show strong reduction in cells expressing zebrafish keratin 8 (*zfk8*) in the head region (white arrow) and exhibited skin blistering in the trunk/tail region of the fish (black arrow)(Bakkers et al., 2002), (F) embryos injected with standard control MO, (G) Embryos injected with *col17a1a* MO show loss of *col17a1a* expression in comparison to the control fish, pericaridal edema (black arrow) and morphological changes in the skin surface, tail region (white arrow)(Kim et al., 2010).

A previous study demonstrated antisense mediated loss of Δ*Np63* leads to epidermal defects in which Δ*Np63* morphants displayed as strong reduction of epidermal keratinocytes, blistering and sloughing the skin (Figure 11 E) (Bakkers et al., 2002). The effect was most prominent in the head region consistent with the phenotype of patients suffering Hay-Wells syndrome, characterized by severe dermatitis in the scalp (J. A. McGrath et al., 2001). A blistering phenotype and perturbation of the basement memebrane zone was also demonstrated by knocking down of the expression of *col17a1a* wich codes for zebrafish type XVII collagen which is homologous to the human type XVII collagen (Figure 11 G) (Kim et al., 2010). Summary of the previous studies on skin diseases conducted in zebrafish are shown in Table 3.

Table 3: Summary of zebrafish models of human genetic skin related defects

Genes	**Disease phenotypes**	**Zebrafish gene**	**References**
EpCAM	Skin defects	*epcam*	(Slanchev et al., 2009)
FRAS1, FREM1 & *FREM2*	Fraser Syndrome	*fras1, frem1* & *frem2*	(Carney et al., 2010)
ITGA3	ECM abnormalities	*Integrin α3*	(Carney et al., 2010)
LAMA5	ECM abnormalities	*laminin α5*	(Carney et al., 2010)
KIND1	Kindler Syndrome	*kindlin-1*	(Postel et al., 2013)
IRF6	Van der Woude Syndrome/Oral cleft	*irf6*	(Sabel et al., 2009)
COL17A1	Junctional epidermolysis bullosa	*col7a1a*	(Kim et al., 2010)
SPINT1	Loss of epidermal integrity,	*spint1a*	(Carney et al., 2007)
Δ*N p63*	Ankyloblepharon-ectodermal dysplasia-clefting(AEC) syndrome, Hay-Wells syndrome	Δ*Np63*	(Bakkers et al., 2002; H. Lee & Kimelman, 2002)
ABCC6	Psuedoxanthoma elasticum(PXE)	*abcc6a*	(Qiaoli Li et al., 2010)

1.8.3. Zebrafish keratins

In zebrafish, the protein expression pattern of keratins is diff erent where they present in the epithelia and many other cell types of diff erent origin (mesenchymal cells) unlike birds and mammals where keratins are almost solely expressed in the epithelia (Conrad, Lemb, Schubert, & Markl, 1998).

There are a total of 23 keratins of which, 16 type I and 7 type II keratins in zebrafish genome, suggesting that fewer keratin genes are found in zebrafish than mammals which contain 54 keratin genes. Approximately equal number of type I and type II keratins are found in humans unlike zebrafish where the number of type II keratins is about double of the type I keratin genes. This decreased number of keratins in zebrafish is because they do not have hard keratins. In mammals, the keratin family comprises hard keratins in addition to the epithelial keratins called soft keratins (Langbein, Rogers, Praetzel, Winter, & Schweizer, 2003; Langbein, Rogers, Winter, Praetzel, & Schweizer, 2001).

In contrast to the two clusters of keratin genes in mammals, zebrafish keratins are partially scattered. The keratin genes in human are located in two different chromosomes as clusters. Besides KRT18, type I keratins are located on chromosome 17 and type II keratins plus KRT18 are clustered on chromosome 12 of the human genome. However, in zebrafish, type I keratin genes are scattered on nine different chromosomes and type II keratins are located on five different chromosomes (Hesse, Zimek, Weber, & Magin, 2004). Except for zebrafish Krt8 and Krt18 which are orthologues of human KRT8 and KRT18, respectively, other

type I and II zebrafish keratins have no clear orthology to mammalian keratin genes. Phylogenetic analysis and chromosomal organization indicated independent duplication in various teleost lineages. For example, five type I keratins are located on chromosome 19 of the zebrafish genome namely, *krtt1c19a, krtt1c19b, krtt1c19c, krtt1c19d,* and *krtt1c19e* and four type I keratins on chromosome 11, *krtt1c11a, krtt1c11b , krtt1c11c* and *krtt1c11d* suggesting that they evolved from relatively recent tandem duplication events. The clustered keratin genes have no direct orthologues in human (Padhi, Akimenko, & Ekker, 2006).

It has been shown that type I keratin of zebrafish had lower molecular weight (48-50 kDa) as compared to the type II keratins (52-56 kDa) and they almost had similar isoelectric point (Markl, Winter, & Franke, 1989). In zebrafish, the first keratin gene to be expressed in all surface cells is K8 at mid blastula stage. In the adult zebrafish Keratin8 is expressed in the intestine, superficial cell layers of the skin and fins.

In zebrafish, *krt4* gene is predominantly expressed in the enveloping layer (EVL) which has been used a strong promoter to label EVL cells(Gong et al., 2002). Another important type I keratin, *krtt1c19e* gene is strongly and predominantly expressed in the basal keratinocytes which can be used as a specific marker for basal cells of the epidermis (R. T. Lee et al., 2014).

1.9. Hypothesis and Approach

The main hypothesis of my project is that zebrafish can serve as a relevant model of epidermolysis bullosa. I aim to do this using CRISPR/Cas9 mutations or a novel epidermis promoter (zebrafish *krtt1c19e*). I hypothesise that; epidermolysis bullosa can be generated in zebrafish by transgenic overexpression of dominant negative keratins (human KRT14 or zebrafish Krtt1c19e) or through mutation of type VII (Col7a1) collagen using CRISPR/Cas9 system.

1.9.1. Significance of the study

Missense mutation of Arginine amino acid at position 125 to different amino acids, such as Cysteine and Proline, is the most frequent mutation in KRT14 which leads to the most severe form of epidermolysis bullosa simplex (Dowling-Meara subtype)(http://www.interfil.org/). The behaviour of basal keratinocytes harbouring keratin mutations is not explored yet in real life and this EBS zebrafish model will help understand how the cells really behave in vivo and provide opportunity to image the real time cellular and subcellular defects at high resolution. The most severe type of EB, DEB is caused by mutations in collagen VII gene, COL7A1. Exploring how collagen VII is required across species is essential. Despite the presence of many different mutations in human patients, viable animal model that recapitulates DEB is required for practical application of new therapies. Thus, generating epidermolysis bullosa zebrafish model will provide further

understanding of the pathophysiology of EB at both genetic and phenotypic levels which can be used as a drug screening platform for developing therapeutic targets.

1.9.2. Objectives

Therefore, the main purpose of this project is to generate zebrafish models of epidermolysis bullosa so as to understand pathomechanism and aetiology.

- To establish zebrafish as a robust model of human epidermolysis bullosa simplex by overexpressing dominant negative zebrafish and human keratins
- To generate collagen VII knockout zebrafish so as to establish dystrophic epidermolysis bullosa zebrafish model
- To assess cellular and subcellular defects related to epidermolysis bullosa phenotypes
- To establish a platform for testing human epidermolysis bullosa patient genetic lesions and therapeutic screens.

2. CHAPTER 2. MATERIALS AND METHODS

2.1. Animal Husbandry

Zebrafish (Danio rerio) were housed in the zebrafish facility, Institute of Molecular and Cell biology (IMCB), Agency for Science, Research and Technology (A*STAR), Singapore. Zebrafish embryos used for experiment were obtained by natural breeding, incubated at 28.5°C and embryo staged as per (C. B. Kimmel, W. W. Ballard, S. R. Kimmel, B. Ullmann, & T. F. Schilling, 1995). Embryos were exposed to 0.003% 1-phenyl-2-thiourea (PTU) from 22 hours post fertilization (hpf) to block pigmentation for whole mount in situ hybridization analysis. Animal management was carried out according to the guidelines of Agri Food and Veterinary Association (AVA), Singapore.

2.2. Transgenesis

To generate transgenes, we employed the gateway cloning method, and the Tol2Kit (Koichi Kawakami, 2004). Middle entry clones were generated in *pDONR221* (Invitrogen). A forward primer containing an attB1 site (GGGGACAAGTTTGTACAAAAAAGCAGGCTNN plus gene specific DNA oligos) and a reverse primer containing a reverse attB2 site (GGGGACCACTTTGTACAAGAAAGCTGGGTN plus gene specific DNA oligos) were used to clone transgenes. One or two nucleotide bases were included in place of N/NN to keep the reading frame of the protein sequence. For all the

transgene constructs by gateway, *p5E krtt1c19e* prom as promoter, *p3E polyA* as 3 clones and *pDestTol2pA2* as destination vector containing Tol2 sequences were used.

Human *KRT14* (*KRT14_WT* and *KRT14_R125P*) cloned in an entry vector, *pEGFP-C1* was obtained from Institute of Medical Biology, Agency for Science, Research and Technology (A*STAR) of Singapore. Overexpression of eGFP tagged dominant negative zebrafish keratin 19 (*krtt1c19e_R124C*) and human *KRT14* (*KRT14_R125P*) under the zebrafish keratin 19 (*krtt1c19e*) promoter was used to establish epidermolysis bullosa simplex in zebrafish.

Tol2 technology enables the generation of transgenic lines by transposase mediated insertion of a plasmid into the genome of zebrafish embryos (K. Kawakami et al., 2004). In order to create a vector system allowing spatial control of gene activation in zebrafish, I inserted human *KRT14* and zebrafish *krtt1c19e* into a destination vector with Tol2 which allows the integration of a gene to the zebrafish genome. Accordingly, transposase mRNA is injected together with the DNA construct containing our gene.

Needles (Borosilicate Glass with filament 10 cm in length) were pulled on a P97-4870 aming/Brown Micropipette Puller (Slutter Instrument). 2% agarose plate was prepared with embryo medium. Injection of transgene was performed by loading the DNA mix into a needle using microloader tip while waiting for the fish to

laying eggs. Eggs were collected in a plate with embryo medium and arranged in the groove of agarose plate and injected using IM 300 Microinjector (NARISHIGE, Japan) or PL-100 microinjector (Harvard Apparatus). *pT3Ts-Tol2* plasmid was used as a template to generate Tol2 mRNA. *SmaI* restriction enzyme was used to linearize pT3Ts-Tol2 DNA and gel extraction kit (Qiagen) was used for purification. mMessage mMachine T3 transcription kit(Ambion) was used to synthesis Tol2 mRNA choosing Lithium chloride precipitation to remove unbound nucleotides and proteins. The DNA constructs were co-injected with transposase mRNA at 30 ng/µl each in to the yolk or cell at the one cell stage. Injected embryos of zebrafish were incubated at 28.5 ^{0}C for three days and those with best expression of the construct were selected using a fluorescent dissecting microscope and raised. After three months, founders were identified and in crossed or outcrossed with AB (wild type) to establish stable lines (F1). F1 embryos were genotyped using primers for zebrafish *krtt1c19e_R124C*; F: CACCTTCTCCAGCGGAAGC and R: ACTTAACAAGGGACGTGGA, human *KRT14_R125P*; F: AGTTCACCTCCTCCAGCTCC and reverse: TCAGTTCTTGGTGCGAAG GAC and sequenced.

2.3. CRISPR/Cas9 System

Clustered regularly interspaced short palindromic repeats (CRISPR) associated Cas9 system was employed for zebrafish mutagenesis (Blackburn, Campbell, Clark, & Ekker, 2013). CRISPR target sites were designed from *col7a1a* Exon10, *col7a1a* Exon29, *col7a1b* Exon2 and *col7a1b* Exon36 using ZiFiT Targeter

Version 4.2 software. The CRISPR target sites used for *col7a1a* Exon10, *col7a1a* Exon29, *col7a1b* Exon2 and *col7a1b* Exon36 are, GGAGGAGCAGTCTGTGGGGG, GGAGGTCTGCCAGGTCGGGG, GGAGGACGTGCCGTATGAGG and GGAGGTATGGAGGTTCTTCC, respectively. To generate single guide RNA (sgRNA) for *col7a1a* Exon10, *col7a1a* Exon29, *col7a1b* Exon2 and *col7a1b* Exon36, PCR performed using a common reverse primer, CRISPR sgR: AAAAGCACCGACTCGGTGCCACTTTTTCAAGTTGATAACGGACTAGCCT TATTTAACTTGCTATTTCTAGCTCTAAAAC and gene specific forward primers; CRISPR gspF: GAAATTAATACGACTCACTATAGGAGGAGCA GTCTGTGGGGGGTTTTAGAGCTAGAAATAGC, GAAATTAATACGACT CACTATAGGAGGTCTGCCAGGTCGGGGGTTTTAGAGCTAGAAATAGC, GAAATTAATACGACTCACTATAGGAGGACGTGCC GTATGAGGGTTTTA GAGCTAGAAATAGC and GAAATTAATACGACTCACTATAGGAGGTA TGGAGGTTCTTCCGTTTTAGAGCTAGAAATAGC were used *col7a1a* Exon10 *col7a1a* Exon29, *col7a1b* Exon2 and *col7a1b* Exon36, respectively. PCR products were purified by PCR purification kit (Zymogen) and checked by gel electrophoresis and nanodrop. RNA transcription was performed using MEGAshortscript T7 kit (Roche). And, Cas9 RNA was prepared by digesting *pCS2-nCas9n* with *NotI* and transcribed by mMESSAGEm-MACHINESP6 transcription kit (Roche).

Cas9 RNA and gRNA were mixed at a concentration of 150-250ng/µl and 100ng/µl, respectively. Phenol red (0.5%) was added to the mixture and injected together into one cell stage of zebrafish embryo. Injected embryos were checked at 24hpf for mutagenesis efficiency by genotyping. Eight injected embryos per plate were taken as a representative sample, lysed by lysis buffer which contains(10mM Tris, 50mM KCl, 0.3% Tween20, 0.3%Nonidet 40; pH 8.3, 0.5mg/ml proteinase K) in a PCR tube at 55 °C for at least three hours and genomic DNA is denatured at 98 ^{0}C for 10 minutes. Short genomic PCR was done using gene specific primers across CRISPR target sites (Table 3). The PCR product was sequenced to check for the Indels in the CRISPR target site.

Table 4: Summary of CRISPR target sites and primers used to knockout zebrafish type VII collagen

Gene	Exon	CRISPR target site	Primers
col7a1a	Exon10	GGAGGAGCAGTCT GTGGGGG	F: 5'- CAGCAAGTCTATTGTTGTTG-3' R: 5'- CTTCAGTTTTCATTAAAAGC-3'
	Exon29	GGAGGTCTGCCAG GTCGGGG	F: 5'- GTGTGACAGTGTTGGCGGTAG-3' R: 5'- GCCTAGCCCTACTTGCTTGTG-3'
col7a1b	Exon2	GGAGGACGTGCCG TATGAGG	F: 5'- GCCTTCCAGGGAAATGTGTTCGG-3' R: 5'- CTCTGCCACCTATGAATGCACTG-3'
	Exon36	GGAGGTATGGAGG TTCTTCC	F: 5'- GACAAGTCTTTAACAGAAATTGAC -3' R: 5'- CTATGTTAACCAGGGGTGTCC -3'

2.4. Morpholino Injection

Antisense morpholino oligonucleotide (MO) for *col7a1* genes were designed and purchased from Gene tools (http://www.gene-tools.com/) as displayed in table 4 and microinjected to one cell stage zebrafish embryos.

Table 5: Morpholino antisense oligonucleotides of zebrafish *col7a1* genes

Gene	MO site	Target Sequence
col7a1a	*col7a1a*_e29i29	ATGGATTTGATCTGACCGTGACACC
col7a1b	*col7a1b*- e20i20	GTACATAAGGTGTTCACCAGTTGCT

e=exon, i=intron

2.5. RNA Extraction, Reverse Transcription and Polymerase Chain Reaction

Larvae at different developmental stage were used for total RNA extraction using trizol (Invitrogen) where 700µl of trizol/10 fish was added and kept at -80 ^{0}C. After thawing embryos were homogenized by homogenizer, incubated at room temperature for about 5 minutes and 140µl chloroform was added, shaken rigorously for about 10 seconds, and centrifuged 12,000xg at 4 ^{0}C for 15 minutes. Top phase was removed and added into a new microfuge tube and then 350ul of isopropanol added and kept for 10 minutes at room temperature, centrifuged at 12,000xg at 4 ^{0}C for 10 minutes, washed with 1ml of 70% ethanol per ml of trizol. Mixture was centrifuged at 7500xg at 4 ^{0}C for 5 minutes. Finally, 20µl RNase free water was used to resuspend the pellet.

After extraction, the purity and concentration of the RNA was evaluated using spectrophotometry (nanodrop) (Thermo Scientific, ND1000) and gel electrophoresis. Total RNA was stored at -80 °C to be used whenever is needed. cDNA was synthesized using Superscript III Reverse Transcriptase (Invitrogen). Expression level of *col7a1a* and *col7a1b* was determined with Reverse Transcriptase Polymerase chain reaction (RT-PCR) using the following oligonucleotides (Table 5). The reference gene used in this experiment was β-actin.

Table 6: Primers used for Reverse Transcription Polymerase chain reaction (RT-PCR) of *col7a1* genes

Gene	**Primers**
col7a1a	F: 5'- TGTGGTCGTCATTATCGCAG -3' R: 5'- CCGTAGAGCTGATTTGCGTC -3'
col7a1b	F: 5'- AAGAATCTGGTTCACGACAC -3' R: 5'- CTCCAGGTGAGTTTGTATTC -3'
B-actin	F: 5'- CTCTTCCAGCCTTCCTTCCT -3' R: 5'- CACCGATCCAGACGGACTAT -3'

Polymerase chain reaction (PCR) was performed using GoTaq Green Master Mix (Promega), The thermal cycler was set according the type of polymerase and primers. For GoTaq Green, Initial denaturing to 95 ^{0}C for 2 minutes, subsequent denaturing to 95°C for 30 seconds, annealing 54 °C (depends on the melting temperature of primers) for 30 seconds, extension at 72 °C for 1 minute/kb

(depends on size of DNA to be amplified), final extension step at 72 °C for 5 minutes and the cycling reaction was programmed to end by holding the tubes at 4^0C. Generally, 25 to 34 cycles were performed to amplify desired DNA templates. To confirm a single band of the correct size was amplified. 1ul of the PCR product was mixed with loading dye and loaded onto a 1% or 2% agarose gel depending on the size of the template.

2.6. Protein Preparation for Mass Spectrometry

To extract protein for mass spectrometry from 30hpf zebrafish embryos a total of 500 embryos were collected in a 90mm petri dish plate. Embryo medium was replaced with embryo medium supplemented with 1mg/ml pronase (Sigma Cat# P-6911; dissolved in water and aliquoted -20°C). Embryos were swirled on shaker for 10min at room temperature. Embryo medium was removed and washed out residual pronase with 5 quick washes with fresh Embryo medium. 1000ul Calcium-free Ringers was added. Yolk was dissociated by pipetting through glass pasteur pipette with tip narrowed by flame polishing. Embryos were shacked at 1100rpm on Eppendorf Thermomixer for 5min at room temperature and spinned at 310xg for 2mins at 4°C. Supernatant was discarded without disturbing the soft pellet. 1000ul Calcium-free Ringers was added and pellet was resuspended. Washing was repeated for a total of five times. After final deyolking wash, spin down and remove Ringers, 500ul (1ul:1embryo) fresh 1x C2SDC lysis buffer was added to deyolked pellet, and short vortexed for 10 seconds. We used a bit different protocol

to extract protein for mass spectrometry from 5dpf and adult fin. Adult zebrafish fin or 5dpf larvae were washed in ice cold PBS twice. PBS was removed and 100ul of lysis buffer was added per fin or 1ul per embryo. Adult fin or larvae were homogenized with homogenizer on ice until tissue fully dissociate. Pellet from 30dpf embryo and homogenized sample from 5dpf larvae and adult fin were incubated on ice for 5min and again short vortexed for 10 seconds then sonicated at 4°C (mid-setting, 6 seconds). After incubating it on ice for 15 min, 0.1ul (25u) benzonase per 100ul of lysate was added and incubated again at RT for 15 mins with shaking (900rpm on thermomixer. It was spinned at 4°C for 60mins and supernatant was taken to fresh tube and snap freezed in Liquid Nitrogen. Finally stored at -80°C for further use.

To prepare MS sample, equal amounts of protein from wild type and knockout samples were first reduced with 5mM dithiothreitol and alkylated with 10 mM iodoacetamide. Proteins were digested with lysyl endopeptidase (1:100 enzyme-to-protein) at 37 ^{0}C for 16 hours, followed by trypsin (1:50 enzyme-to-protein) for 8 hours. The digested peptides were cleaned-up using Empore C18-SD Extraction Disk Cartridge (3M), vacuum-dried and reconstituted in 0.1% formic acid for MS analysis.

To generate spectral library, equal aliquots from wild type biological replicates were pooled together and injected into ekspert nanoLC-425 system (Eksigent) coupled to TripleTOF 6600 system (SCIEX) as three technical replicates. Online reversed-phase separation was performed using buffer A (2% acetonitrile, 0.1% formic acid) and buffer B (95% acetonitrile, 0.1% formic acid). Peptides were first

trapped on a trap column (350 µm x 0.5 mm, ChromXP C18CL 3 µm 120Å), then separated on an analytical column (75 µm x 15 cm). Peptides were gradient eluted at 10-18% solvent B over 55 min, followed by 18-30% solvent B over 60 min at a flow rate of 300 nL/min. Eluted peptides were analyzed in the information dependent mode on the MS, with precursor mass range from 400-1600 m/z, 250 ms accumulation time, and maximum 50 precursors selected for fragmentation. MSMS fragmentation analysis was performed in high sensitivity mode, with mass range 100-1800 m/z, 50ms accumulation time, dynamic exclusion 15s and rolling collision energy enabled. Protein identification was performed by searching generated spectra in the ProteinPilot 5.0 software (SCIEX) against the zebrafish UniProt Reference Proteome, with search parameters for adjusted for cysteine alkylation by iodoacetamide and biological modifications specified by the algorithm. False discovery rate (FDR) was determined by searching against decoy reversed protein sequences generated from the zebrafish UniProt database.

MS analysis for individual wild type and knockout samples were performed as above, except that the MS was running on SWATH-MS mode, specifying for 120 variable windows across 400-1200 m/z with 1 m/z overlap, minimum window width of 3 m/z and rolling collision energy enabled. Fragmentation information was collected for 25ms across 100-1800 m/z in high sensitivity mode. Generated SWATH data were analyzed against the reference spectral library using the SCIEX OneOmics workflow on the BaseSpace cloud analysis platform (Illumina). Up to ten peptides with six transitions each were selected for each protein with 75 ppm ion tolerance, 10 min extracted-ion-chromatogram (XIC) window, considering only

peptides with > 99% confidence and excluding those which were shared. Retention time calibration was performed using the indexed retention time (iRT, Biognosys) synthetic peptides. (Done by Larry Wai Leong LOW and Qifeng LIN from Institute of Molecular and Cell Biology, A*STAR, Singapore).

2.7. Immunostaining

Immunostaining of wild type and transgenic zebrafish larvae at different stages (3dpf and 6dpf) for eGFP tagged keratins (human KRT14 and zebrafish Krtt1c19e) at (3dpf and 6dpf) was performed. Embryos were dechorionated by adding 400µl pronase per plate and kept at room temperature for about 20 minutes. Embryos were transferred into microfuge tube and fixed in 4% PFA at room temperature for about two to three hours or overnight at 4 °C shaker incubator.

After fixation, Embryos were washed using PBS Tween 20(0.5% PBT) three times for five minutes, followed by a methanol series wash (25% MeOH, 50% MeOH, and 75% MeOH) and then washed extensively in 100% MeOH (at least 3x 100% MeOH). Embryos were stored at -20°C for at least two hours.

Embryos were removed from methanol by gradual replacement by PBT. Embryos were pre incubated in 0.75ml blocking buffer (0.01% DMSO and 0.05% sheep serum in PBT) for at least two hours at room temperature. Pre blocking solution was removed and (rabbit anti-eGFP (1:400, Abcam) , mouse anti E-cadherin

(1:250, BD Bioscience), rabbit anti DsRed (1:250, BD Bioscience) and (mouse anti- p63(1:200; Santa Cruz)), primary antibodies were added in 0.75ml blocking buffer and incubated at 4°C overnight.

Embryos were washed with PBT (1x fast, 3x 1hr) and Secondary antibodies (Invitrogen) of donkey anti rabbit (488nm) and anti-mouse (546nm) were used at a dilution of 1:400 and added in 0.75ml blocking buffer and incubated at 4 °C overnight on shaker incubator. Unbound antibodies were washed with PBT (1x fast, 3x 30 minutes) and counter staining of the nuclei was performed using DAPI (5mg/ml, Invitrogen). Stained embryos were kept in 50% glycerol and incubated on shaker incubator for 15 minutes. Embryos were screened using epifluorescence and stored in 80% glycerol diluted in 1xPBS.

2.8. Whole Mount *In Situ* Hybridization

To show expression pattern of *col7a1* gene, in situ hybridization was performed as previously described (Thisse & Thisse, 2008). Antisense RNA probes for *col7a1a*, *col7a1b* and *col6a2a* were synthesized from cDNA of a wild type fish using primers shown in table 6. *pGEM-T* easy vector (promega) was used to clone PCR products in which cloned circular DNA was linearized by *SpeI* restriction enzyme. Antisense DIG labelled RNA were prepared and transcribed with T3 RNA polymerase (Roche). Alkaline phosphatase (AP) coupled anti digoxigenin fab

fragment antibody for detection and NBT/BCIP for development of the probe was used as stated (Thisse & Thisse, 2008).

Table 7: Primers used for probe preparation

Gene	Primers
col7a1a	F: 5'- CAGGGCAGCCAGGTGTCCCAG -3' R: 5'- CAGCGCAGGGTATAGCGGGA -3'
col7a1b	F: 5'- CTTCCCGGGACTGATGGTATTC -3' R: 5'- GAGGTGCCTGGTAAACCGATC -3'
col6a2a	F: 5'- GATGCGGTGCCCTGGATATTG -3' R: 5'- CCAGATCAGCGAAACGCCTC -3'

2.9. Cryosectioning

To identify the layer of the epidermis with the expression of eGFP tagged keratins, we performed cryosectioning of immunostained zebrafish larvae at 5dpf and 16dpf. Embryos in 80% glycerol were washed with PBT (3x wash in 5 minutes) and incubated overnight in 30% sucrose which is a cryoprotectant and partial dehydrant that prevents the formation of ice crystal artefact in frozen tissue sections. Embryos were removed from sucrose and embedded in the embedding molds in an embedding medium optical cutting temperature (OCT), orientated and frozen on dry ice. Frozen blocks were wrapped in aluminum foil and incubated at -80 ^{0}C. Sectioning of the frozen blocks was conducted at 30µm.

2.10. Histology

Four months old adult zebrafish were anaesthetized, euthanized with tricaine and fixed in 4% PFA overnight and submitted for histopathology. Fish were processed through graded alcohol, xylene and wax to dehydrate the tissue for paraffin embedding. Paraffin blocks were made with the required orientation and transverse sectioning was performed at 4-6um thickness. The sections were placed into microscope slides and dried. The slides were then hydrated through xylene followed by graded alcohol to hydrate the section for Hematoxylin and Eosin staining. The slides were stained in Hematoxylin for 5min, followed by acid alcohol and finally Eosin for 2min. The slides were once again dehydrated with graded alcohol and xylene for cover slipping with xylene based mountant. (Done by Marcus Wai Yean YONG from Institute of Molecular and Cell Biology, A*STAR, Singapore).

2.11. Imaging

For imaging live larvae, tricaine buffered to pH 7.0 at 0.02% was used for anesthesia and mounted in 0.8-2% low melting agarose. Immunostained embryos were mounted in 80 to 100% glycerol and cryosectioned samples were mounted with Vectashield. Images were taken using Leica MZ16FA, Zeiss AxioImager M2, Olympus Fluoview Confocal (Multi-photon) and Zeiss LSM700 Confocal

(Environmental Chamber). TEM Images were acquired with SIA model 12C high resolution full-frame CCD camera.

2.12. Statistical Analysis

Data analysis was carried out using Matlab software. Two sample t-test was employed to compare two independent populations and determine whether there is statistical evidence that the associated population means are significantly different. Significance level was set at a default value of 5%. (Done by Kok Haur ONG and Dr. Weimio YU from Institute of Molecular and Cell Biology, A*STAR, Singapore).

CHAPTER 3. RESULTS

3. GENERATION OF EPIDERMOLYSIS BULLOSA ZEBRAFISH MODEL

3.1. Epidermolysis Bullosa Simplex (EBS) Zebrafish Model

Epidermolysis bullosa is a heterogeneous group of genetic diseases characterized by blistering of the skin for which there is no cure. It is mostly caused by dominant-negative mutations in either *KRT5* or *KRT14* genes. In human EBS, the most commonly mutated amino acid residue in keratins is arginine at position 125(R125) which is located at the helix initiation motif of human KRT14 (Figure 11). This mutation perturbs duplex formation and results in epidermolysis bullosa simplex in humans, characterized by aggregates in the cytoplasm of the cell (Szeverenyi et al., 2008).

3.1.1. Human KRT14 and Zebrafish Krtt1c19e have conserved domains in the helix initiation motif

To establish a zebrafish model of EB, I looked to introduce the KRT14 (R125) mutant gene into the basal keratinocytes. I also attempted to make the equivalent mutation in an endogenous basally expressed keratin, Krtt1c19e. The sequence alignment between human KRT14 and zebrafish Krtt1c19e shows a conserved region where arginine is located at position 124 (Arg124) in zebrafish Krtt1c19e (Figure 12).

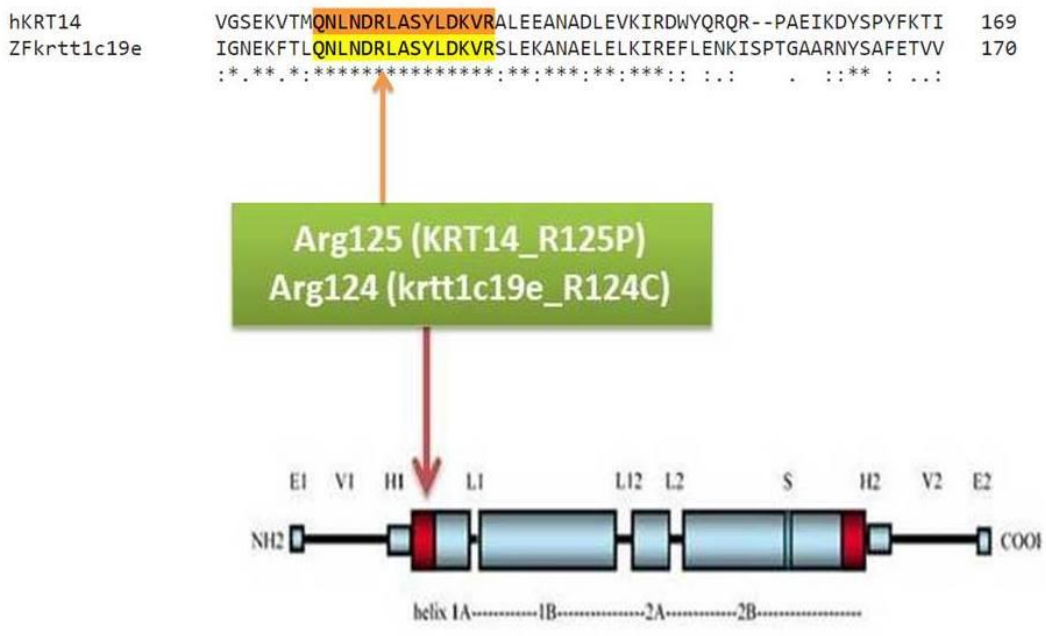

Figure 12: Diagram of intermediate filament protein domain structure

Diagram illustrating sequences of the conserved domain at the helix initiation motif of human KRT14 and Zebrafish Krtt1c19e, the helix initiation motif is conserved, as is the arginine at position 125 in human KRT14 and 124 in zebrafish Krtt1c19e.

In this present study, to generate epidermolysis bullosa simplex (EBS) zebrafish model, zebrafish *krtt1c19e* was used as a promoter which is predominantly expressed in the basal keratinocytes (R. T. Lee et al., 2014). A point mutation was introduced to human KRT14 (KRT14_R125P) and zebrafish Krtt1c19e (Krtt1c19e_R124C), where the amino acid arginine is changed to proline and cysteine, respectively (Figures 13 A).

3.1.2. Generating transgenes and transgenic zebrafish lines

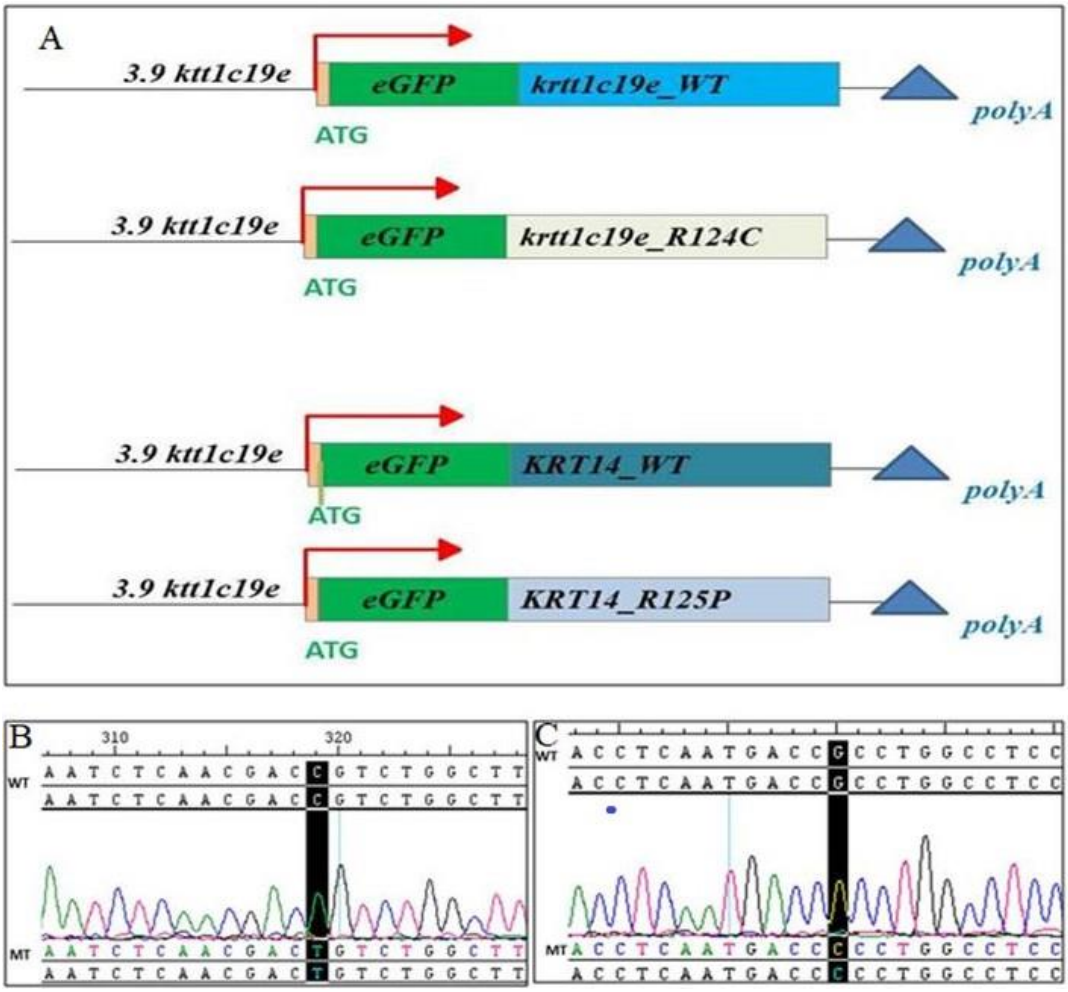

Figure 13: Generating transgenes to establish epidermolysis bullosa simplex in zebrafish:

(A) Zebrafish *krtt1c19e* promoter driving expression of human keratins (KRT14 _WT and KRT14 _R125P) and zebrafish keratins Krtt1c19e_WT and Krtt1c19e_R124C) tagged with enhanced green fluorescent protein. (B) Sequence of human *KRT14_WT* and *KRT14_R125P*, the point mutation indicated was checked by sequencing where Guanine (G) is replaced by cytosine(C) and results the change in amino acid residue, arginine(R) to proline (P). (C) Sequence of zebrafish *krtt1c19e_WT* and *krtt1c19e_R124C*, the point mutation indicated was checked by sequencing where cytosine(C) is replaced by thymine (T) and results the change in amino acid residue, arginine(R) to cysteine(C).

All the transgenes used were tagged with enhanced green fluorescent protein (eGFP) at their N-terminus region as indicated (Figure 13A). Expression of eGFP on the skin of zebrafish larvae was used for screening founders and F1 generations after 3dpf (Figure 14). To confirm that the expression of eGFP is in the basal keratinocytes, I performed a co-immunostain for eGFP and ΔNp63 at 3dpf. eGFP positive cells showed nuclear expression of ΔNp63 (specific to basal keratinocytes) (Figures 15 B & C).

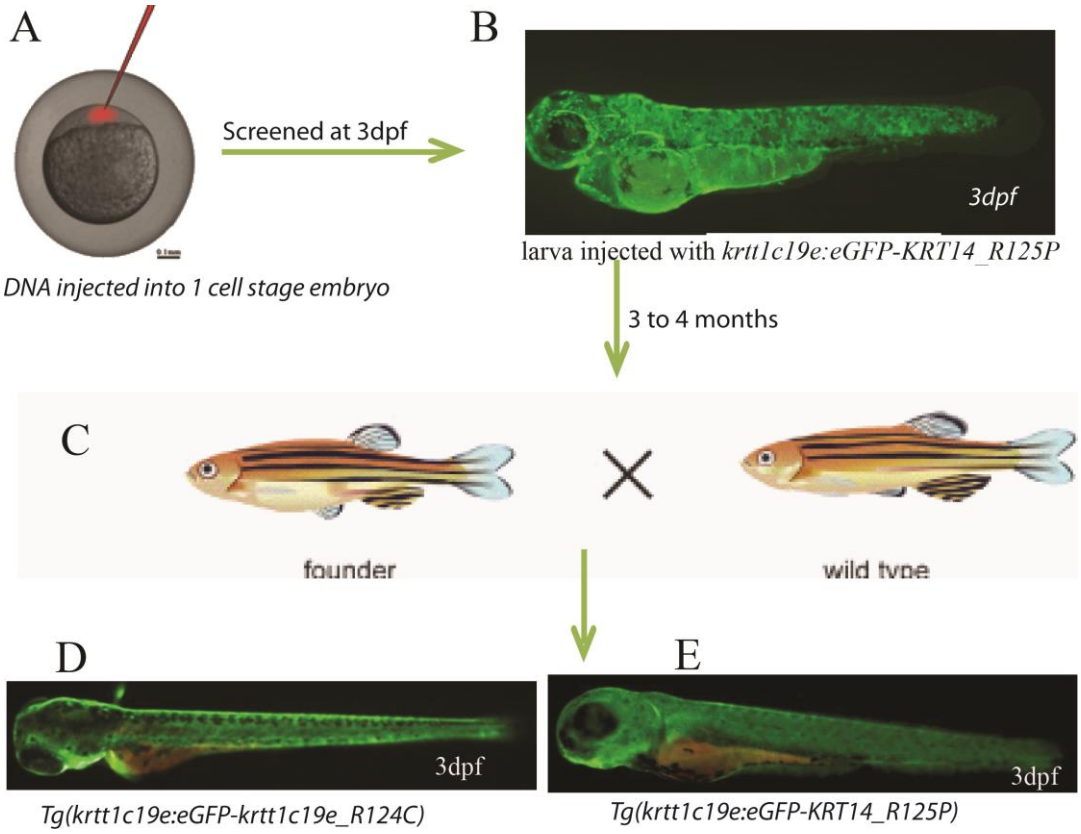

Figure 14: Injection of transgenes into zebrafish to generate epidermolysis bullosa simplex (EBS) zebrafish model

(A) Image showing injection of plasmid construct at one cell stage. (B) eGFP expression in epidermis of 3dpf zebrafish larva injected with *krtt1c19e:eGFP-KRT14_R125P*, (C) At 3 to 4 months of age, potential founders were out crossed with wild type to screen for

stable transgenic lines. (D) Image of transgenic larvae indicating eGFP expression in the basal keratinocytes Krtt1c19e_R124C at 3dpf. (E) Image of transgenic larva indicating eGFP expression in the basal keratinocytes KRT14_ R125P at 3dpf.

To establish epidermolysis bullosa simplex zebrafish model, 30ng/µl DNA construct and 30 ng/µl transposase mRNA (Tol2) were mixed and co-injected into one cell stage zebrafish embryos using a micro injector. About 0.5nl of the mixture was injected directly into the yolk or cell. Three days after injection, embryos were examined for eGFP expression by fluorescent dissecting microscopy. In each transgene, I observed variable number of injected embryos showing eGFP expression in the epidermis and I screed embryos with a broad eGFP expression. These are raised to adulthood.

After three months, these were screened for founders (F0) by incrossing and examining offspring again for broad eGFP expression. F1 embryos were screened by fluorescent expression (eGFP). In some of the transgenics, I noticed that eGFP expression was in the EVL cells as well as basal keratinocytes, and I was able to identify founders with specific eGFP expression in the basal keratinocytes and these were raised and used as stable transgenic lines for each transgene.

The stable transgenic lines were named as; *Tg(krtt1c19e:eGFP-KRT14_WT)* and *Tg(krtt1c19e:eGFP-KRT14_R125P),* and zebrafish transgenic lines *Tg(krtt1c19e:eGFP-krtt1c19e_WT)* and *Tg(krtt1c19e:eGFP-krtt1c19e_R124C)*

(Figure 14). Thereafter, these are referred to as KRT14_WT, KRT14_R125P, Krtt1c19e_WT and Krtt1c19e_R124C.

3.1.3. Confocal analysis of transgenic lines generated by overexpression of zebrafish and human keratins

To examine our stable transgenic fish lines, I used immunofluorescent staining and confocal imaging. Three regions of the transgenic larva were assessed at different stages of development for any epidermolysis bullosa simplex phenotype. As shown below (Figure 15 A) I used the head, trunk and tail area to obtain images for comparison. All three regions expressed similar levels of eGFP. The images shown (Figure 15 B & C) were taken from the head region for cellular and subcellular level comparison.

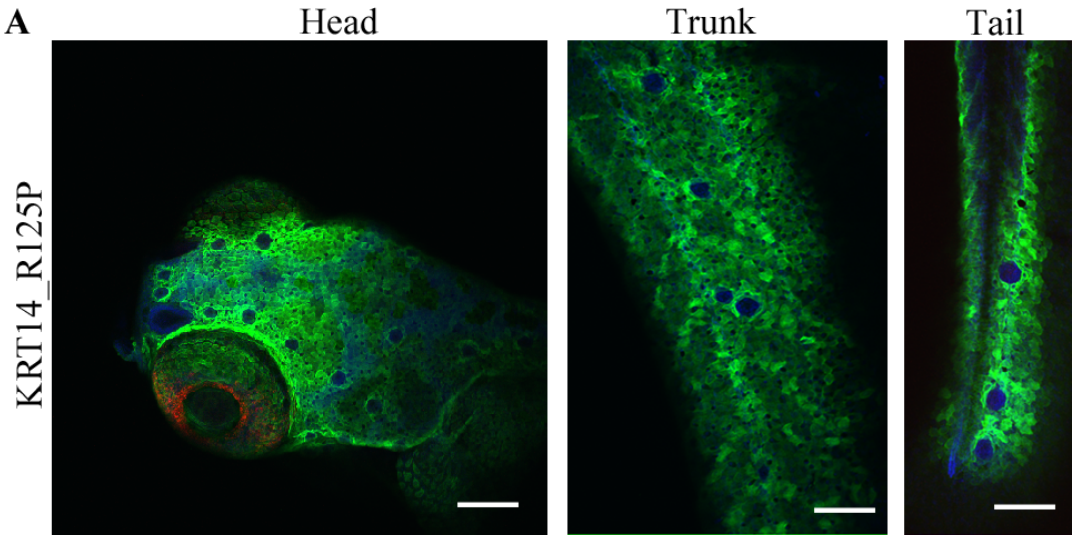

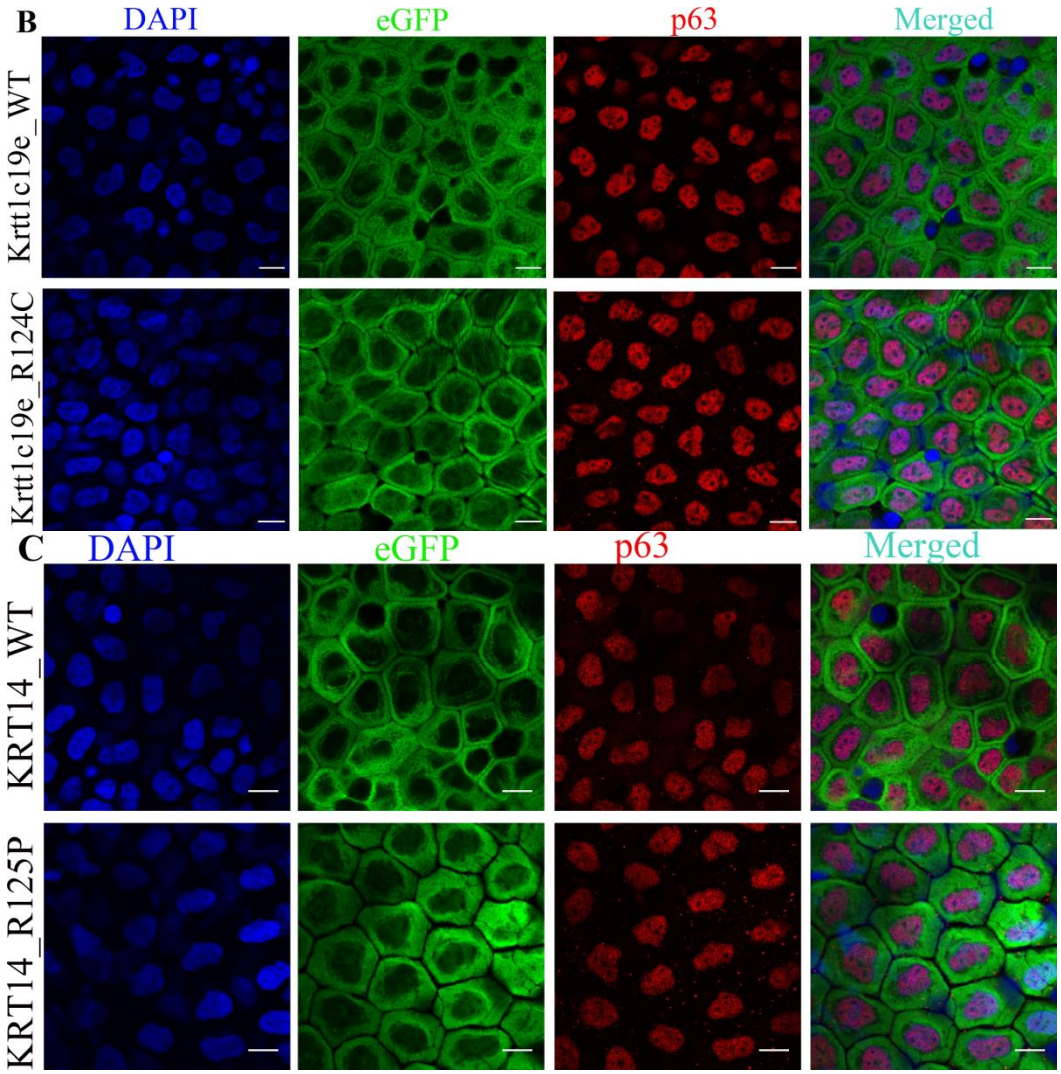

Figure 15: Confocal analysis on transgenic lines generated by overexpression of zebrafish and human keratins:

(A) Examining transgenic zebrafish expressing human KRT14_R125P for possible blistering phenotype at different parts of the body. Images taken with 10x objective lens, (B & C) Immunofluorescence image of Krtt1c19e_WT, Krtt1c19e_R124C, KRT14_WT and KRT14_R125P under normal/unstressed condition: DAPI (blue nucleus), eGFP (Green cytoplasm) and ΔNp63 (Red staining the nucleus) positive basal keratinocytes captured together at 16dpf. All images displayed Images shown (B and C) were obtained with a 100xOil objective lens (Olympus). Bars = 100µm (A), 10µm (B, C).

I used immunofluorescent staining of ΔNp63 and eGFP to demonstrate that the keratins are expressed in the basal cells and indicating that all eGFP positive cells

are ΔNp63 positive basal keratinocytes (Figure 15 B & C). In order to compare any difference in cell organization, all images in figure 15 were taken at the same confocal plane using the center of the nucleus a reference point.

For all zebrafish transgenic lines, I checked for any cellular phenotype of the basal keratinocytes from 3dpf to adult stage and I used 5dpf and 16dpf. Here I presented immunofluorescent images taken from zebrafish larvae at 16dpf. Confocal analysis of the immunostained zebrafish line for *Tg(krtt1c19e:eGFP- krtt1c19e_WT* and *KRT14_WT)* revealed that the basal keratinocytes expressing eGFP tagged wild type zebrafish and human keratins showed no global visible defects in keratin architecture (Figure 15 B & C).

However, basal cells expressing mutant keratins (Krtt1c19e_R124C and KRT14_R125P) displayed a smoother keratin network than that of the wild type keratins which appeared more diffuse, with less evidence of keratin bundles. Additionally, the basal cells in the transgenic fish expressing wild type zebrafish and human keratins seems tightly connected to each other, while in the transgenic fish expressing mutant zebrafish and human keratins, visible gap among cells was observed (Figure 15).

Cryosection of transgenic zebrafish expressing wild type and mutant zebrafish and human keratins

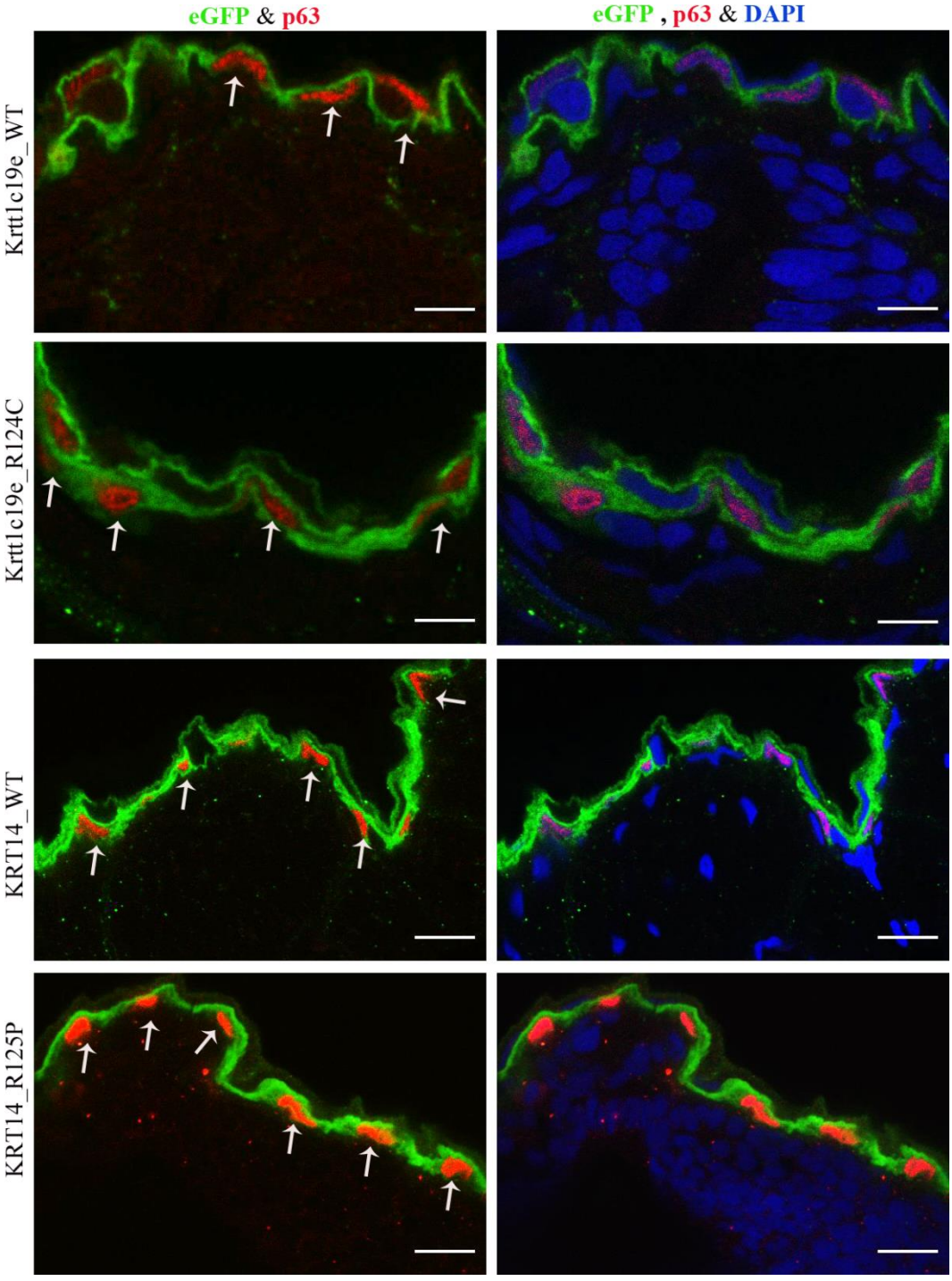

Figure 16: Cryosection of zebrafish skin overexpressing zebrafish and human keratins

Cryosections of basal keratinocytes overexpressing eGFP tagged wild type and mutant zebrafish Krtt1c19e and human KRT14. In all cases, eGFP positive cells have ΔNp63

positive nuclei captured at 16dpf (white arrow). All images shown here were obtained with a 100xOil objective lens (Olympus). Bars= 25μm

I performed cryosection to confirm our overexpression of eGFP tagged wild type and mutant keratins was specific to basal cells (Figure 16). eGFP expressing cells had ΔNp63 positive nuclei, and this can be considered basal. In addition, I examined cryosections for any blistering phenotype between the dermis and the epidermis of the zebrafish skin in the mutant expressing transgenics. As shown in figure 16, no visible defect was observed in which this section was done at normal condition.

3.1.4. Cellular and subcellular characterization of epidermolysis bullosa simplex zebrafish model

Given that we suspected a mild change in keratin architecture in the mutant keratins as visualized by eGFP tag, we employed computational method to quantify the difference in keratin architecture, shape of basal cells and cell adhesion defects between the wild type and mutant keratins. Representative images were segmented using ImageJ and analyzed using Matlab software.

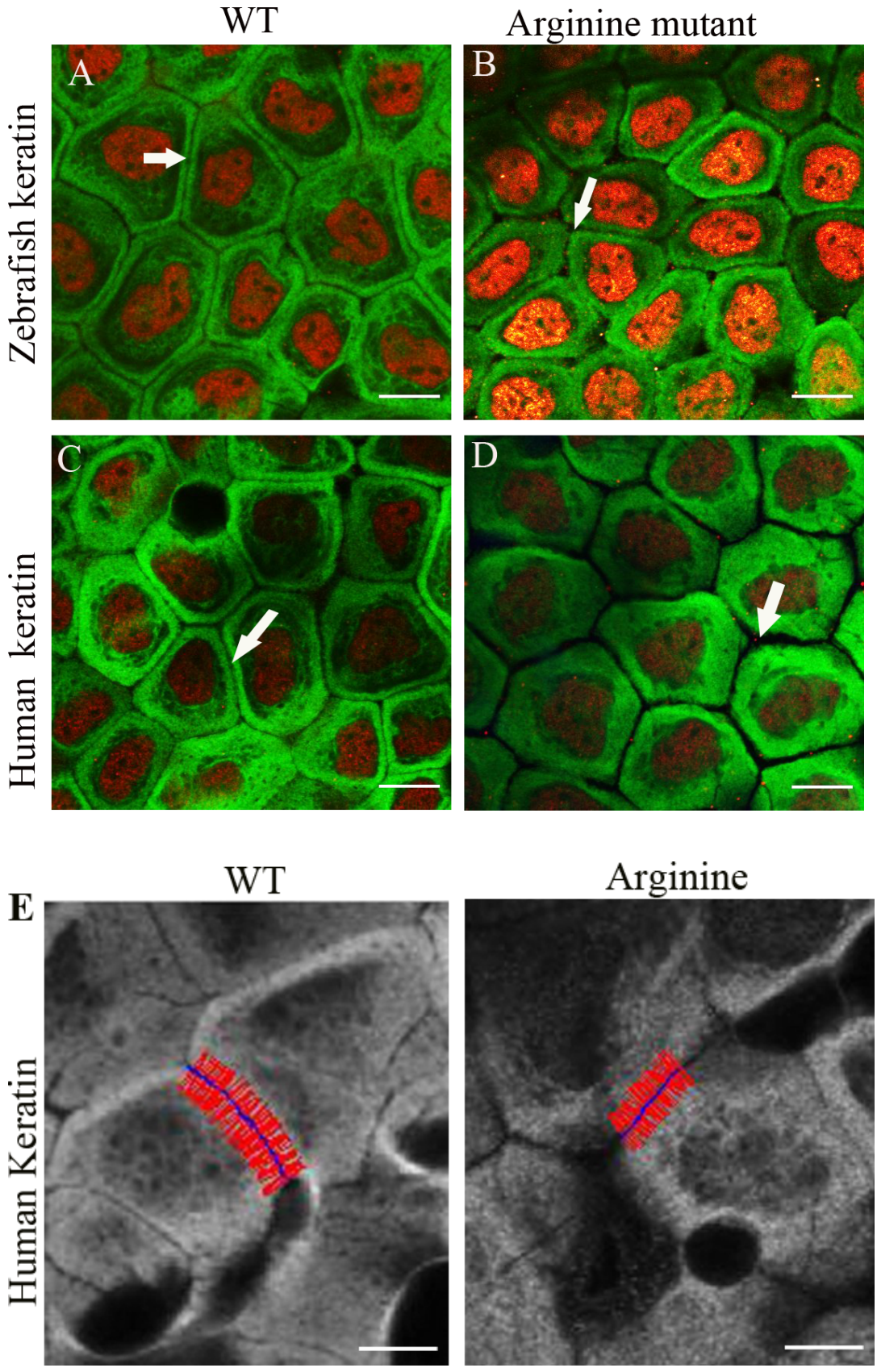
WT
Arginine mutant
A
B
Zebrafish keratin
C
D
Human keratin
E
WT
Arginine
Human Keratin

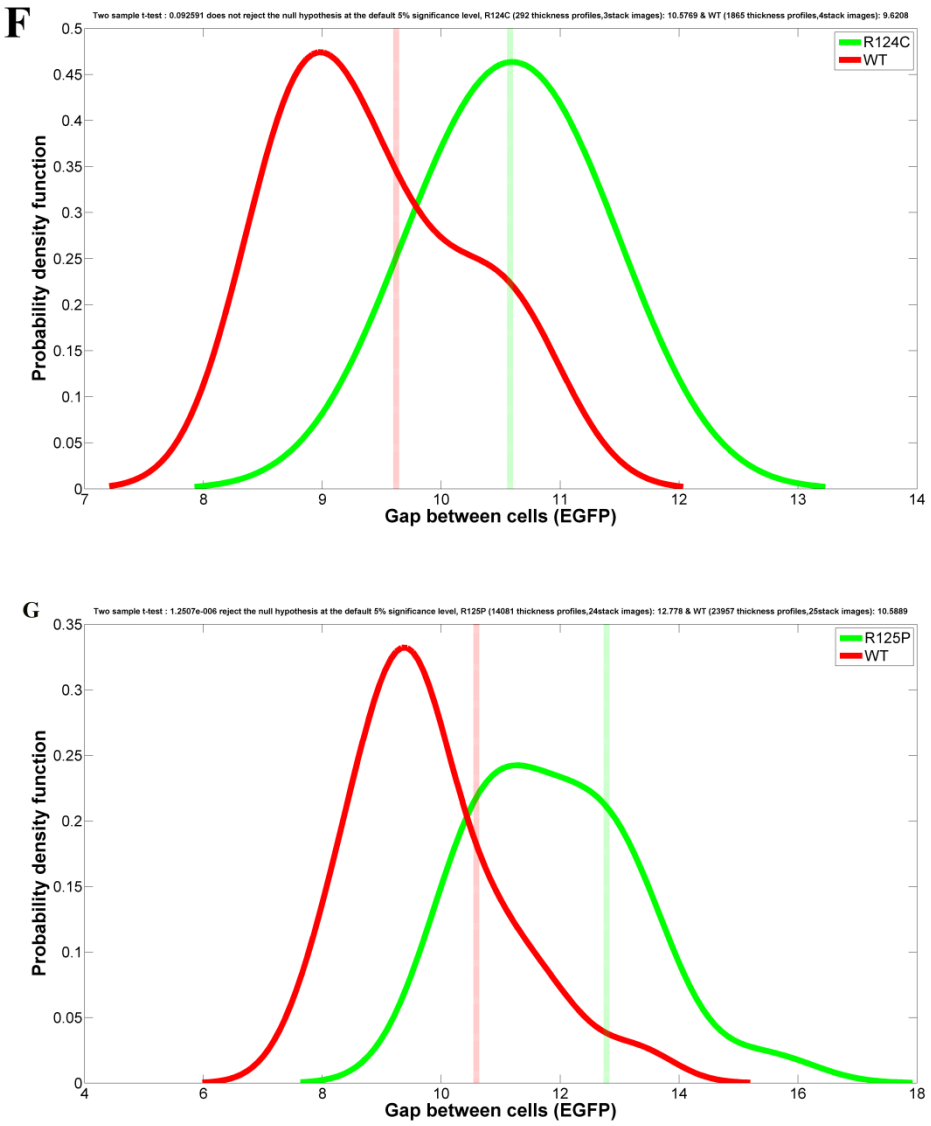

Figure 17: Cellular and subcellular characterization of EBS zebrafish model

(A) Transgenic zebrafish expressing Krtt1c19e_WT at 16dpf, (B) Transgenic zebrafish expressing Krtt1c19e_R124C at 16dpf, (C) Transgenic zebrafish expressing human KRT14_WT at 16dpf and (D) Transgenic zebrafish expressing human KRT14_R125P at 16dpf: eGFP (Green cytoplasm) and ΔNp63 (Red staining the nucleus) positive basal keratinocytes captured together at 16dpf. White arrow indicating a gap between eGFP signal of basal cells. The X-axis represents gap distance between basal keratinocytes and calculated using a pixel value. The size of the original image is 0.124 μm/pixel. All

images shown here were obtained with a 100xOil objective lens (Olympus). (E) Wild type keratin expressing transgenic line (WT) and ES zebrafish model (arginine mutant), each red line is a profile measuring a distance from the eGFP signal of cell to the neighboring cell. (F) Quantitative analysis of probability of basal keratinocytes gap between eGFP signal of neighboring basal keratinocytes where in wild type keratins (red) is smaller than the mutant keratins (green). (G) Quantitative analysis of probability of basal keratinocytes gap between eGFP signal of adjacent cells where there is a statistically significance difference between the wild type and mutant keratins ($p < 0.001$). All images shown here were obtained with a 100xOil objective lens (Olympus). Bars = 25μm.

In this experiment, we compared a number of basal keratinocytes from zebrafish expressing both zebrafish and human keratins. 47 and 32 basal keratinocytes overexpressing Krtt1c19e_WT and Krtt1c19e_R124C, and 50 and 71 cells overexpressing human KRT14_WT and KRT14_R125P, respectively, were analyzed to determine the gap between basal keratinocytes.

The gap between eGFP signal cells is computed by the number of profiles created using Matlab software (Figure 17 E (red lines)). The difference in cell-cell adhesion (a gap between eGFP signal of neighboring cells) of the wild type keratin expressing transgenics and the EBS zebrafish model is highly statistically significant with a $p<0.0001$ (Figure 17 F & G).

3.1.4.1. Cell adhesion defect in epidermolysis bullosa simplex zebrafish model

In human, EB simplex is characterized by blistering of the epidermis where the site of cleavage is above the basement membrane involving lysis of basal keratinocytes that arises from cell-cell and/or cell-matrix adhesion defects. For example, basal keratinocytes from EBS patient carrying KRT14_R125P revealed weak intercellular adhesion from down regulation of desmosome protein complexes, important to associate neighboring basal cells (Liovic et al., 2009). The keratin intermediate filament network attaches to the intracellular component of hemidesmosomes and stabilizes the connection of basal keratinocytes to the underlying basement membrane (Litjens, de Pereda, & Sonnenberg, 2006). However, mutation in keratin proteins and failure in intermediate filament assembly can give rise to epidermolysis bullosa simplex.

Here in this study, from the confocal images, I noticed that mutant protein expressing cells, had a gap between cells, compared to cells expressing wild type keratins, where the eGFP signal was contiguous from one cell to another. This can be seen in Figure 17 comparing the separation of eGFP signal between cells in the mutant keratin expressing transgenics (Figure 17 B & D) and the wild type keratin expressing transgenics (17 A&C).

If there is a gap between the eGFP signals of neighboring cells, it could mean that cells are detaching from each other or that the keratin network is detaching from the cell junction, or both. To evaluate if the overexpressed dominant negative keratin is causing cell adhesion defects, we used transgenic fish expressing lyn-

tdTomato on the cell membrane of basal keratinocytes and E-cadherin, a component of cell-cell junction to label cell membrane.

3.1.4.2. Examining basal keratinocytes behavior in EBS zebrafish model

The observation that the transgenic fish overexpressing mutant human keratin exhibited a gap between basal keratinocytes led us to examine whether it is due to retraction of keratin intermediate filament networks from the edge of the cell to the center or detachment of cells from each other, or both.

To demonstrate how the gap is formed between eGFP signal of basal cells, I crossed both *Tg*(*krtt1c19e: eGFP-KRT14_WT)* and *Tg*(*krtt1c19e: eGFP-KRT14_R125P*), with *Tg(krtt1c19e:lyn-tdtomato*) zebrafish to obtain a double transgenic fish in which keratin intermediate filaments of basal keratinocytes are labeled by eGFP (Green) and cell membrane of basal keratinocytes are labeled by tdTomato (Red).

In order to examine the behavior of basal keratinocytes and determine the gap noticed in EBS zebrafish model, I incubated 5dpf double transgenic larva at 18 ^{0}C for one hour. Immediately after incubation (cold treatment), the double transgenic larva was fixed and immunofluorescent staining was performed using antibodies against eGFP and DsRed.

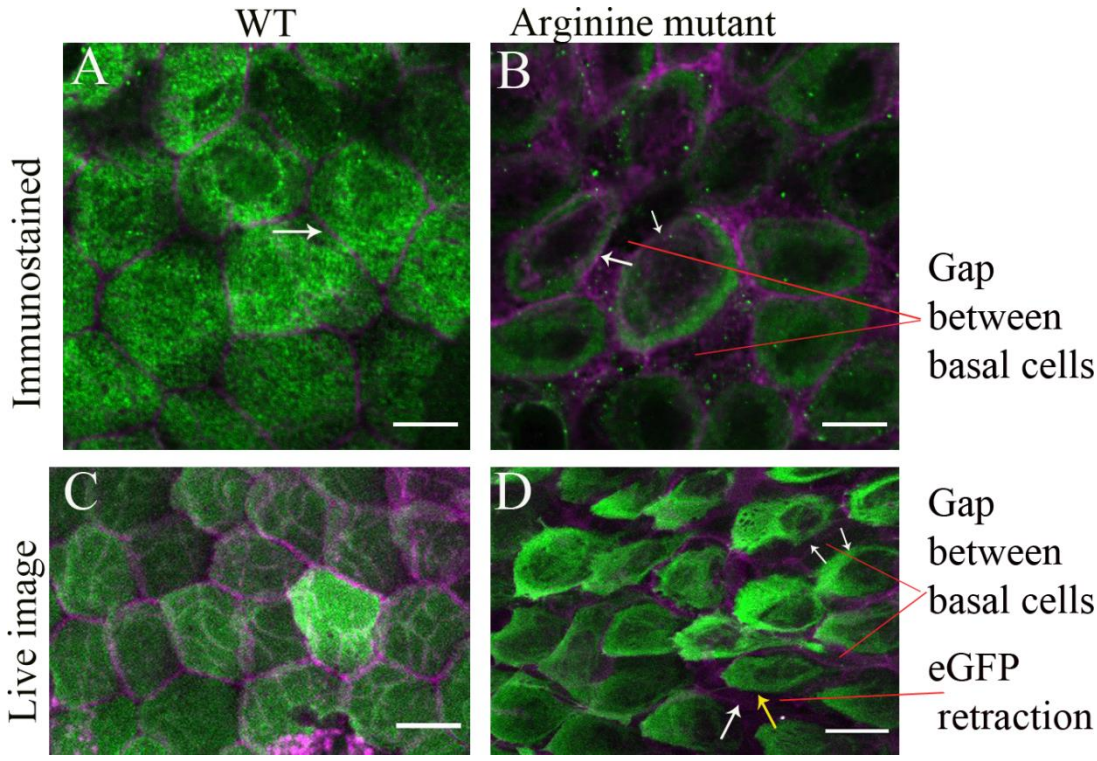

Figure 18: EBS zebrafish model subjected to cold shock showing adhesion defects in basal keratinocytes

Confocal image of basal keratinocytes obtained from the head region of double transgenic zebrafish *Tg(krtt1c19e:lyn-tdtomato;krtt1c19e:eGFP-KRT14_WT)* and *Tg(krtt1c19e:lyn-tdtomato;krtt1c19e:eGFP-KRT14_R125P)* at 5dpf. In both transgenic zebrafish expressing wild type and mutant human keratins, (A & B) Immunostaining was performed using antibody DsRed against lyn-tdTomato (white arrow) and the live image was taken from a z-stack of multiple planes and projected into a single image for better visualization and comparison of the gap. (C & D) Live Images showing keratin intermediate filaments of basal keratinocytes expressing eGFP (Green cytoplasm) and basal keratinocytes expressing lyn-tdTomato which is a membrane protein as indicated (violet). Cell membrane labeled by tdTomato (white arrow) and edge of eGFP signal of basal cells (yellow arrow). In the EBS zebrafish model detachment of basal keratinocytes and eGFP retraction from the membrane was observed when subjected to cold shock stress. Bars = 25µm.

The fluorescent staining showed that the eGFP and lyn-tdTomato signal of the basal cells of the double transgenic larva expressing wild type human keratin

remained contiguous, however a gap between neighboring basal keratinocytes expressing mutant human keratin was observed as indicated in figure 17, suggesting that the detachment of basal cells in EBS zebrafish model.

Whilst, the live image of the double transgenic larva overexpressing wild type human keratin, showed tightly connected basal keratinocytes and no gap between eGFP signal of basal cells and from eGFP to lyn-tdTomato within cells was observed before and after cold treatment. In contrast, the double transgenic line overexpressing mutant human keratin exhibited change in cell morphology and notable gap between and within the basal cells after cold stress. Thus, detachment of neighboring basal keratinocytes and gap between eGFP signal and lyn-tdTomato of basal cells was observed in EBS zebrafish model (Figure 18 D).

E- Cadherin

E-cadherin is a membrane protein involved in cell-cell adhesion mechanism. Intracellularly, E-cadherin interacts with the actin microfilaments and associate neighboring cells (Takeichi, 1988). To assess the cell adhesion of basal keratinocytes of the transgenic lines overexpressing wild type and mutant zebrafish and human keratins, I performed E-cadherin staining and performed quantification analysis.

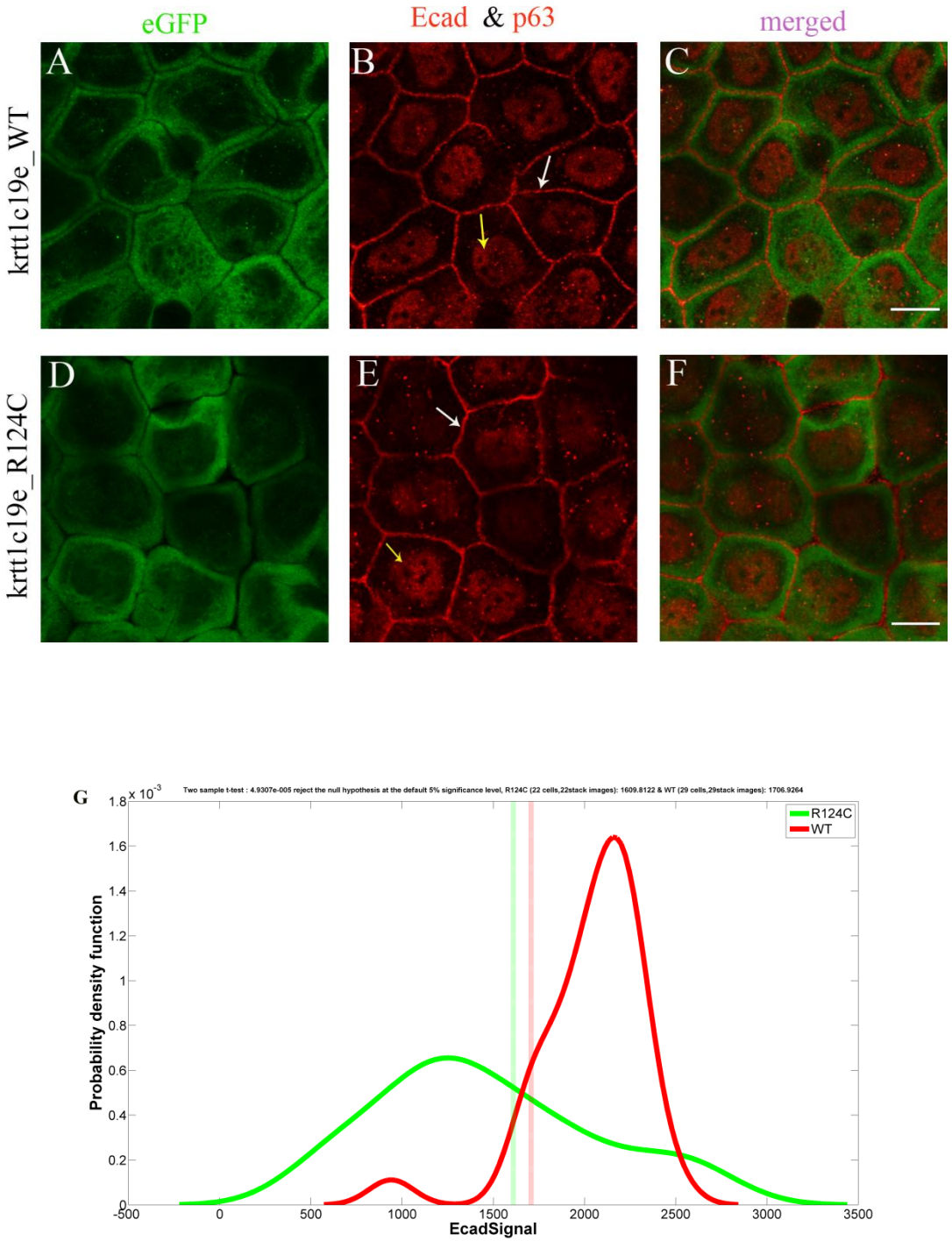

Figure 19: Analysis of immunofluorescent images of E-cadherin expression in wild type and mutant keratin expressing zebrafish transgenic lines

eGFP (green) cytoplasm, E-cadherin and ΔNp63 (red) staining the membrane (white arrow) and nucleus (yellow arrow) of basal keratinocytes, respectively. (A, B & C) Transgenic line expressing Krtt1c19e_WT immunostained against eGFP, E-cad and

ΔNp63 at 16dpf, (D, E & F) Transgenic line expressing Krtt1c19e_R125C immunostained against eGFP, E-cad and ΔNp63 at 16dpf, (G) Quantification analysis of E-cad signal, showing no statistical difference between the wild type (red) and the mutant keratin (green) ($p>0.05$). All images shown here were obtained with a 100xOil objective lens (Olympus). Bars = 25μm.

As shown in figure 19, basal keratinocytes overexpressing Krtt1c19e_WT are contiguous to each other as compared to the basal cells overexpressing Krtt1c19e_R124C. To determine E-cadherin signal of the basal keratinocytes, we compared 29 and 22 cells overexpressing wild type and mutant zebrafish keratins, respectively. No statistically significant difference in E-cadherin signal was found between the basal cells overexpressing wild type and mutant zebrafish keratin.

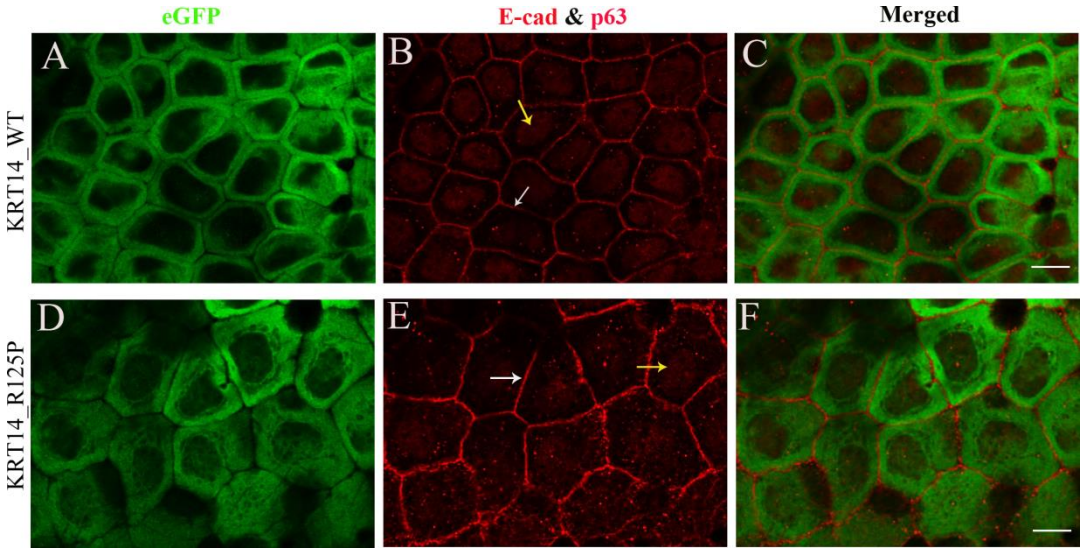

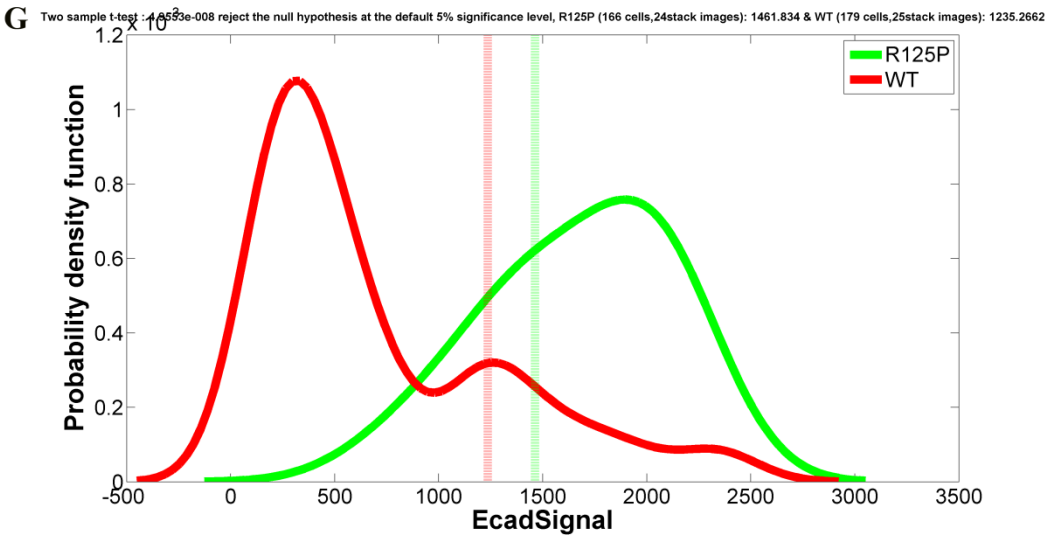

Figure 20: Analysis of immunofluorescent images of E-cadherin expression in wild type and mutant human keratin expressing zebrafish transgenic lines

eGFP (Green) cytoplasm, E-cadherin and ΔNp63 (red) staining membrane (white arrow) and nucleus (yellow arrow) of basal keratinocytes, respectively. (A, B & C) Transgenic line expressing human KRT14_WT immunostained against eGFP and E-cadherin at 16dpf, (D, E & F) Transgenic line expressing human KRT14_R125P immunostained against eGFP and E-cad at 16dpf, (G) Quantification analysis of E-cad signal, describing the intensity of E-cadherin on the boundary of the basal cells, showing E-cadherin signal is higher in the mutant keratin (Green) than the wild type (red) with a statistically significant difference ($p<0.05$). All images shown here were obtained with a 100xOil objective lens (Olympus). Bars = 25μm.

Conversely in the transgenic lines expressing human keratins, basal keratinocytes are again tightly connected to each other in the transgenic line overexpressing wild type human KRT14 as compared to the transgenic line overexpressing human KRT14_R125P which seem to have a gap between the adjacent cells (Figure 20).

To determine E-cadherin signal, we compared 179 and 166 cells from zebrafish expressing wild type and mutant human keratin, respectively. Accordingly, basal

cells overexpressing mutant human KRT14 have high E-cadherin signal as compared to basal cells overexpressing wild type human KRT14 with statistically significant difference ($p<0.05$) as indicated in figure 20 G.

3.1.4.3. Shape of basal cells

Our imaging indicated that in addition to separation between the cells, cells of mutant transgenics had a less polygonal shape and were more rounded. We analyzed the area, curvature and circularity of cells in the wild type and mutant fish using Matlab as shown (Figure 20 and 21).

Circularity

To appreciate the difference in shape resulted by the overexpression of dominant negative keratins, circularity and curvature of the basal keratinocytes of the head area were compared. Circularity is used in image analysis to sort or identify objects. A useful measure of circularity compares two objects so that the outcome does not depend on size or units. Circularity is calculated as four times pi times the area divided by the perimeter squared: $C = 4\pi A/P^{2,}$ where C is the circularity, A is the area and P is the perimeter. A circle will have a C value of 1, whilst less circular shapes will be less than 1.

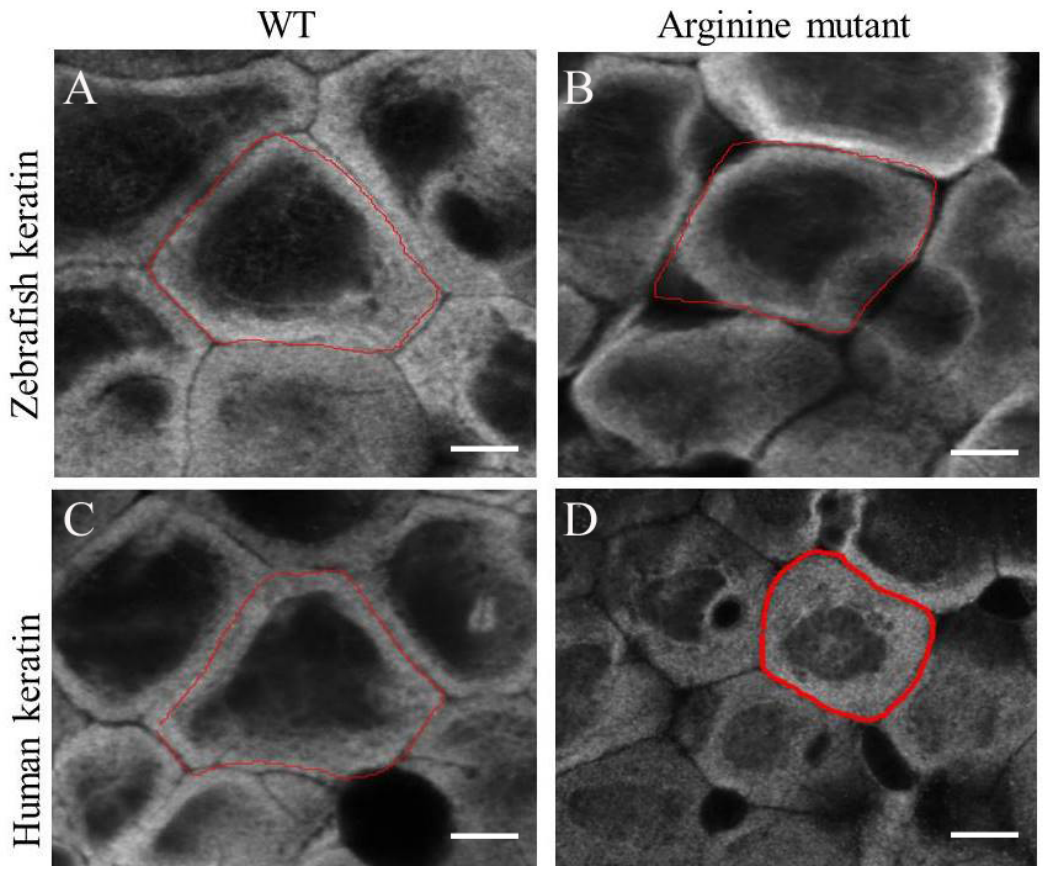
WT
Arginine mutant
A
B
C
D
Zebrafish keratin
Human keratin

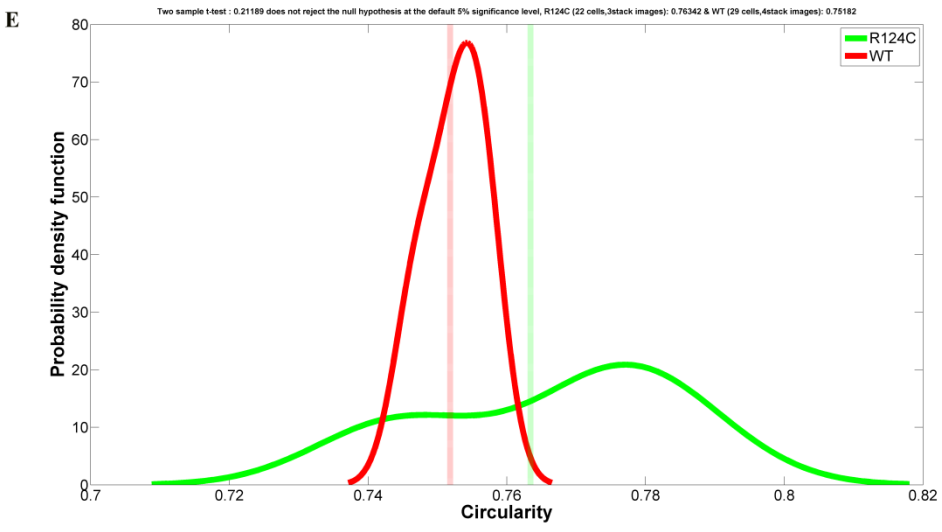
E
Two sample t-test : 0.21189 does not reject the null hypothesis at the default 5% significance level, R124C (22 cells,3stack images): 0.76342 & WT (29 cells,4stack images): 0.75182
R124C
WT
Probability density function
Circularity
0
10
20
30
40
50
60
70
80
0.7
0.72
0.74
0.76
0.78
0.8
0.82

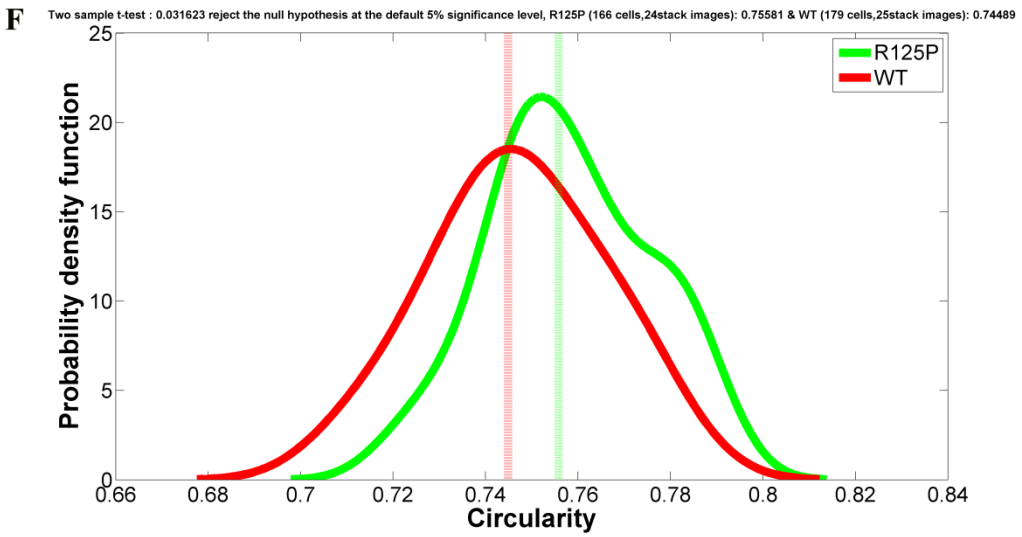

Figure 21: Circularity of basal keratinocytes overexpressing zebrafish and human keratins

Cells circumscribed by red path in both wild type and mutant transgenics, and zebrafish and human keratins are examples to compare and showing how we segmented them for computing circularity.(A) transgenic line expressing Krtt1c19e_WT at 16dpf, (B) transgenic line expressing Krtt1c19e_R124C at 16dpf, (C) transgenic line expressing KRT14_WT at 16dpf, (D) transgenic line expressing KRT14_R125P at 16dpf, (E) Quantitative analysis of probability of basal cells circularity expressing Krtt1c19e _WT (Red) and Krtt1c19e_R124C (Green) showing no difference. (F) Quantitative analysis of the probability of basal keratinocytes circularity expressing KRT14_WT (Red) and KRT14_R125P (Green) indicating statistically significant difference ($p<0.05$).

Circularity of 29 wild type and 22 mutant keratin expressing basal cells, respectively, were compared for the zebrafish transgenic lines overexpressing zebrafish keratins. No statistical significant difference was found ($p>0.05$) (Figure 21 A,B & E). In contrast, a statistical significant difference ($p<0.05$) was found when we compare 179 basal cells from transgenic zebrafish expressing wild type human keratin and 166 basal cells from EBS zebrafish model, with the basal cells

expressing mutant human keratin more rounded or circular than those basal cells expressing wild type human keratin as shown (Figure 21 C, D & F).

Curvature

The curvature is used to describe how sensitive its tangent line is to moving one point to a nearby point. A straight line is defined as zero curvature. To determine the curvature of the perimeter of basal cells from transgenic zebrafish expressing wild type and mutant keratin proteins from human and zebrafish, we used a mathematical formula as follows

2D plane curve with Cartesian coordinate, $\gamma(t) = \big(x(t), y(t)\big)$,

$$k = \frac{|x'y'' - y'x''|}{(x'^2 + y'^2)^{\frac{3}{2}}}$$

Where k sign > 0 represent the counterclockwise and < 0 represent the clockwise. The primes indicate the derivative with respect to the parameter t. The standard of curvature is used to describe the standard deviation of curvature in each cell. In the final results, mean of standard of curvature (CurvatureStd) and their distribution for wild type and mutant fish was computed respectively.

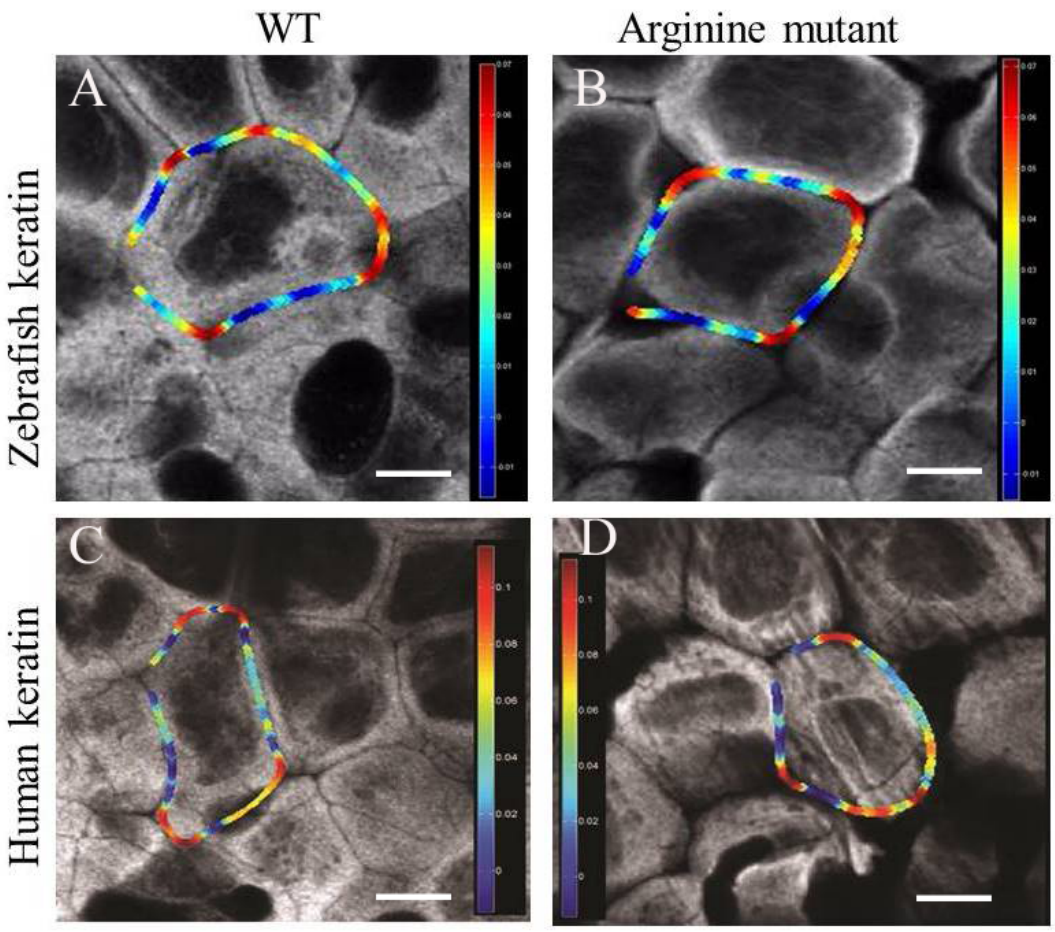
WT
Arginine mutant
Zebrafish keratin
Human keratin
A
B
C
D

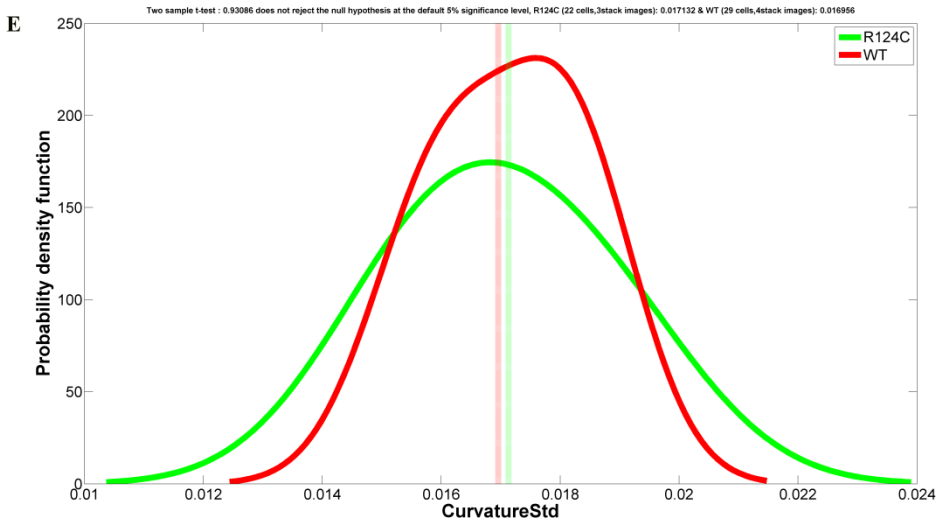
E
Two sample t-test : 0.93086 does not reject the null hypothesis at the default 5% significance level, R124C (22 cells,3stack images): 0.017132 & WT (29 cells,4stack images): 0.016956
R124C
WT
Probability density function
CurvatureStd
0
50
100
150
200
250
0.01
0.012
0.014
0.016
0.018
0.02
0.022
0.024

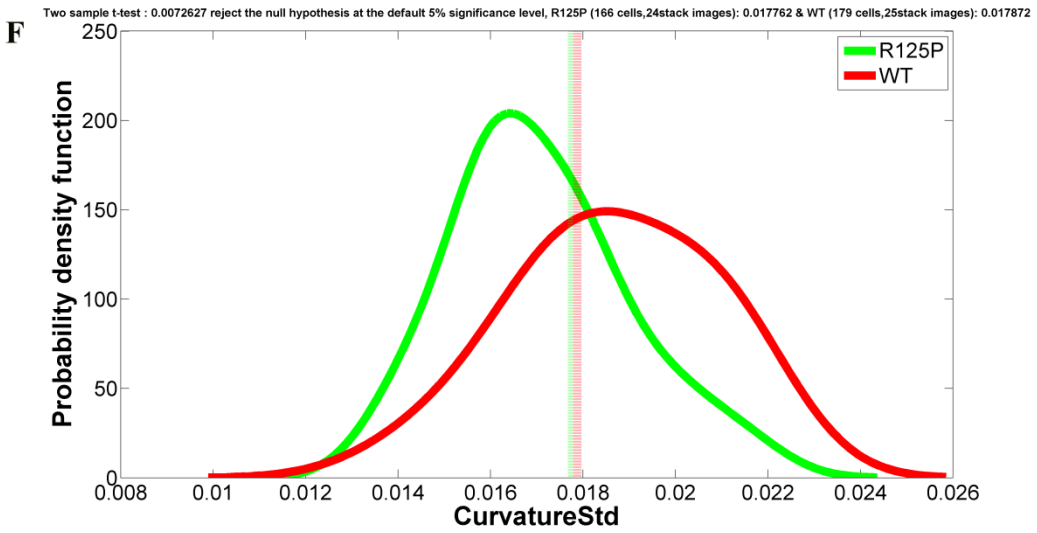

Figure 22: Curvature of basal keratinocytes overexpressing zebrafish and human keratins

Cells bounded by different colors in both wild type and mutant, and zebrafish and human keratins showing measurement of the curvature of individual basal keratinocytes. (A & B) Curvature of transgenic lines expressing zebrafish Krtt1c19e _WT and Krtt1c19e_R124C, respectively, (C& D) Curvature of transgenic lines expressing human KRT14_WT and KRT14_R125P, (E) Quantitative analysis of the probability of basal keratinocytes curvature expressing zebrafish keratins showing no statistically significant difference ($p>0.05$), and (F) Quantitative analysis of the probability of basal keratinocytes curvature expressing human keratins showing statistical significant difference between the wild type and mutant human expressing fish lines ($p<0.05$). Bars = 25μm.

We determined the curvature of basal keratinocytes on the head area. Curvature of basal cells (same cells and numbers assed for circularity) were compared for the transgenic lines overexpressing zebrafish keratins and found no difference. In contrast, a statistical significant difference ($p<0.05$) was found when we compare curvature of basal cells of the zebrafish expressing wild type versus mutant human keratins, meaning that the mutant keratin expressing cells are less curved where

they appear circular and rounded than the wild type keratin expressing cells as shown (Figure 22).

3.1.5. Transmission electron microscope analysis of zebrafish skin overexpressing dominant negative zebrafish and human keratins

Wild type and mutant zebrafish and human keratin expressing transgenic lines were analyzed for possible detachment of the epidermis from the basement membrane resulting from the defects in the integrity of keratin networks in the basal keratinocytes. Any defect in the attachment of basal cells to the basement membrane via hemidesmosomes, or in the attachment between adjacent basal cells via desmosomes caused by keratin mutation (Krtt1c19e_R124C and KRT14_R125P) was analyzed.

Ultrathin transverse cross sections were taken from approximately the same area in the mid tail region of transgenic zebrafish embryos overexpressing wild type and mutant human and zebrafish keratins (Figure 23). Electron micrographs of the epidermis, basement membrane and dermis were captured at 4,000X, 10,000X and 40,000X magnifications for transmission electron microscope analysis.

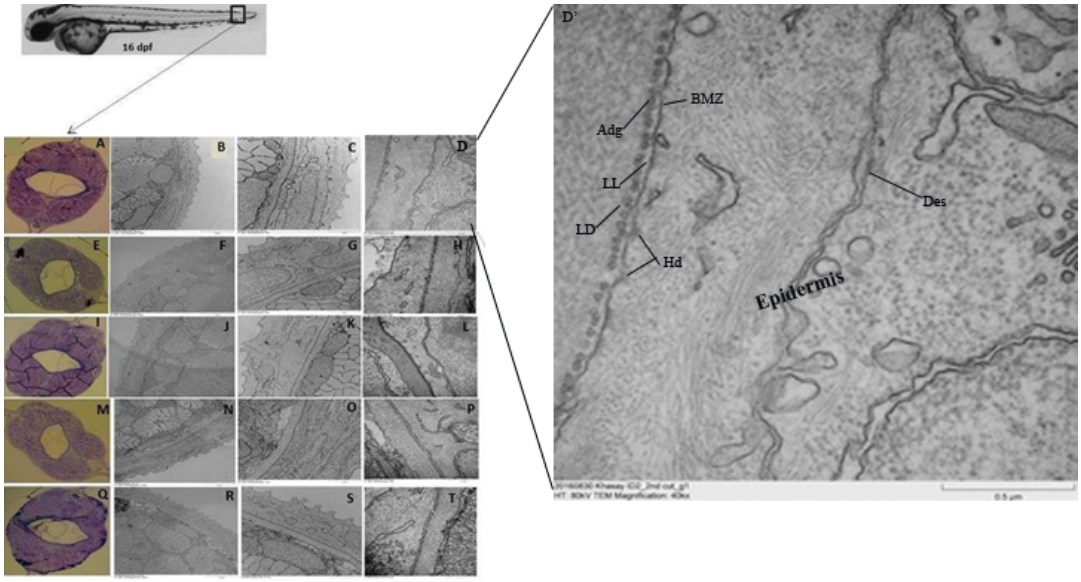

Figure 23: Electron micrograph of zebrafish skin at 16dpf

Detailed ultrastructure of zebrafish skin at original magnification of 4kx (B, F, J, and N &R), 10kx (C, G, K, and O & S), 40kx (D, H, L, P &T), Bar =5 µm, 2 µm and 0.5µm. Ultrathin transverse cross sections were taken from the mid tail region of zebrafish embryos at 16dpf. (A-D) TEM images of wild type fish, (E-H) transgenic zebrafish expressing Krtt1c19e_WT, (I-L) transgenic zebrafish expressing Krtt1c19e_R124C, (M-P) transgenic zebrafish expressing human KRT14_WT and (Q-T) transgenic zebrafish expressing KRT14_R125P, (D') detailed ultrastructure of the zebrafish skin displaying desmosome (Des), hemidesmosomes (Hd), basement membrane zone(BMZ), adepidermal granules (Adg), lamina lucida (LL) and lamina densa (LD).(Done by Qiaohui Yang and Dr. David Liebl from IMB-IMCB joint electron microscopy suite, A*STAR, Singapore)

Electron micrographs taken at 4000x, 10,000x and 40,000x magnification showed the presence of all skin structures including desmosomes between adjacent basal cells, as well as hemidesmosomes. No major difference in the prevalence of these two types of cell junctions in both the wild type and keratin mutants were found. Results of the transmission electron microscope analyses showed no visible defects in the integrity of the attachment of the basement membrane to the epidermis

attributed to overexpression of mutant keratin. No evidence of microblisters was found in all the transgenic zebrafish expressing zebrafish and human keratins.

In an unstressed condition, no obvious difference was noted between transgenic lines expressing zebrafish keratins. However, the transgenic fish harboring mutations in KRT14_R125P showed differences in keratin network distribution, cell adhesion defects and shape of basal keratinocytes as compared to the wild type human keratin expressing transgenic line. To understand the behavior of the basal cells expressing dominant negative keratins and to induce blister formation in the transgenic fish, I exposed them to different stressors known to induce blistering of the skin in EBS patients.

3.1.6. Effect of osmotic stress on keratin intermediate filaments of epidermolysis bullosa simplex zebrafish model

Osmotic shock is physiological stressor due to change in solute concentration around the cell and causes movement of water across the cell membrane. This causes cells to rapidly shrink on hyperosmotic stress or swell on hypoosmotic stress.

To determine the effect of osmotic stress on basal keratinocytes overexpressing both wild type and mutant zebrafish and human keratins, I used E3 medium (5mM NaCl, 0.17mM KCl, 0.33mM $MgCl_2.6H_2O$, 0.33mM $CaCl2.2H_2O$, and pH 7.2) at different dilutions. For this reason, transgenic fish lines of 16dpf were transferred from 1XE3 medium (standard embryo medium) into 0.1X, 0,5X, 2X, 4X, 10X or

20X E3 medium to expose them to hypo-osmotic and hyper-osmotic stress conditions.

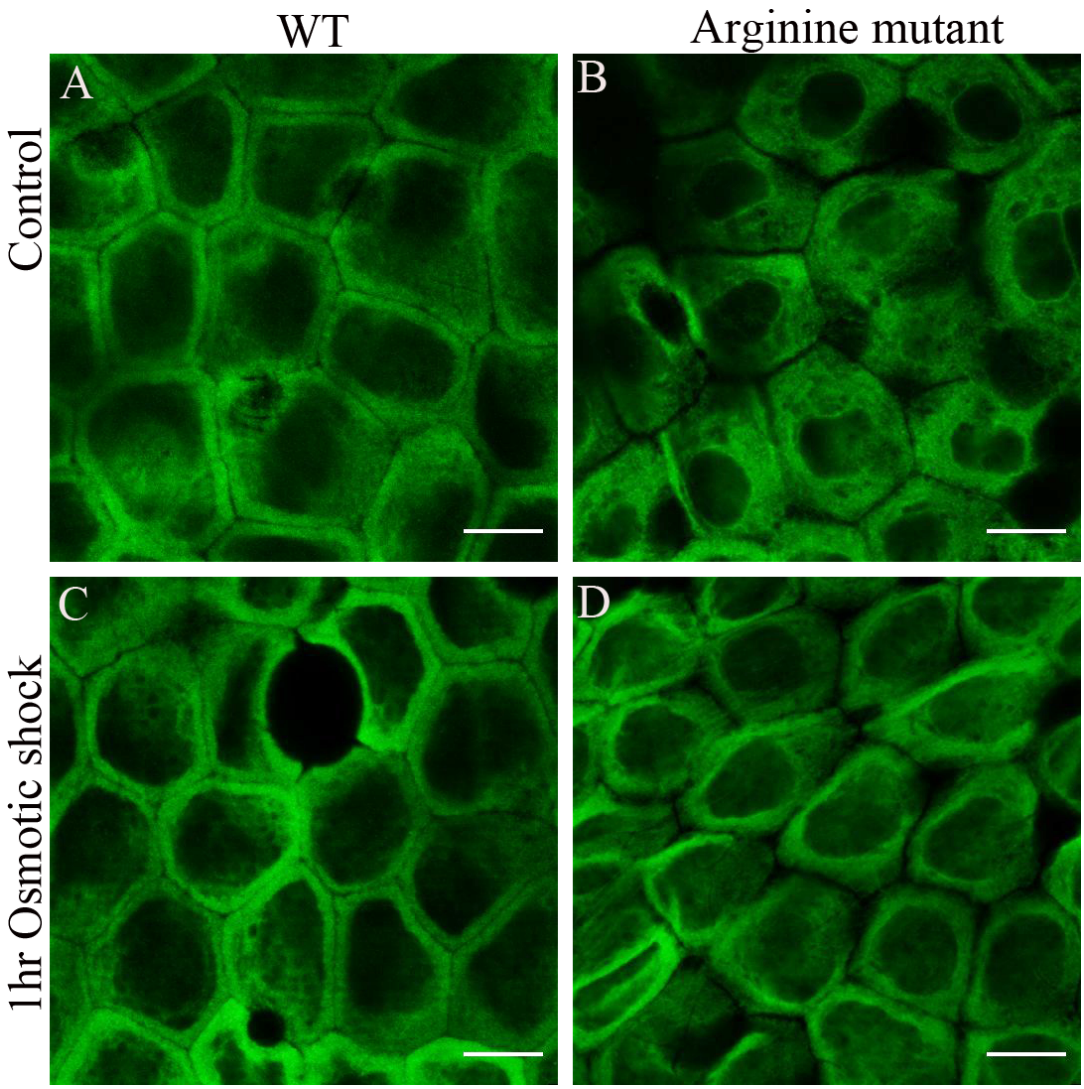

Figure 24: Effect of osmotic shock in epidermolysis bullosa simplex zebrafish model

All transgenic zebrafish lines were subjected to hyper-osmotic shock (4X E3 medium) and immunostained for eGFP after 1 hour incubation. (A) controls zebrafish model overexpressing human KRT14_WT at 16dpf in 1X E3, (B) controls EBS zebrafish model overexpressing human KRT14_R125P at 16dpf in 1X E3, (C) Osmotic shock treated zebrafish overexpressing human KRT14_WT at 16dpf, (D) Osmotic shock treated EBS zebrafish overexpressing human KRT14_R125P at 16dpf. I presented only

basal keratinocytes exposed to 4X E3 medium as a representative image for the reason that, no difference was observed in all the dilutions used and cells analyzed. All images shown here were obtained with a 100xOil objective lens (Olympus). Bars = 25μm.

With the hypothesis that osmotic shock might induce defects in keratin intermediate filament organization or cell shape changes, 16dpf larvae of both transgenic lines were incubated for an hour.

Immediately after osmotic shock, the fish were examined under dissecting scope for global skin phenotypes, then fixed and immunostained against eGFP. No evidence of keratin aggregates or changes in cell structure in all basal keratinocytes overexpressing the wild type or mutant zebrafish or human keratins (Figure 24) was observed.

3.1.7. Heat shock treatment induces keratin aggregate formation in epidermolysis bullosa simplex zebrafish model

In EBS patients, basal keratinocytes breakdown in response to different stress factors. The cells with mutant keratins are susceptible to cytolysis upon mechanical trauma or thermal changes(Coulombe & Omary, 2002) which results in blistering of the skin epidermal layer. I attempted to recapitulate this in the EBS zebrafish model where I incubated the transgenic fish at 40 ^{0}C for an hour to stress the fish and induce EBS related phenotypes. I used two different age groups to perform this experiment; zebrafish at 5dpf and 16dpf for transgenic lines overexpressing both wild type and mutant zebrafish and human keratins. I examined the whole fish larva immediately after treatment (heat shock) using a dissecting scope to visualize any global skin defects. No visible changes were observed in any fish lines. I

employed immunofluorescent to evaluate whether there is any change at cellular and subcellular level in the heat treated fish and respective controls (Figure 25). In both line expressing zebrafish keratins, there was no obvious difference in the keratin intermediate filament network in both transgenic lines expressing Krtt1c19e_WT and Krtt1c19e_R124C after heat shock. The basal cells appear quite similar to the untreated fish line (data not shown).

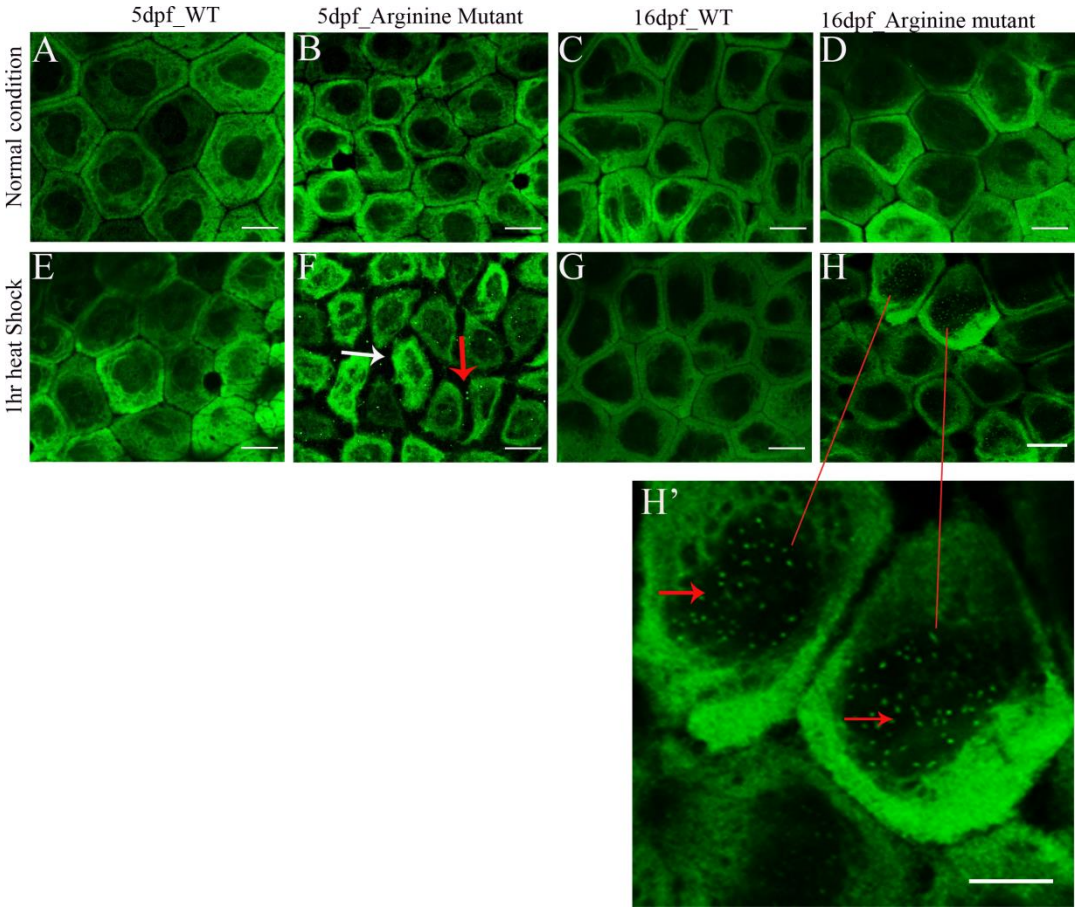

Figure 25: EBS zebrafish model displaying eGFP aggregates and detachment of basal keratinocytes from each other upon heat shock

EBS zebrafish model was treated with heat shock at 40 ^{0}C for one hour to induce EBS related phenotypes. (A) Untreated control of transgenic zebrafish overexpressing human KRT14_WT at 5dpf, (B) Untreated EBS zebrafish overexpressing human KRT14_R125P at 5dpf, (C) Untreated control of transgenic zebrafish overexpressing human KRT14_WT at 16dpf, (D) Untreated EBS zebrafish overexpressing human KRT14_R125P at 16dpf, (E)

Heat treated transgenic zebrafish overexpressing human KRT14_WT at 5dpf, (F) Heat treated EBS zebrafish overexpressing human KRT14_R125P at 5dpf revealing aggregates (red arrow) and detachment of basal keratinocytes from each other (white arrow), (G) Heat treated transgenic zebrafish overexpressing human KRT14_WT at 16dpf, (H & H') Heat treated EBS zebrafish overexpressing human KRT14_R125P at 16dpf showing aggregates in the basal keratinocytes predominantly in the nucleus (red arrows). All images shown here were obtained with a 100xOil objective lens (Olympus). Bars = 10μm (A-H), 50μm (H').

However, following heat shock at 40 ^{0}C for 1 hour a striking phenotype was observed in the zebrafish line overexpressing mutant human keratin (eGFP-KRT14_R125P) proteins in basal keratinocyte, which displayed numerous small eGFP positive aggregates and detachment of basal cells from each other (Figure 25, compare F with B and H & H' with D). At 16dpf, after 30 minutes of heat shock, basal keratinocytes started to show tiny aggregates and the phenotype become increasingly evident after one hour heat treatment. The keratin aggregates in the 16dpf EBS zebrafish model become pronounced within the nucleus (Figure 25 H&H'). Similarly, heat treated basal cells from the 5dpf EBS zebrafish model showed tiny aggregates which was dispersed throughout the cytoplasm (Figure 25D). A total of 65 (at 5dpf) and 159 (at 16dpf) EBS zebrafish model were analyzed using confocal microscopy following heat treatment and antibody staining, 89% (5dpf) and 84% (16dpf) fish were found with mild to severe phenotype.

3.1.8. Cold shock disrupts intermediate filament organization in epidermolysis bullosa simplex zebrafish model

The observation that the humanized fish overexpressing mutant human keratin displayed formation of aggregates and detachment of basal cells upon heat shock in our EBS zebrafish model, led us to use the opposite stressor factor, cold shock. To elucidate whether the mutant keratins are also sensitive to cold temperature, both transgenic fish lines, overexpressing eGFP tagged zebrafish keratins (Krtt1c19e_WT and Krtt1c19e_R124C) and human keratins (KRT14_WT and KRT14_R125P*)* were incubated at 18 ^{0}C for one hour with the hypothesis that cold shock might have an effect of cytoskeletal protein organization.

No global blistering of the skin was observed following examination via dissecting scope immediately after cold shock in either zebrafish lines and I assessed for any change at cellular and subcellular level through immunofluorescence as I did for the heat treated EBS fish. There was no visible effect of cold shock on the zebrafish transgenic lines overexpressing either wild type or mutant zebrafish keratins where both appeared similar at 5dpf and 16dpf (data not shown).

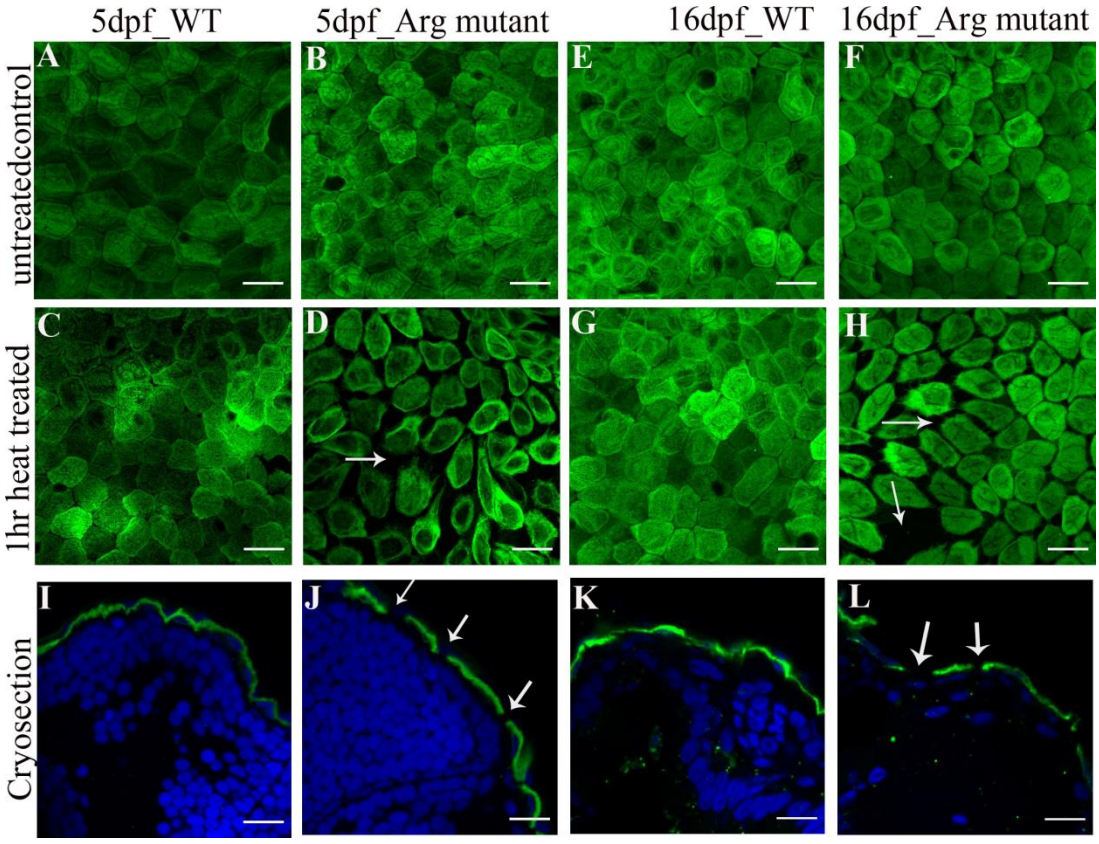

Figure 26: Humanized zebrafish overexpressing mutant human KRT14 showed dramatic alterations in keratin architecture upon cold shock

EBS zebrafish model was treated with cold shock at 18 ^{0}C for one hour to induce EBS related phenotypes. (A) Untreated control of transgenic zebrafish overexpressing human KRT14_WT at 5dpf, (B) Untreated EBS zebrafish overexpressing human KRT14_R125P at 5dpf, (C) Cold treated transgenic zebrafish overexpressing human KRT14_WT at 5dpf, (D) Cold treated EBS zebrafish overexpressing human KRT14_R125P at 5dpf showing a gap between eGFP signal of cells (indicated in white arrow), (E) Untreated control of transgenic zebrafish overexpressing human KRT14_WT at 16dpf, (F) Untreated EBS zebrafish overexpressing human KRT14_R125P at 16dpf, (G) Cold treated transgenic zebrafish overexpressing human KRT14_WT at 16dpf, (H) Cold treated EBS zebrafish overexpressing human KRT14_R125P at 16dpf demonstrating a gap between eGFP signal of basal keratinocytes (indicated in white arrow), (I) Cryosection of cold treated transgenic zebrafish overexpressing human KRT14_WT at 5dpf, (J) Cryosection of cold treated EBS zebrafish overexpressing human KRT14_R125P at 5dpf presenting a gap between eGFP signal of cells (indicted in white arrow), (K) Cryosection of cold treated transgenic zebrafish overexpressing human KRT14_WT at 16dpf, (L) Cryosection of cold treated

EBS zebrafish overexpressing human KRT14_R125P at 16dpf showing a gap between eGFP signal of basal keratinocytes (indicated in white arrow). Basal keratinocytes were fluorescently stained for eGFP (anti-eGFP) (Green) and DAPI (Blue). All images shown here were obtained with a 100xOil objective lens (Olympus). Bars = 25μm.

Similar to the observation we had upon heat shock (Figure 25); cold shock had no effect on the zebrafish line expressing wild type human keratin (Figure 26C&G). Interestingly, the humanized fish overexpressing mutant human KRT14 exhibited a remarkable phenotype in response to cold shock. After one hour of cold shock the EBS zebrafish model revealed alteration in keratin intermediate filament distribution in both 5dpf (Figure 26D) and 16dpf (Figure 26H). The keratin network appeared to be retracted from the edge of the cell towards the center and tiny keratin aggregates were observed at the edge of the cells (Figure 26D & H). In some cases, we have also observed empty spaces between basal keratinocytes (Figure 26H), potentially due to complete detachment of cells or cytolysis.

To determine whether the eGFP signal is detached from the dermis as well from neighboring keratinocytes upon cold shock, I performed cryosection of the cold treated fish at 5dpf and 16dpf. The gap between cells was evident in sections (Figure 26J & L), although there was no visible separation of the epidermis from the underlying dermis. This confocal analysis enable us to suggest that after cold shock, the basal cells from transgenic expressing mutant human KRT14 appeared more rounded and may have lost cell-cell adhesion, whilst eGFP of the basal cells from the wild type remained contiguous between cells (Figure 26). In the transgenic fish expressing mutant human KRT14, we noted differences in severity of phenotype upon on exposure to cold treatment whereby out of 96 EBS zebrafish

larva examined at 5dpf, 10 (~10%) fish were with no obvious phenotype and 86 (~90%) fish had a mild to severe phenotype.

3.1.9. Cold shock affects cell-cell adhesion between basal keratinocytes in epidermolysis bullosa simplex zebrafish model

Because we could not distinguish if the phenotype of EBS keratins under cold shock was due to the retraction of keratin intermediate filaments or detachment of cells from each other, we used immunofluorescent analysis, examining E-cadherin distribution following cold shock to observe cell–cell adhesions. Unfortunately there are no antibodies readily available for imaging fish desmosome components.

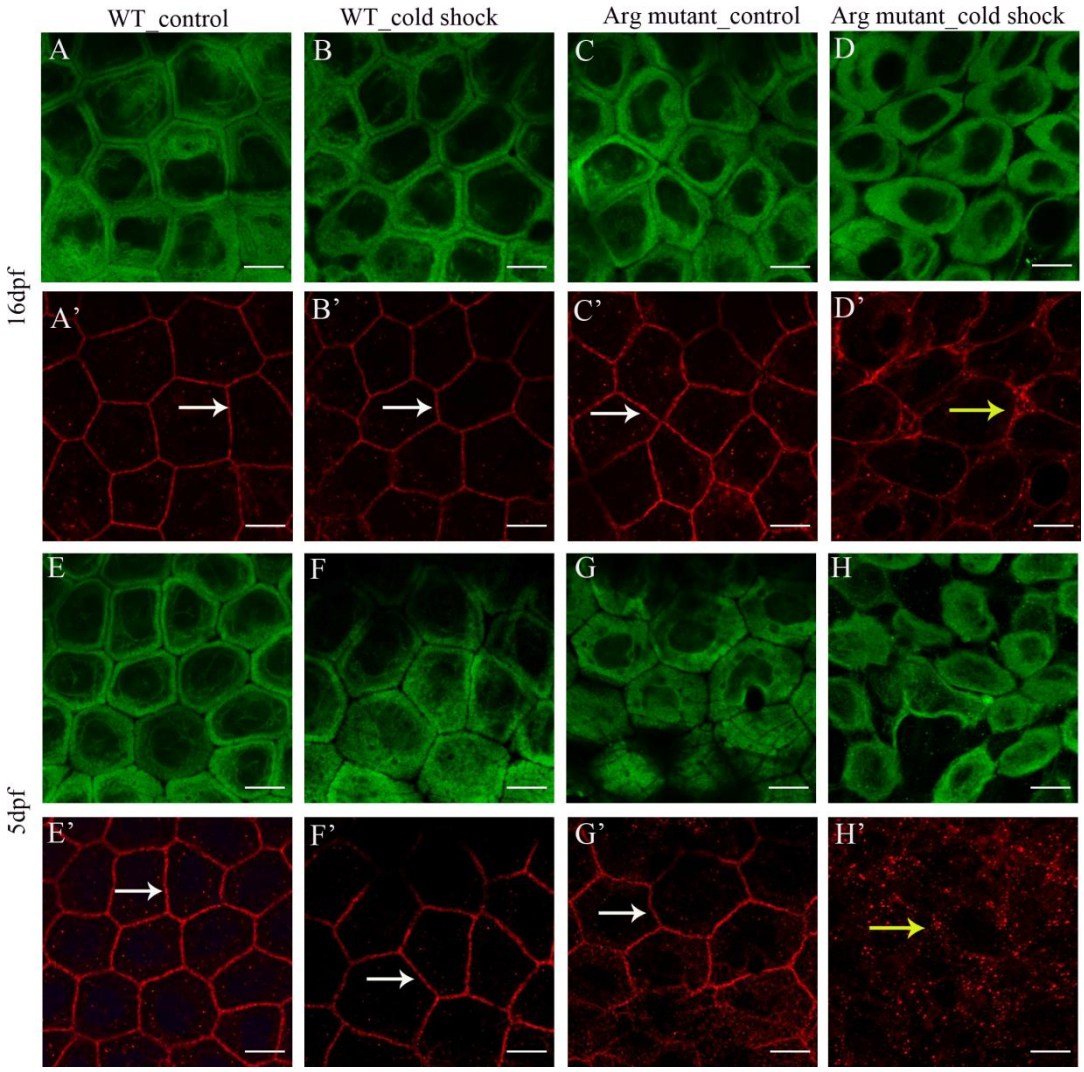

Figure 27: Cold shock causes cell adhesion disruption in EBS zebrafish model

Confocal image of EBS or wild type transgenic zebrafish treated with cold shock at 18 ^{0}C for one hour and stained for E-cadherin (Red), eGFP (Green) and DAPI (Blue). (A&A') Untreated KRT14_WT transgenic zebrafish at 16dpf, (B &B') Cold treated transgenic zebrafish overexpressing human KRT14_WT at 16dpf, (C&C') Untreated EBS zebrafish overexpressing human KRT14_R125P at 16dpf, (D&D') Cold treated EBS zebrafish overexpressing human KRT14_R125P at 16dpf showing a gap between eGFP signal of cells and punctuated E-cadherin staining (indicated in white arrow), (E&E') Untreated transgenic zebrafish overexpressing human KRT14_WT at 5dpf, (F &F') Cold treated transgenic zebrafish overexpressing human KRT14_WT at 5dpf, (G&G') Untreated EBS zebrafish overexpressing human KRT14_R125P at 5dpf, (H & H') Cold treated EBS zebrafish overexpressing human KRT14_R125P at 5dpf demonstrating a gap between

eGFP signal of adjacent cells and diffuse or no staining of E-cadherin observed (indicated in yellow arrow). The white arrows indicates a normal staining of E-cadherin (A', B', C', E', F' &G'). All images shown here were obtained with a 100xOil objective lens (Olympus). Bars = 25μm

Both transgenic fish expressing wild type and mutant human keratin were subjected to cold shock at 18 ^{0}C for one hour. Fish were fixed immediately and immunostained using antibodies against eGFP and E-cadherin. First, we examined the morphology of the basal keratinocytes by imaging eGFP positive cells captured from the head area at 5dpf and 16dpf zebrafish larvae (Figure 27). Upon cold shock, unlike the basal cells from KRT14_WT fish which were quite similar in shape, the basal keratinocytes from the KRT14_R125P transgenic fish were very different in their morphology. The size and shape of the cells expressing mutant human keratins was uneven of which we observed small, large, narrow, shrunk and elongated basal cells, with most losing polygonal appearances (Figure 27 D & H). As before, immunofluorescent staining revealed that tiny aggregates of eGFP positive intermediate filaments dispersed at the cell edge with retraction of eGFP signal from neighboring cells (Figure 27H).

E-cadherin staining was similar in the wild type fish before and after cold shock (Figure 27A', B', E'& F'), and was similar in the KRT14_R125P transgenic fish before cold shock (Figure 27C, C', G & G') where E-cadherin was seen predominantly around the periphery of the cells (Figure 27C' & G'). However, after cold shock the E-cadherin localization in mutant humanized fish was highly

punctuated, with diffuse staining at the cell periphery (Figure 27D') and almost no staining of E-cadherin was observed at 5dpf (Figure 27H').

The striking difference in cell morphology and E-cadherin expression between the wild type and mutant human keratin expressing basal cells, upon cold shock indicated the transgenic fish overexpressing the mutant human KRT14 exhibited a notable defect in cell-cell adhesion, where there was loss of close adhesion between the basal keratinocytes and dispersed localization of E-cadherin unlike the transgenic fish expressing KRT14_WT where the basal cells retained tight connection to each other under the same stress condition(Figure 27 B & F).

Accordingly, we hypothesize that basal keratinocytes overexpressing mutant human keratins display dramatic alteration in keratin intermediate filament networks, and are more susceptible to temperature stress, showing major alterations in intermediate filament distribution, cell adhesion and formation of aggregates.

3.1.10. Histology of epidermolysis bullosa simplex zebrafish model

Whilst there were cellular defects in the 5dpf and 16dpf KRT14_R125P transgenic larvae after temperature shock, we wanted to see if there were tissue level defects in the adult zebrafish (4 months) upon similar perturbations.

For the analysis of the epidermolysis bullosa simplex zebrafish model, transverse sections were performed in the trunk region of the transgenic adult zebrafish expressing wild type and mutant human keratin. The histological sections were

stained using hematoxylin (nuclear stain) and eosin (cytoplasmic stain) (Done by Marcus Wai Yean YONG from Institute of Molecular and Cell Biology, A*STAR, Singapore).

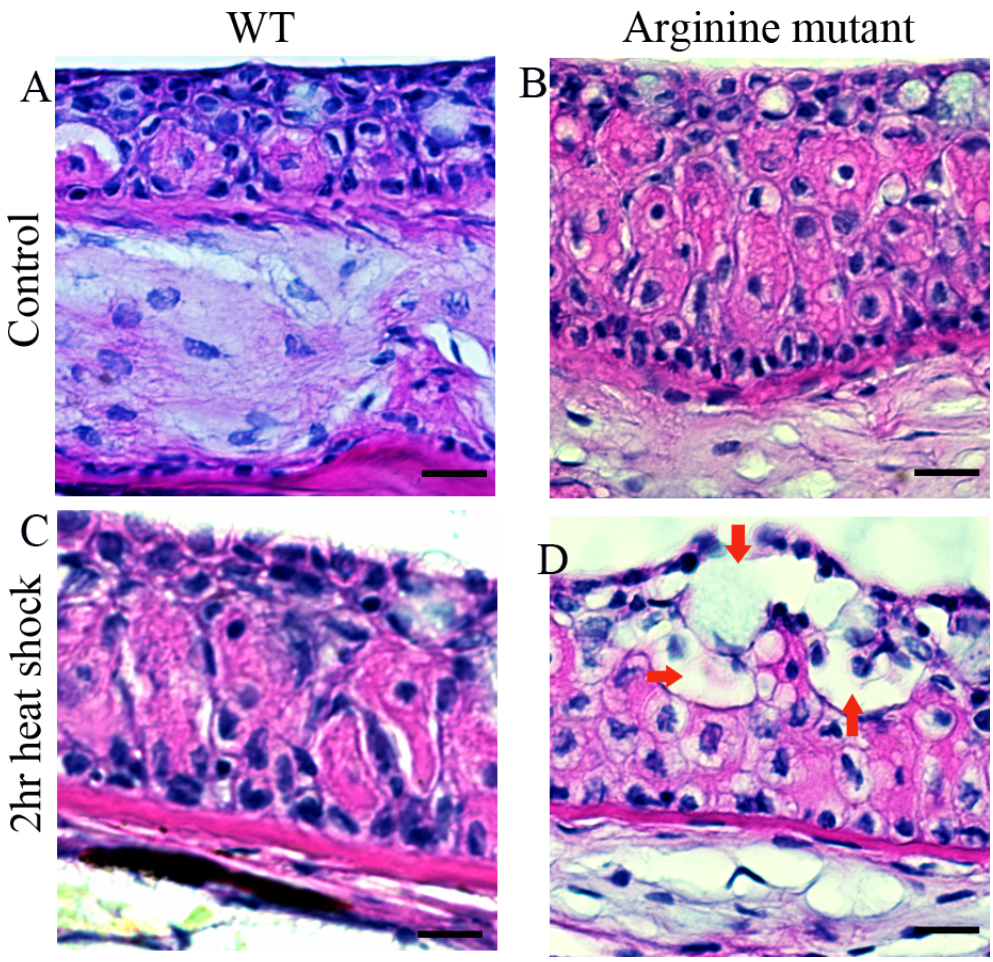

Figure 28: Transverse sections and hematoxylin and eosin staining of adult zebrafish skin

(A) Transverse section of untreated control of transgenic adult zebrafish overexpressing wild type human keratin (KRT14_WT), (B) Transverse section of untreated EBS adult zebrafish overexpressing mutant human keratin (KRT14_R125P), (C) Transverse section of heat treated transgenic adult zebrafish overexpressing wild type human keratin (KRT14_WT), (D) Transverse section of heat treated EBS adult zebrafish overexpressing mutant human keratin (KRT14_R125P) exhibiting disruption of the superficial layer of the epidermis (red arrows). All images shown here were obtained with a 63xOil objective lens (Zeiss). Bars = 25µm.

To investigate the histological changes of epidermolysis bullosa simplex zebrafish model, two adult fish were taken from each transgenic line overexpressing wild type and mutant human keratin and were kept at 40 ^{0}C for two hours. Fish were examined immediately for any blistering phenotype using dissecting scope and fixed overnight for histological sectioning.

In all the sectioned and H& E stained zebrafish no visible defects in the basal layer/basal keratinocytes were observed. Interestingly, in the histological section of humanized fish overexpressing mutant keratin, evidence of cellular disintegration and blistering at the superficial layer of the epidermis was revealed only following heat shock (Figure 28D). This phenotype at the superficial layer of the skin of the EBS zebrafish model was observed in 72% of the images taken from the H & E stained slides.

3.1.11. Live imaging analysis of epidermolysis bullosa simplex zebrafish model

In zebrafish live imaging studies using reporter transgenic lines have enabled understanding of cell behavior *in vivo.* I used this opportunity to understand the behavior of basal keratinocytes and keratin intermediate filament networks in the EBS zebrafish model.

It has not been previously reported how basal keratinocytes behave in epidermolysis bullosa simplex patients *in vivo*. Zebrafish provides the ability to image in *vivo* with cellular and subcellular resolutions.

My investigations began by comparing basal keratinocytes overexpressing wildtype versus the mutant human keratins based on their response to stress (heat and cold shock) *in vivo* at 5dpf and 16dpf (Figure 29 & 30).

3.1.11.1. Heat shock reveals aggregate formation and detachment of basal keratinocytes in vivo in EBS zebrafish model

To visualize the effect of heat on EBS keratins *in vivo*, both 5dpf and 16dpf EBS zebrafish larvae were subjected to a heat chamber which was set to 40 ^{0}C for one hour and time-lapse confocal recording was conducted.

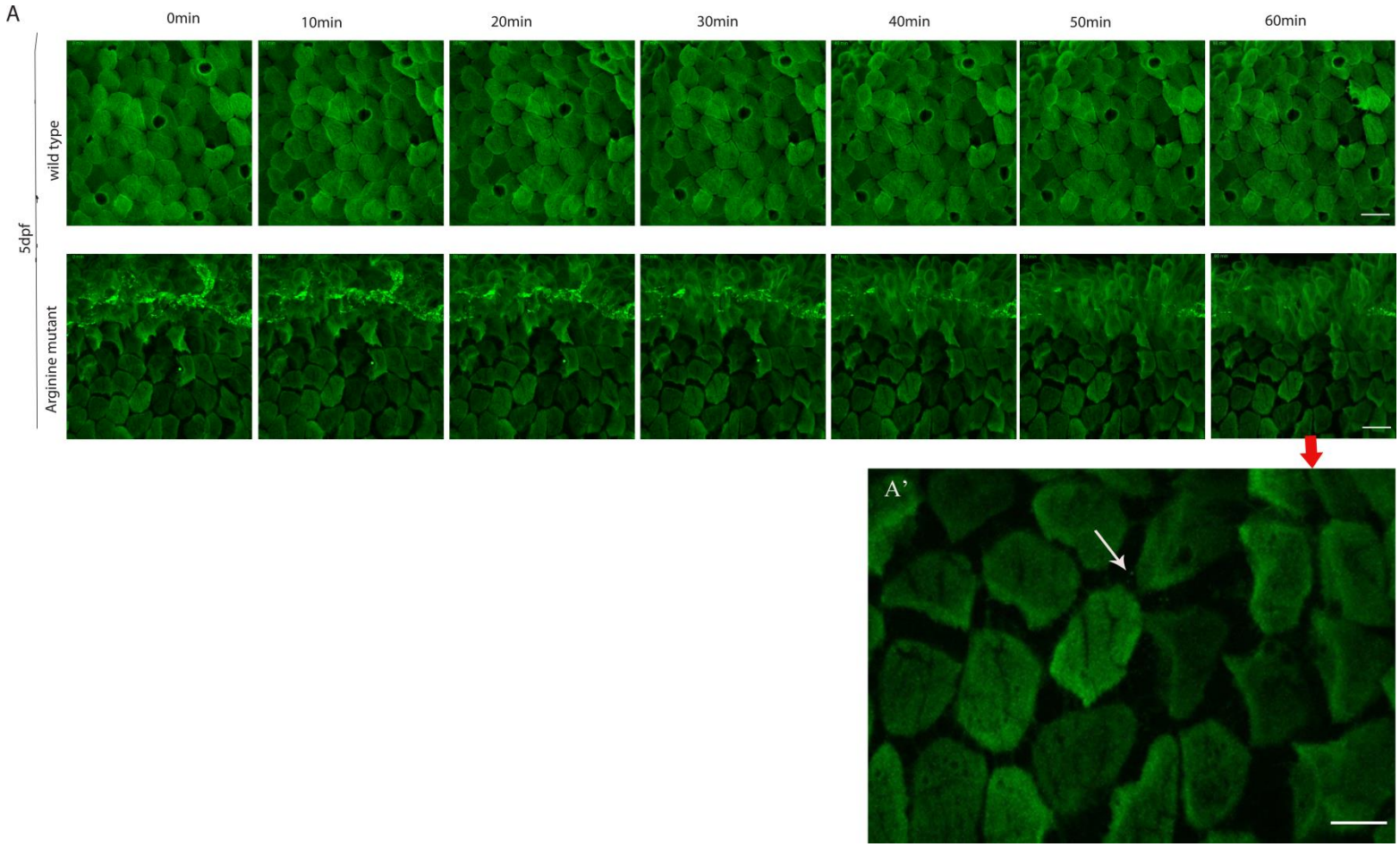
A
0min
10min
20min
30min
40min
50min
60min
5dpf
wild type
Arginine mutant
A'

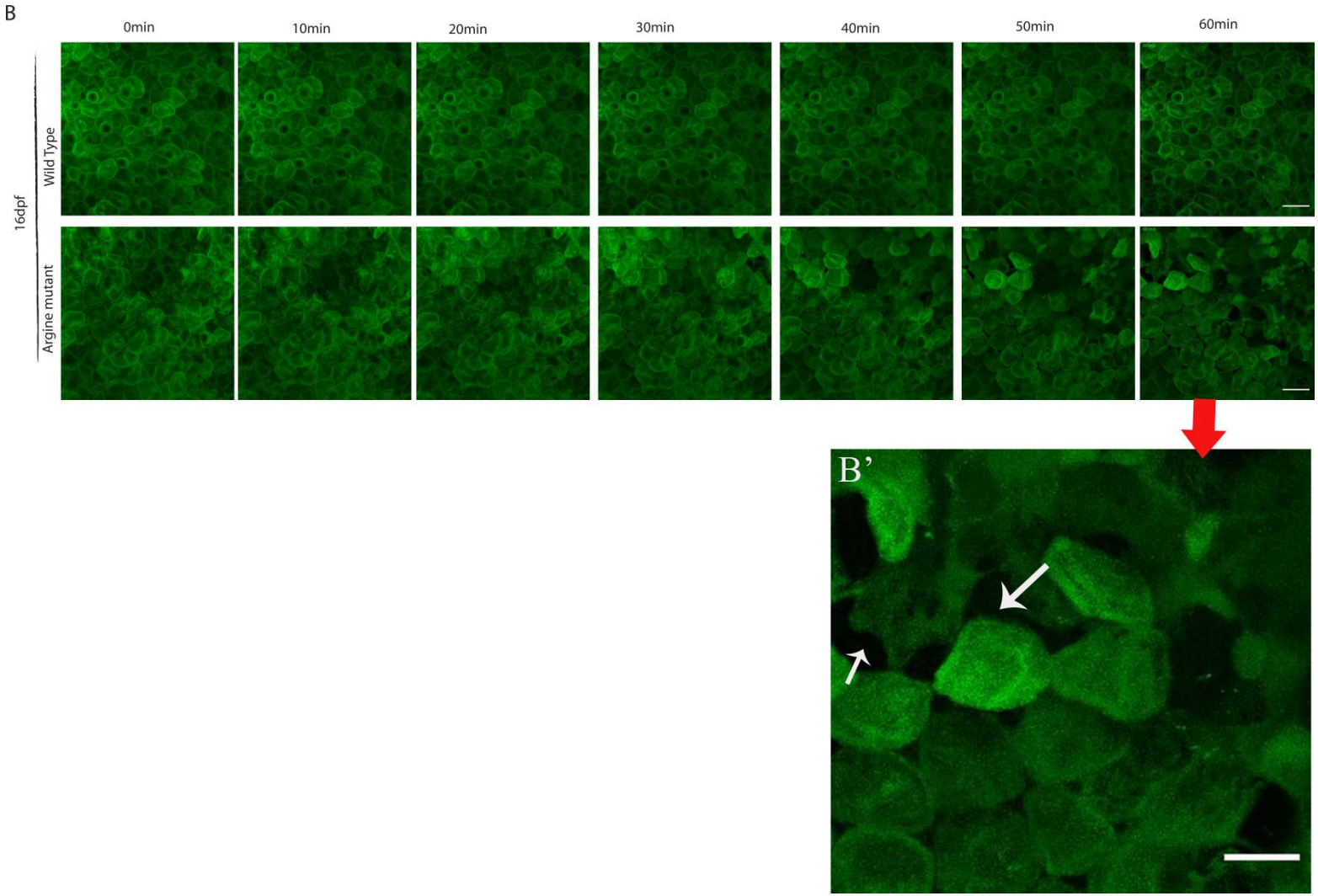
B
0min
10min
20min
30min
40min
50min
60min
16dpf
Wild Type
Argine mutant
B'

Figure 29: Time-lapse analysis of basal keratinocytes of epidermolysis bullosa simplex zebrafish model in response to heat shock

(A) Time-lapse recordings of the basal keratinocytes of the transgenic zebrafish overexpressing wild type human keratin at 5dpf (top row) and EBS zebrafish overexpressing mutant human keratin at 5dpf (bottom row), (A') tiny aggregates and detachment of cells (white arrow), (B) Time-lapse recording of the basal keratinocytes of the transgenic zebrafish overexpressing wild type human keratin at 16dpf (top row) and EBS zebrafish overexpressing mutant human keratin at 16dpf (bottom row), (B') detachment cells (white arrow). In both A&B, representative images were taken every 10minutes. White arrows on the EBS zebrafish expressing mutant human keratin indicating the detachment and tiny aggregate formation in response to heat shock. All images shown here were obtained with a 40xOil objective lens (Zeiss). Bars = 25µm (A, B), 100µm (A', B').

After one hour incubation, the KRT14_WT transgenic fish displayed no change in keratin intermediate filament network and hardly any basal cells deformation of either 5dpf(A) or 16dpf (B) (Figure 29 A & B). In contrast, in the Arginine mutant transgenic fish, detachment of the basal keratinocytes was observed. This resulted in the formation of small aggregates visible in the periphery of basal cells and started to appear after 30min heat treatment. In addition, morphological changes, partial disruption and sliding of the basal keratinocytes over the dermis were observed (Figure 29 A & B).

3.1.11.2. Cold shock reveals aggregate formation and detachment of basal keratinocytes in vivo in EBS zebrafish model

Similar to the heat shock stress, I used cold shock as stress factor to gain an insight into characterization of keratin intermediate filament networks in the EBS zebrafish model. Transgenic fish at 5dpf and 16dpf were cold treated. I could not find a microscope with a cooling chamber and I added a cold E2 medium at 18 ^{0}C as a means of stressing the fish. In this case, E2 medium at 18 ^{0}C was added for the first 20minutes and replaced every 20 minutes for an hour and time-lapse recording was performed.

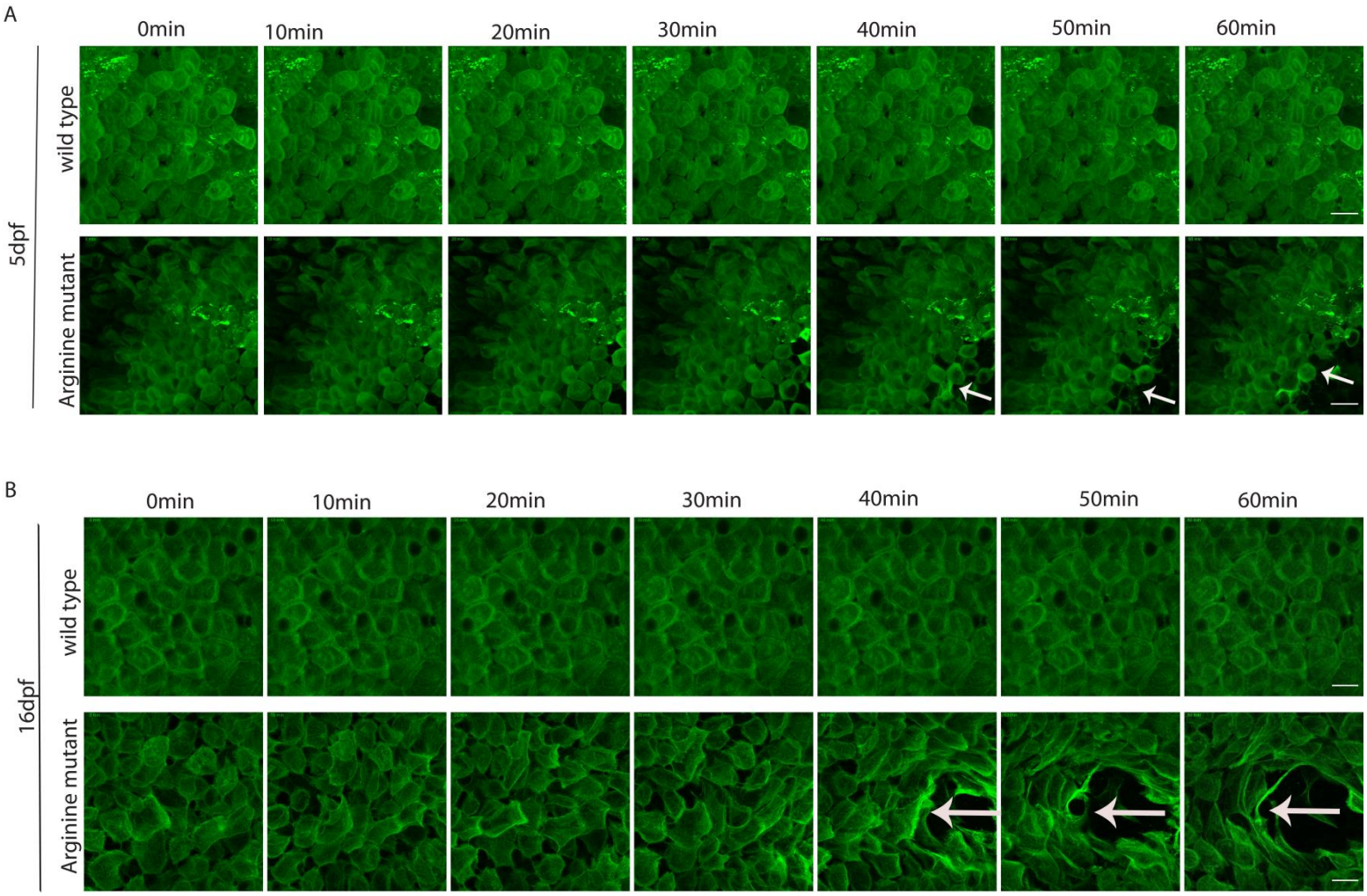
A
0min
10min
20min
30min
40min
50min
60min
5dpf
wild type
Arginine mutant
B
0min
10min
20min
30min
40min
50min
60min
16dpf
wild type
Arginine mutant

Figure 30: Time lapse analysis of basal keratinocytes of epidermolysis bullosa simplex zebrafish model in response to cold shock

(A) Time-lapse recordings of the basal keratinocytes of the transgenic zebrafish overexpressing wild type human keratin at 5dpf following cold shock and basal keratinocytes of the EBS zebrafish overexpressing mutant human keratin at 5dpf following cold shock (B) Time-lapse recordings of the basal keratinocytes of the transgenic zebrafish overexpressing wild type human keratin at 16dpf following cold shock and basal keratinocytes of the EBS zebrafish overexpressing mutant human keratin at 16dpf following cold shock. In both A&B, representative images were taken every 10 minutes. Red arrows in the EBS zebrafish model (A&B) indicating sliding of basal keratinocytes over the underlying dermis. All images shown here were obtained with a 40xOil objective lens (Zeiss). Bars = 25μm.

In the transgenic zebrafish expressing wild type human keratin, no visible sign of keratin intermediate filament fragmentation or deformity of basal keratinocytes morphology was identified during the cold shock treatment. The basal keratinocytes appeared, tightly connected to each other and their morphology was similar throughout time-lapse recording. In contrast, in the EBS zebrafish, alterations in keratin intermediate filament architecture, changes in basal cell morphology and sliding of basal keratinocytes over underlying tissue was detected (Figure 30).

3.2. Generation of Dystrophic Epidermolysis Bullosa-Like Zebrafish Model

3.2.1. Identification and characterization of zebrafish *col7a1* genes

In addition to a zebrafish EBS model I attempt to establish a DEB zebrafish model. To do this, I first identified zebrafish *col7a1* orthologous genes by BLAST search using human COL7A1 protein sequences and cross checked ZFIN (https://zfin.org/) and Ensembl (https://asia.ensembl.org/index.html). The human *COL7A1* gene is located in chromosome 3 and has 118 exons which encodes for a protein of 2944 amino acids. Accordingly, we found two paralogues of zebrafish *col7a1* genes namely *col7a1a* and *col7a1b* in chromosome 6 and 4, respectively (Figure 31). The zebrafish *col7a1a* and *col7a1b* genes have 118 and 90 exons which encodes for a protein of 3093 and 2302 amino acids that have 49.32% and 37.61% identity at amino acid level to their human counterpart, respectively (Figure 31).

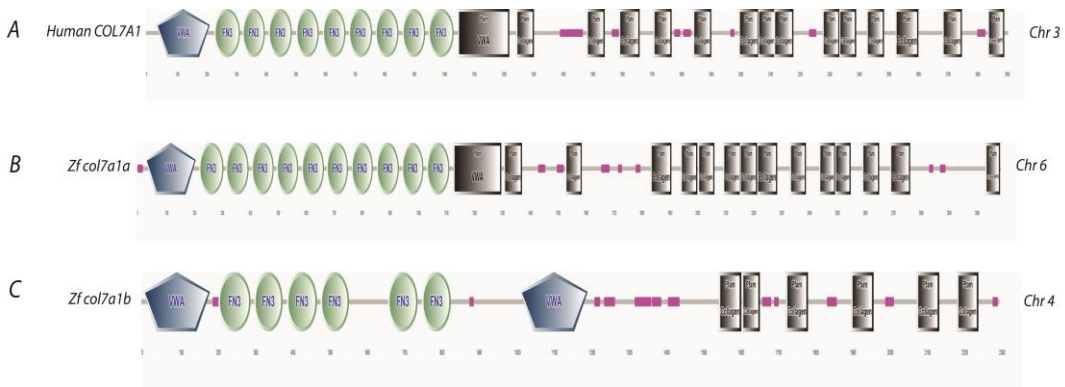

Figure 31: Domains comparing the genes coding for type VII collagen between human and zebrafish

The protein domains were obtained using Simple Modular Architecture Research Tool (SMART) and the protein sequence was based on the Ensembl database. (A) Human type

VII collagen domain located on chromosome 3. (B &C) Zebrafish type VII collagen located on chromosome 6 & 4, respectively.

Protein sequence of Col7a1a and Col7a1b was taken from Ensembl and the domains of both genes were identified using Simple Modular Architecture Research Tool (SMART), a biological database that is used in the identification of protein domains and analysis of protein sequences (Letunic, Doerks, & Bork, 2008; Schultz, Milpetz, Bork, & Ponting, 1998).

In human, DEB arises from dominant negative or loss of function mutations in the gene encoding type VII collagen (*COL7A1*) which leads to dominant DEB (DDEB) or recessive DEB (RDEB), respectively (Titeux et al., 2006). Recessive DEB is generally the most severe form of DEB where the skin is extremely fragile, often with extensive blistering and wounds (Varki et al., 2007). There is no animal viable model for this yet as the disease condition is severe and lethal shortly after birth. To mimic DEB in zebrafish, I started by characterizing the two *col7a1* genes as follows.

I evaluated the spatio-temporal expression pattern of the two zebrafish *col7a1* genes; the expression of both zebrafish *col7a1* genes was detected by RT-PCR from 15 somite stages (16hpf) to adult stage of zebrafish which was similar (Figure 32). The RT-PCR result indicated that RNA of neither *col7a1a* nor *col7a1b* is maternally deposited. B-actin was used as a reference gene (Figure 32).

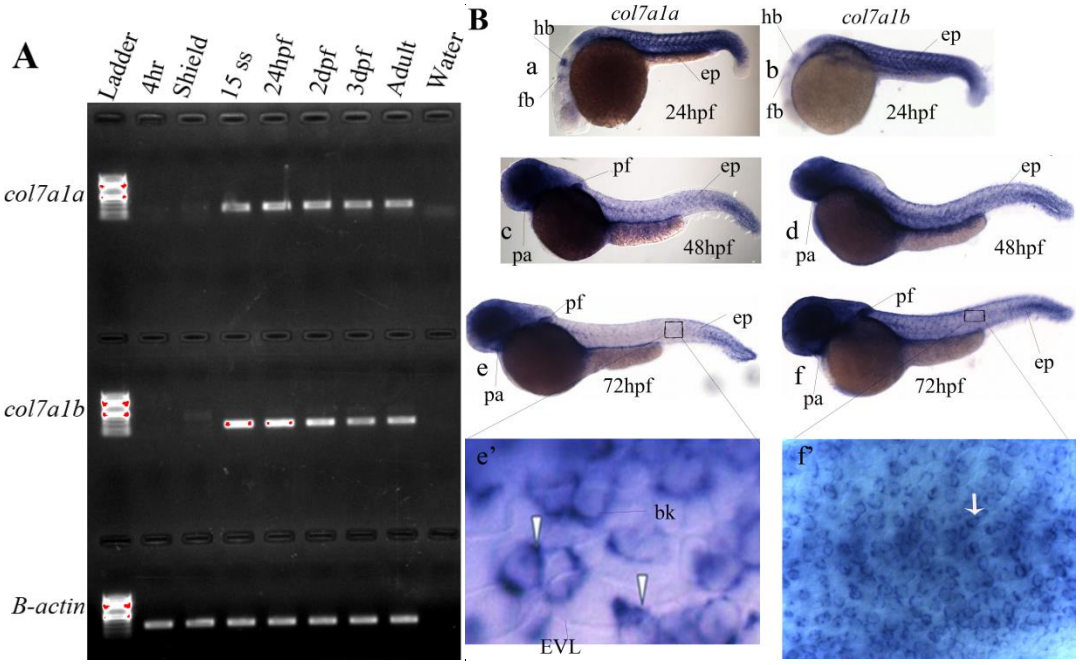

Figure 32: Zebrafish *col7a1* genes are expressed in the basal keratinocytes

(**A**) RT-PCR of *col7a1a*, *col7a1b* and *β-actin* (reference gene), where both of *col7a1a* and *col7a1b* expression starts from 15 somatic stage (after about 16hpf) indicating type VII collagen is not maternally deposited. (**B**) Whole mount in situ hybridization of *col7a1a* and *col7a1b* at 24hpf, 48hpf and 72hpf showing expression of both *col7a1* genes in the zebrafish epidermis (ep), pectoral fin (pf), pharyngeal arch(pa), hindbrain (hb) and forebrain (fb) (e') In situ hybridization of *col7a1a* at 72hpf and the white arrows showing expression of *col7a1a* in the basal keratinocytes(bk) where it is beneath the enveloping layer (EVL) cells (f') In situ hybridization of *col7a1b* at 72hpf showing strong expression of *col7a1b* in the basal keratinocytes of the zebrafish epidermis.

To further assess the spatio-temporal expression pattern of zebrafish *col7a1* genes, I performed whole mount *in situ* hybridization (WISH). Based on this, expression of both transcripts of *col7a1*, *col7a1a* and *col7a1b* is shown to be expressed in zebrafish epidermal basal keratinocytes at different developmental stages of zebrafish larvae (24hpf, 48hpf and 72hpf) (Figure 32B). According to my in situ hybridization images, the expression level of *col7a1a* gene is much weaker than

the expression level of *col7a1b* which is strongly expressed in the epidermal basal keratinocytes as displayed in (Figure 32 B).

3.2.2. Generation of dystrophic epidermolysis bullosa zebrafish model

In order to knockdown col7a1 genes and generate dystrophic epidermolysis bullosa-like model in zebrafish, I injected morpholino designed against *col7ala* and *col7a1b* genes into wildtype zebrafish embryos. Gross examination of morpholino injected and uninjected wild type embryos as a control were performed using dissecting scope at different stages of development. However, no phenotype was noted. This lack of phenotype up on morpholino knockdown leads us to knockout the *col7a1* genes using targeted nucleases.

To knockout both zebrafish *col7a1* genes I employed the CRISPR/Cas9 system with an intention of generating dystrophic epidermolysis bullosa in zebrafish. To introduce indels in both *col7a1* zebrafish genes, I identified a target sequence for each of the genes. The CRISPR target site for *col7a1a* and *col7a1b* were designed against Exon10 (Figure 33A) and Exon2 (Figure 33B), respectively. *col7a1a* and *col7a1b* are located in the FN3 repeats and von Willebrand factor (vWF) type A (VWA) domain of zebrafish type VII collagen, respectively.

Thus, I designed single guide RNAs (sgRNA) able to direct Cas9 nuclease to exons of both genes. I injected the sgRNA together with Cas9 RNA into one cell stage zebrafish embryo to introduce mutations. I have generated founder fish with 2bp deletions in *col7a1a* Exon10 and founder with 2bp deletion in *col7a1b* Exon2

(Figures 33 A&B). Whilst these do not show a phenotype when in the individual homozygous phase, I have generated *col7a1a*; *col7a1b* double heterozygotes. This again didn't show phenotype, where adult fish viable and fertile.

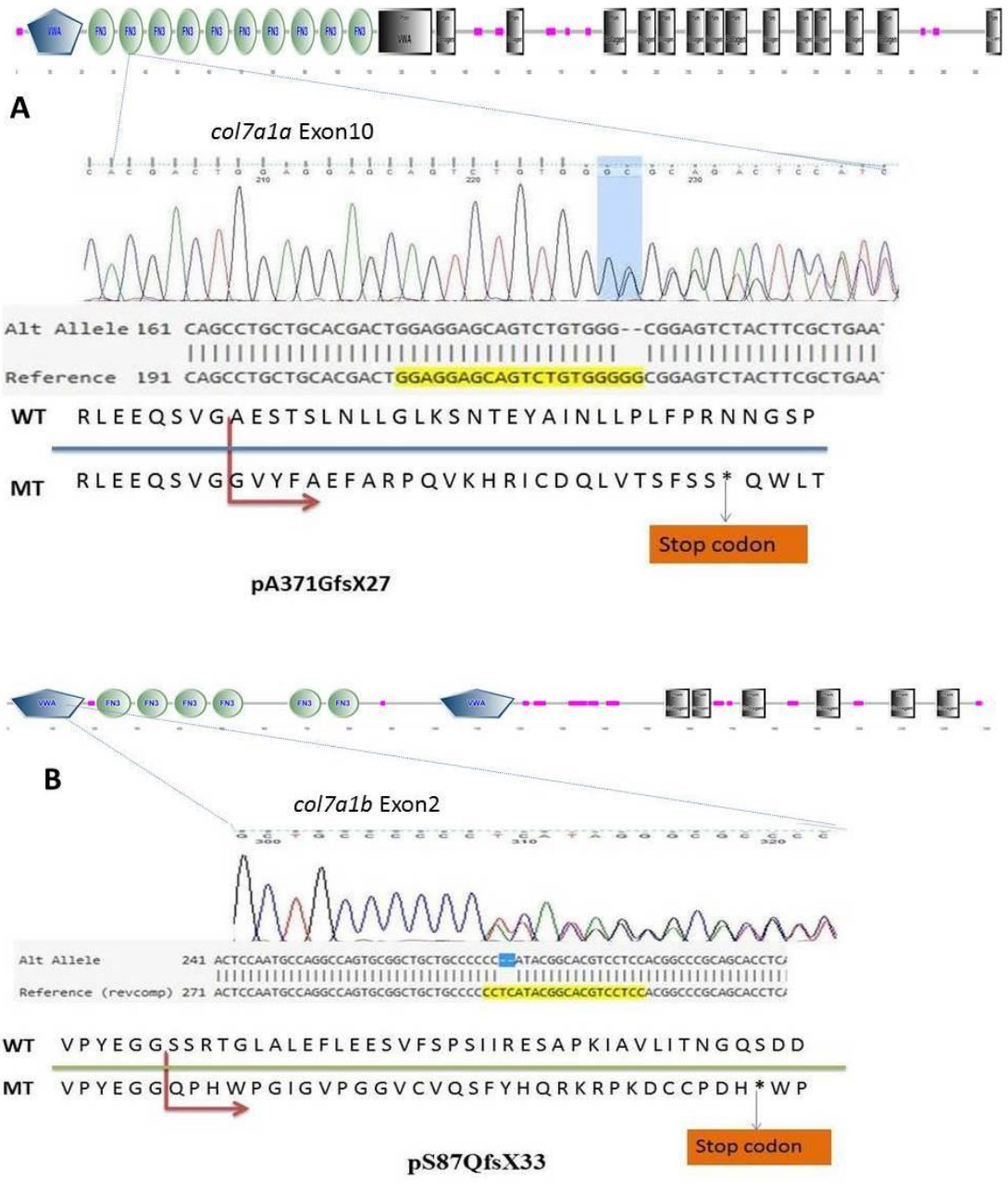

Figure 33: Generation of dystrophic epidermolysis bullosa targeting zebrafish *col7a1* genes using CRISPR/Cas9 system

Domain of collagen VII, CRISPR target site of *col7a1a* and *col7a1b* showing an example of deleted nucleotide bases right in the CRISPR target sites in both genes. (a) Is indicating the location of *col7a1a* Exon10 CRISPR site with a deletion of 2bp and resulting in premature stop codon after 27 amino acids, (b) is illustrating the location of *col7a1b* Exon2 with a deletion of 2bp resulting in frameshift mutation which led to premature stop codon after 33 amino acids.

As illustrated in figure 33A and B, *col7a1a* and *col7a1b* homozygous founders were generated with 2bp deletion each where the deletion caused a frameshift mutation. In *col7a1a,* the mutation resulted in amino acid change from Alanine (A) to Glycine (G) at position 371 led to a premature stop codon after 27 subsequent amino acids (Figure 33A). Similarly, in *col7a1b*, the mutation caused in amino acid change from Serine (S) to Glutamine (Q) at position 87 which resulted in premature stop codon after 33 subsequent amino acids (Figure 33B). This premature stop codon hypothetically results in truncated, incomplete, and nonfunctional protein product.

I examined the double knockout fish from embryological stage to adult stage for any defect, especially skin related phenotypes. However, no obvious sign of blistering of the skin was observed. I further continued to explore if any micro-blisters in the dermal-epidermal layer of the double knockout fish using transmission electron microscope analysis.

3.2.2.1. Transmission electron microscope analysis of col7a1 double knockout

Ultrathin transverse cross sections were taken from the mid tail region of zebrafish larvae at 16dpf. Electron micrographs of the epidermis, basement membrane and dermis were captured at 4,000x and 10,000x magnification for transmission electron microscope (TEM) analysis. Wild type zebrafish embryo and *col7a1* double knockout mutant were analyzed for possible detachment of the underlying dermis from the basement membrane resulting from the absence of collagen VII in the double mutants. Results of the TEM analyses showed no visible defects in the integrity of the attachment of the basement membrane to the dermis attributed to *col7a1* double knockout (Figure 34).

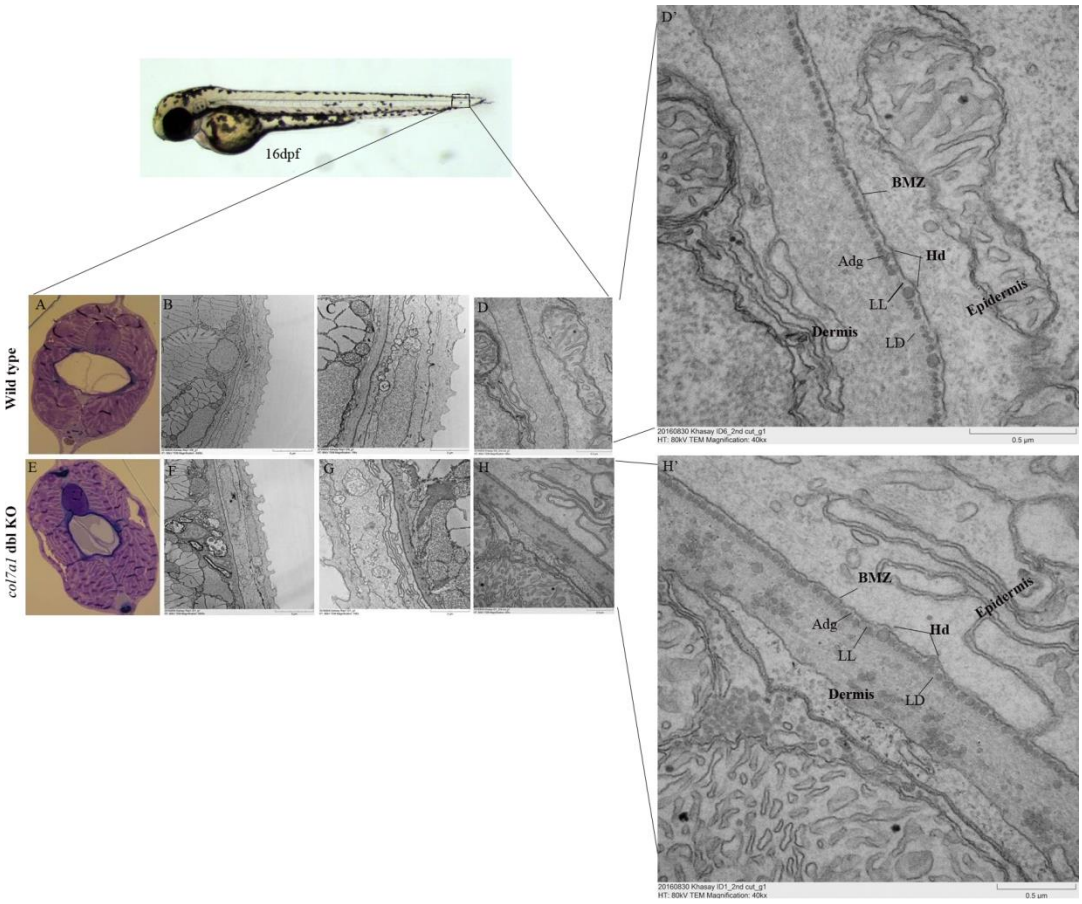

Figure 34: Transmission electron microscope analysis of *col7a1* double knockout fish

Detailed ultrastructure of zebrafish skin, wild type fish (A-D &D') and *col7a1* double knockout (E-H&H'), at original magnification of 4kx, 10kx and 40kx, Bar =5 µm, 2 µm and 0.5µm. Ultrathin transverse cross sections were taken from the mid tail region of zebrafish embryos at 16dpf. In both wild type (D') and *col7a1* double knockout (*col7a1* dbl KO) (H') fish, similar structures of the skin were noted such as, Adepidermal granules (Adg), Lamina lucida (LL), Lamina densa (LD), hemidesmosomes(Hd) and basement membrane zone(BMZ). (Done by Qiaohui Yang and Dr. David Liebl from IMB-IMCB joint electron microscopy suite, A*STAR, Singapore).

Lack of phenotype of the double knockout fish could be due to at least three main reasons:

1) c*ol7a1* genes knockout may be compensated by endogenous paralogues or other extracellular proteins of basement membrane.

2) The presence of a transcription or translation start site after the site of mutation.

3) Type VII collagen may not be totally knocked out due to exon skipping

Thus, in an effort to determine the status of type VII collagen in the double knockout zebrafish, we performed different evaluations at RNA and protein level where the total RNA and protein was harvested form the double knockout fish and wild type control.

3.2.2.2. Detecting alternative splices using reverse transcription polymerase chain reaction

Alternative splicing is an important cell process when a single gene codes for multiple proteins during gene expression whereby certain combination of exons in a transcribed pre-mRNA are included or excluded to form different splice isoform transcripts (Black, 2000; Blencowe, 2006; Graveley, 2001).

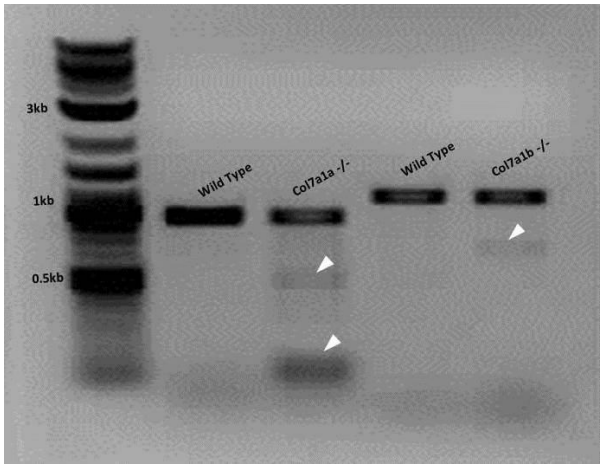

Figure 35: Detection of alternative splice isoforms in *col7a1* double knockout fish using reverse transcription polymerase chain reaction

cDNA from wild type fish was used as a control in each case as labeled (Wild Type). Alternative splices which might be resulted due to the introduction of deletion in both *col7a1* genes (*col7a1a* and *col7a1b*) is indicated by the white arrow.

To assess the availability of RNA splicing that might be introduced due to the 2bp deletion, I extracted total RNA from *col7a1* double knockout fish and prepared cDNA. According to RT-PCR analysis other bands were identified in the mutants for both *col7a1a* and *col7a1b*, but only single bands in wild type control (Figure 35). This suggest that the deletion might lead to exon skipping (most common form of alternative splicing), where one or more variable exons are either included or skipped from the final transcript to make up the array of spliced isoforms of a gene (Anderson et al., 2017; Keren, Lev-Maor, & Ast, 2010) and thereby possibly maintaining type VII collagen function. Alternatively, cryptic splice sites might have been employed.

3.2.2.3. Proteomics analysis

As there are no antibodies available against zebrafish collagen VII, global proteome analysis was conducted using sequential window acquisition of all theoretical fragment ion spectra mass spectrometry (SWATH MS), to determine whether type VII collagen is efficiently knocked out using CRISPR/cas9 system and explore how the loss of collagen VII expression may change cellular protein homeostasis.

First, we looked for how many peptides of zebrafish *col7a1* genes could be detected using MS analysis from a spectral library derived from wild type fish as a control, we could not find collagen VII peptides from the spectral library.

To assess the status of collagen VII in the double knockout fish, we harvested protein from 30hpf embryo, 5dpf larvae and adult fin of the double knockout fish and performed MS analysis to assess the status of type VII collagen in comparison to the wild type control.

According to the proteomics analysis, we found different evidence at the three age stages of our double knockout fish whereby we could not draw a conclusion on the status of collagen VII.

The first information we obtained from 30hpf embryo, no collagen VII peptide was detected, consistent with loss of protein. In addition, the only significant change in the double knockout fish compared to the wild type control was spectrin beta chain, a protein that in zebrafish is encoded by *sptbn1* gene, was upregulated (~2 fold) (Annex 1). This is a key cytoskeleton protein important for membrane integrity,

cell morphology, organelle transport, and cell polarity of varied cell types during development (Liao et al., 2000).

Secondly, in the 5dpf double knockout zebrafish, a total of 10019 proteins were found and no CollagenVII was detected. 26 proteins were found upregulated with the cut value of fold change greater than 1.5. Most importantly, we found three collagens upregulated from the SWATH MS data namely, Col28a2, Col6a2 and Col14a1b, which might potentially be compensating the function of CollagenVII. Upregulation of the three collagens was not statistically significant ($p>0.5$), however the fold change confidence was relatively high (Table 8). Other upregulated and down regulated proteins are stipulated in Annex 2.

Table 8: List of upregulated collagens in col7a1 double knockout zebrafish

Gene names	Protein names	Fold Change	log2 Fold Change	Fold Change confidence	p-value	No of peptides
col28a2a	Collagen, type XXVIII, alpha 2a	13.99	3.81	0.99	0.1068	2
col6a2	Collagen, type VI, alpha 2	10.40	3.38	0.70	0.8075	1
col14a1b	Collagen, type XIV, alpha 1b	16.29	4.02	0.71	0.07	4

To evaluate the presence of collagen VII in the adult double knockout zebrafish, protein was harvested from the fin for the reason that Type VII collagen is expressed in the fin like the other parts of the skin (see RT_PCR figure 32) and the fin is more convenient to collect without sacrificing the fish. A total of 9499

proteins were found in adult knockout fish out of which 15 proteins were found upregulated with fold change value greater than 1.5. We also detected a single peptide from the SWATH MS data. The peptide "**ALSDFGIEVR"** was found from type VII collagen encoded by *col7a1a* at exon 72 to 73 after 1699 subsequent amino acids from the CRISPR target site as indicated below (Figure 36). Though we did detect the single peptide from the adult fin data, the quantification was not confident. Therefore, we still cannot conclude anything regarding the status of collagen VII. (Done by Larry Wai Leong LOW and Qi Feng LIN from Institute of Molecular and Cell Biology, A*STAR, Singapore).

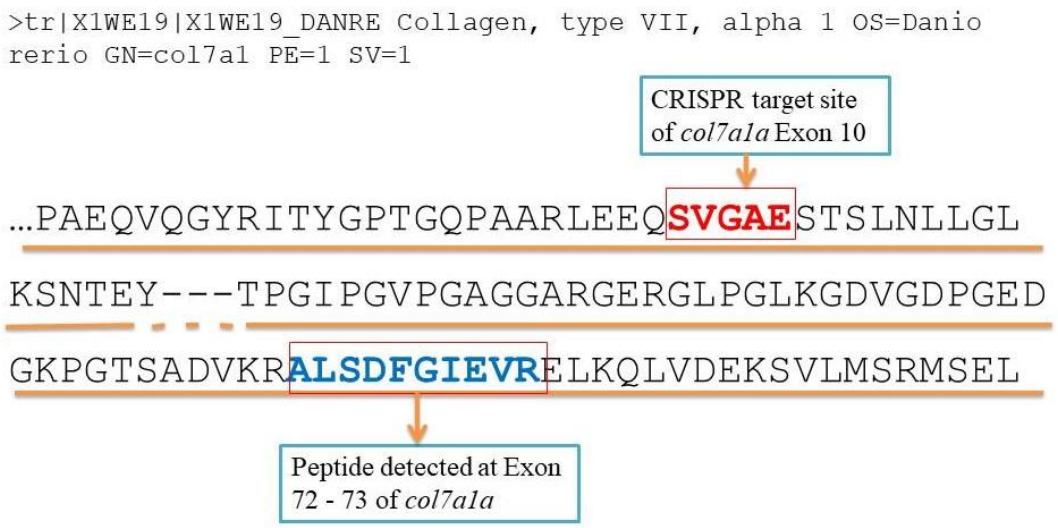

Figure 36: Detection of type VII collagen peptides encoded by zebrafish *col7a1a* gene

Partial protein sequence of zebrafish type VII collagen encoded by *col7a1a* illustrating the CRISPR target site in Exon 10 of *col7a1a* (highlighted in Red) and the peptide found at Exon 72 to 73 of col7a1a (highlighted in Blue).

Taken together, the proteomics analysis to some extent suggested that the type VII collagen is knocked out where no peptide was detected at 30hpf and 5dpf of our

double knockout fish; however, a single peptide was found in the adult. The other possibility is genetic compensation (upregulation of other collagens) and/or retained function in the collagen VII in our adult double knockout fish.

In an effort to knock down any possible presence of type VII collagen in our knockout fish, I injected morpholino designed against *col7a1* genes, *col7a1a* and *col7a1b* into double mutant and wild type fish. I performed a gross examination of morpholino injected embryos of our double knockout and wild type fish using dissecting scope at different stages of development. However, no gross skin defect was noted in both double knockout fish and wild type control up to adult stage.

In order to evaluate and confirm whether the loss of zebrafish type VII collagen function resulted in upregulation of the collagens found in our proteomics analysis, I tend to assess their temporal and spatial expression using whole mount in situ hybridization in our double knockout fish and wild type as a control. Among the three collagens (*col28a2a*, *col6a2a* and *col14a1b*), the spatiotemporal expression of *col6a2a* is presented below (Figure 37). I could not manage to get the spatiotemporal expression of the other two genes due to failure of the in situ or extremely low expression levels.

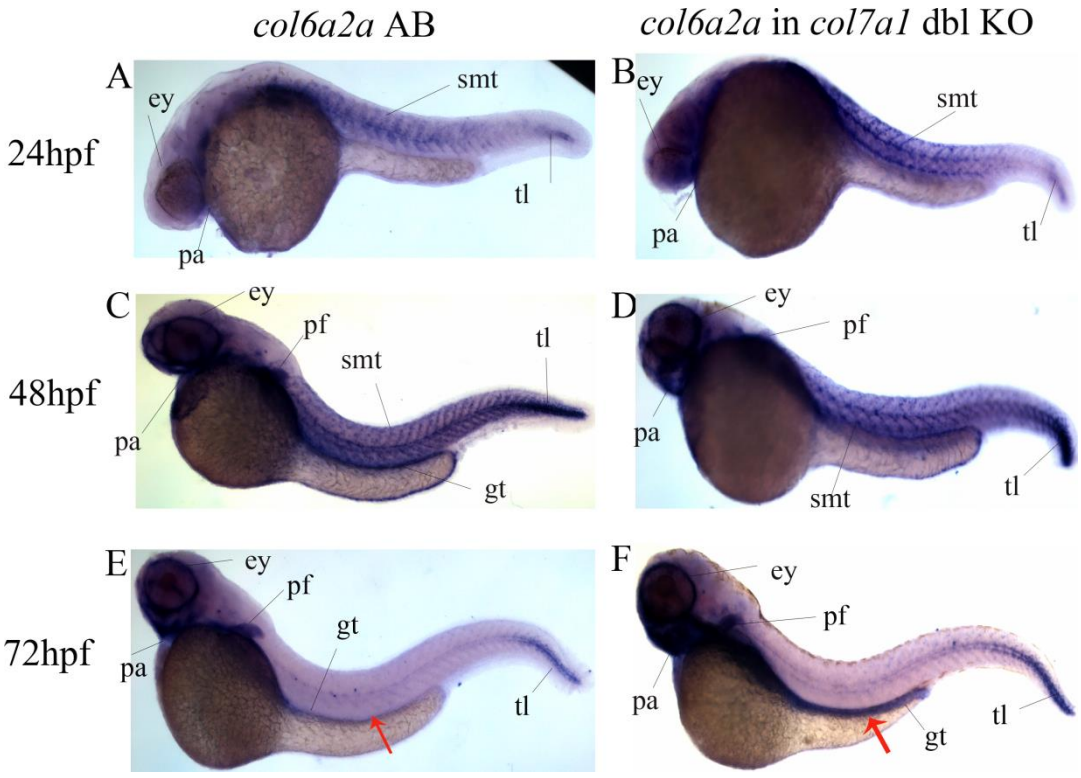

Figure 37: Comparison of spatiotemporal expression of *col6a2a* in wild type and *col7a1* double knockout fish

Whole mount in situ hybridization of *col6a2a* at 24hpf, 48hpf and 72hpf in AB (wild type fish) and in type VII collagen double knockout fish showing expression of in the epidermis, somites (smt), pectoral fin(pf), eye (ey), gut (gt), pharyngeal arch (pa) and tail (tl). (E) In situ hybridization of *col6a2a* at 72hpf showing weak expression in the gut of the wild type fish (red arrow) and (F) strong expression of *col6a2a* in the gut of type VII collagen double knocked out fish at 72hpf (red arrow).

The whole mount in situ hybridization demonstrated that *col6a2a* is expressed in a variety of tissues skin epidermis, as well as the somites, tail, gut and pharyngeal arch of zebrafish (Figure 37). We observed similar expression pattern of *col6a2a* in the wild type fish and the double knockout fish in all stages, however stronger expression was noted in the gut of 72hpf double knockout fish as compared to the wild type control (Figure 37 Red arrow).

Since exon10 and exon2 are early exons of *col7a1a* and *col7a1b*, respectively the 2bp deletion introduced in each gene may lead to another transcription start site after the deletion site and produce functional protein which may be enough to maintain the structural integrity of the skin. Thus, I designed new gRNAs targeting more 3' exons (Figure 38).

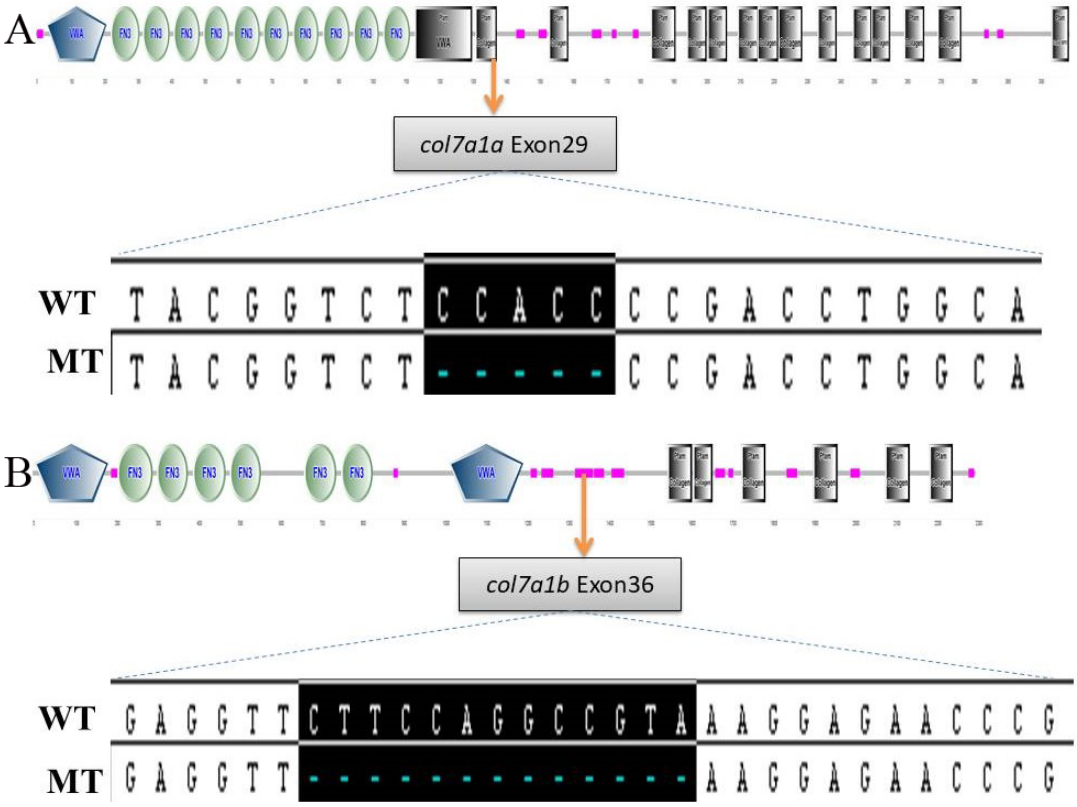

Figure 38: Generation of zebrafish model of dystrophic epidermolysis bullosa

Arrows indicating CRISPR target sites of zebrafish *col7a1* genes, *col7a1a* Exon29 and *col7a1b* Exon36, respectively.

SgRNA *col7a1a* Exon29 was injected into *col7a1b* Exon2 homozygous embryos and sgRNA *col7a1b* Exon 36 was injected into *col7a1a* Exon10 homozygous embryos. I have generated *col7a1a* Exon29 and *col7a1b* Exon36 heterozygotes on *col7a1b* Exon2 and *col7a1a* Exon10 homozygote background, respectively. Upon

sequence analysis, embryos from *col7a1a* Exon29 heterozygotes contained a 5bp deletion (Figure 38A) and *col7a1b* Exon36 heterozygotes containing a 13bp deletion were found (Figure 38B). I have generated *col7a1a* Exon29$^{-/-}$; *col7a1b*Exon2$^{-/-}$, *col7a1a* Exon29$^{-/-}$; *col7a1b* Exon36$^{-/-}$ and *col7a1a* Exon10$^{-/-}$; *col7a1b* Exon36$^{-/-}$ and could not see skin related phenotype. I have now double knockout of *col7a1a* Exon29$^{-/-}$; *col7a1b* Exon36$^{-/-}$ fish. The adult double knockout fish were examined on dissecting scope and didn't show evidence of skin defects.

CHAPTER 4. DISCUSSION, CONCLUSIONS AND FUTURE DIRECTIONS

4.1. Epidermolysis Bullosa Simplex

As a first line of defense of the body, the skin must accommodate continuous challenges and must be strong enough to bear physical trauma to allow a large range of movement. The intermediate filaments expressed by epidermal skin cells are crucial to maintain the physical resilience of the basal cells and mutations in keratins of the epidermis leads to inherited skin fragility disorder such as epidermolysis bullosa simplex in which the basal keratinocytes of patients exhibit fragility and keratin aggregates upon mechanical trauma (Anton-Lamprecht & Schnyder, 1982; Bonifas et al., 1991; Coulombe, Hutton, Vassar, & Fuchs, 1991; Lane et al., 1992).

Epidermolysis bullosa simplex is mostly due to dominant negative mutations in either *KRT5* or *KRT14* genes, which affects the keratin intermediate filament assembly, causes cytolysis and blistering of the skin (Coulombe et al., 2009) for which effective treatment is still lacking.

The complex and specific regulation of keratin intermediate filaments reflect their indispensable role in maintaining the structure of epithelia. Evidence for these functions was first discovered by expressing cDNA of KRT14 deletion mutants in cells (Albers & Fuchs, 1987, 1989; Coulombe, Chan, Albers, & Fuchs, 1990). The protein products of these cDNAs were shown to have a dominant negative effect on the endogenous keratin intermediate filament networks in keratinocytes (Albers

& Fuchs, 1987, 1989; Coulombe et al., 1990). We used this approach to mimic human epidermolysis bullosa simplex in zebrafish by overexpressing dominant negative proteins of zebrafish Krtt1c19e and human KRT14 and equivalent mutations in Krtt1c19e.

Animal models have been developed to help improve our knowledge on the pathomechanism of epidermolysis bullosa simplex (Bruckner-Tuderman, McGrath, Robinson, & Uitto, 2010; Q.-J. Jiang & Uitto, 2005). Transgenic animal models for EBS by expression of mutant form of KRT14 or its absence were developed in mice (Arin & Roop, 2004; Cao, Longley, Wang, & Roop, 2001; Lloyd et al., 1995; Vassar, Coulombe, Degenstein, Albers, & Fuchs, 1991). The first two mouse models generated for EBS (Lloyd et al., 1995; Vassar et al., 1991) exhibited abnormalities in epidermal architecture, alteration in keratin intermediate filament formation, cytolysis of basal cells, and blistering of the epidermis which resembles EBS, but neither of them survived for long as they died immediately after birth which were not helpful in leading to therapeutic approaches. Inducible mouse models have been developed for epidermolysis bullosa simplex (Arin & Roop, 2004; Cao et al., 2001) that mimics EBS at both genetic and phenotypic levels. These inducible mouse models have provided a tool to study the molecular and cellular basis of inherited skin disorders and have shown implications for gene therapy approaches for EBS and other dominantly inherited diseases. Another interesting model of EBS has been developed by co-overexpression of human KRT5 and KRT14_R125C which resulted in a blistering phenotype in Drosophila and this model was useful to investigate the effect of different keratin mutations, their

cellular consequences and provide opportunity for rapid genetic and therapeutic screens (Bohnekamp et al., 2015). However, these animal models have not provided the opportunity of direct *in vivo* imaging of basal keratinocytes which express mutant keratins to understand their behavior. Regardless of the incredible progress made in understanding the molecular basis of different forms of epidermolysis bullosa, there is no cure for this disease. Generating alternative model that recapitulates human EBS is necessary and zebrafish will play a role in further dissecting the molecular mechanisms, cellular and subcellular aspects of the disease *in vivo*, but also establishing commonalities, converging and diverging mechanisms and realize a cure.

In the present study, I created transgenic lines of zebrafish by overexpressing dominant negative zebrafish and human keratins, *Tg*(*krtt1c19e:eGFP-krtt1c19e_R124C*) and *Tg*(*krtt1c19e:eGFP-KRT14_R125P*), and their wild type forms, driven by a 3.9kb basal cell promoter type I keratin, zebrafish *krtt1c19e* (R. T. Lee et al., 2014). I demonstrated that both zebrafish and human keratins are specifically expressed in the basal keratinocytes by this promoter activity.

To my knowledge, this is the first epidermolysis bullosa simplex zebrafish model, and I have examined the EBS zebrafish model for any abnormalities including skin defect from embryo to adult stage. I used zebrafish larva at 5dpf and 16dpf to characterize basal keratinocyte behavior and to look for possible epidermolysis bullosa simplex phenotypes. These time points were selected for the following reasons. (1) During development, basally localized cytokeratin becomes apparent in basal epidermal cells by 3dpf in which the zebrafish larval epidermis consists of

an outermost periderm called enveloping layer (EVL) and the basal epidermis (Sonawane et al., 2005). (2) The formation of important cell adhesion protein complexes such as hemidesmosome starts at 4 to 5dpf (Sonawane et al., 2005). This is the time when the basal layer become more flattened and their cytoplasm is more electro dense than earlier developmental stages and the BM facing the basal keratinocytes is thicker (Le Guellec et al., 2003). (3) The *krtt1c19e* promoter is strongly active by this point (R. T. Lee et al., 2014). (4) Zebrafish basal keratinocytes starts to stratify beyond 16dpf. At this stage the epidermis is thick because of a third layer formation and specialized mucous goblet cells start to differentiate (Le Guellec et al., 2003), these extra cells make imaging difficult as they also express *krtt1c19e.* In the EBS zebrafish model, I have been able to image basal keratinocytes expressing dominant negative zebrafish and human keratins *in vivo* in an attempt to understand their behavior.

I found that overexpression of the zebrafish Krtt1c19e_R124C protein does not appear to have an effect on the assembly of keratin intermediate filaments in basal keratinocytes either at normal condition or upon stress. The keratin intermediate filament networks formed in transgenic fish overexpressing mutant zebrafish keratin do not differ from the transgenic line overexpressing the wild type form. And, I observed no evidence of blistering, aggregate production, and keratin bundle or network rupture even when the transgenic fish were subjected to stress such as temperature. This could be because of the presence of highly adapted chaperones. Protein folding disorders of type I and type II keratin intermediate filaments can be

stabilized by interacting with associated proteins including small chaperones (Coulombe & Wong, 2004).

Likewise, transgenic zebrafish overexpressing dominant negative human keratins were healthy, refractory to blisters and showed no gross alterations in phenotype under normal condition, confirmed by immunofluorescent, histological and ultrastructural analysis, similar to the previous observations in inducible mouse model developed for epidermolysis bullosa simplex (Arin & Roop, 2004; Cao, Longley, Wang, & Roop, 2001). However, subtle cellular phenotypes such as changes in keratin distribution in the basal keratinocytes, cell shape and cell adhesion defects between neighboring basal cells was observed, only in the EBS zebrafish model harboring the mutation, KRT14_R125P. These cellular phenotypes observed under normal condition in our epidermolysis bullosa simplex zebrafish model were not reported in previous studies, potentially because of the experimentally inaccessibility of the animal models to visualize cellular and subcellular behavior *in vivo*.

In the unstressed EBS zebrafish model, I noticed a slight yet reproducible gap between neighboring basal cells expressing mutant human keratin. Potentially the overexpression of dominant negative human keratin is affecting proper polymerization processes with the endogenous partner protein and impairs formation of keratin intermediate filaments leading to dysfunction of desmosomes. The perturbation in connection between the IF and desmosomes and hemidesmosomes may underlie detachment between the basal cells and cytolysis (Uttam et al., 1996). Previous studies have demonstrated that overexpression of

mutant keratins and loss of keratins caused cell-cell adhesion defects due to destabilization of desmosome protein complexes (Bär et al., 2014; Kröger et al., 2013; Seltmann et al., 2013). For example, a study on human keratinocytes cell lines, derived from KRT14_R125P mutation carrying EBS patients, have shown down regulation of desmosome protein complexes such as desmoplakin, plakoglobin and desmoglein 3 (Liovic et al., 2009). In this study, immunostaining analysis showed high E-cadherin signal in basal keratinocytes of the mutant fish under normal condition suggesting that E-cadherin might be compensating for the function of desmosomes. However, E-cadherin expression become diffuse and punctuated when subjected to thermal stress. Keratin- hemidesmosome (cell-matrix) adhesion is essential in maintaining the structural integrity of the skin (Ridley et al., 2003). Mutations in keratin-hemidesmosome protein complex leads to disruption of the adhesion complex and causes skin blistering disorder such as epidermolysis bullosa (J. D. Fine, 2010). Nevertheless, no defect in cell-matrix adhesion was noted in our unstressed EBS zebrafish model according to cryosection and TEM analysis.

I employed the physiologically relevant stressors that have been previously used to test the behavior of keratinocytes in vitro from epidermolysis bullosa simplex patients such as osmotic stress and thermal stress. To induce epidermolysis bullosa simplex phenotypes in our transgenic fish, I tested osmotic shock (different dilution of E3 medium) and thermal shocks (heat shock at 40 ^{0}C and cold shock at 18 ^{0}C), and treated them for an hour.

I found that osmotic stress had no effect on the transgenic zebrafish overexpressing mutant zebrafish or human keratins. In contrast, previous in vitro studies revealed keratin filament fragmentation and keratin aggregates at the edge of the cells following osmotic shock in cells expressing KRT14_R125P (considered a severe mutation of the keratin protein as the position of the mutations in the keratin protein is generally correlated with the severity of the disease phenotype) (D'Alessandro, Russell, Morley, Davies, & Lane, 2002). In the same in vitro study, no aggregates were present in less severe mutations (e.g. KRT14_V270M) when subjected to osmotic shock.

I demonstrated that the production of keratin aggregates and detachment of basal keratinocytes in epidermolysis bullosa zebrafish model overexpressing mutant human keratin through immunofluorescent and live imaging upon heat and cold stress. This finding is in agreement with previous studies which have shown the same phenotype in vitro using epidermolysis bullosa simplex cell lines where they used heat stress at 43 ^{0}C for 30 minutes to induce keratin aggregate production where most of the cytoskeletal network was affected and keratin aggregates mostly confined to the cell periphery (Chamcheu et al., 2009). In our case, the keratin aggregates were more pronounced in the nucleus of the basal cells. This might be because keratins traffic to the nucleus during stress (Hobbs, Jacob, & Coulombe, 2016). Although experimental evidence is lacking on the effect of cold shock in keratin intermediate filaments of EBS patients, I showed here in this study that the

basal keratinocytes from the EBS zebrafish model exhibited a dramatic alterations in keratin intermediate filament networks when subjected to cold stress.

In addition, morphological changes, partial disruption and sliding of the basal keratinocytes over the dermis were observed through time-lapse imaging. This might be due to the lack of connection between the keratin intermediate filament network of the basal layer and hemidesmosomes connecting to the underlying basement membrane. This may cause microblisters in the basal layer of the epidermis (Coulombe et al., 2009). In addition, histological sections of heat treated EBS adult zebrafish model overexpressing mutant human keratin (KRT14_R125P) showed disruption of the superficial layer of the epidermis.

I have demonstrated that the overexpression of dominant negative human keratin can interfere with keratin filament assembly *in vivo* and perturb proper keratin network formation in zebrafish upon exposure to stress factors. Thus, this mirrors aspects of epidermolysis bullosa simplex as an inherited skin blistering disorder characterized by blistering of skin in response to mild mechanical trauma due to rupture of basal keratinocytes (Bonifas et al., 1991; M. Coulombe et al., 1991; Lane et al., 1992).

Skin fragility may result in bacterial infection which is one of the major problems of EB patients (Arnold, Bruckner-Tuderman, Züger, & Itin, 2009). The EBS zebrafish model is well suited for infection analysis via live imaging which could help to look for any difference in immune response between wild type and mutant. This EBS zebrafish model could also be used to study wound healing and evaluate

the effect of mutant keratins on the re-epithelization process. It will allow *in vivo* visualization of the recovery process and mimicking and viewing relapses and healing, through controlling temperature the mutants are exposed to. This is unprecedented as an *in vivo* tool in the EB field.

4.2. Dystrophic Epidermolysis Bullosa

Dystrophic epidermolysis bullosa is the most severe and lethal form of EB due to loss of function in type VII collagen in human (Webber et al., 2017). The gene (*COL7A1*) coding for collagen VII is produced by basal keratinocytes and fibroblasts and associates the lamina densa with the underlying papillary dermal collagen fibrils (Burgeson, 1993). Different mutations in *COL7A1* gene result in a variety of phenotypes. Identical *COL7A1* mutations often result in disease variability even in monozygotic twins, suggesting that additional modifiers contribute to DEB (Odorisio et al., 2014). *Col7a1* knockout mice have been generated to understand the molecular mechanism of dystrophic epidermolysis bullosa (Heinonen et al., 1999). However, the *Col7a1* null mice, born with extensive skin blistering, died during the first two weeks of life. Another collagen VII hypomorphic mouse model for DEB was generated which expressed one tenth of the normal level of collagen VII and developed phenotypes similar to human DEB (Fritsch et al., 2008) and this mouse model have suggested that fibroblast based therapy can be used to treat DEB. Despite the presence of more than 700 different mutations in DEB patients (Wertheim- Tysarowska et al., 2012), no effective treatment is available at the moment. because of lack of aminal models

that recapitulates the disease condition at both phenotypic and genotypic levels which will be valuable to further understand the pathophysiology of the disease.

In order to establish a dystrophic epidermolysis bullosa model in zebrafish, I have identified zebrafish *col7a1* genes from ensembl genome browser and I found two paralogues, *col7a1a* and *col7a1b*, at chromosome 6 and 4, respectively. I characterized their spatio-temporal expression by RT_PCR and whole mount in situ hybridization whereby both zebrafish *col7a1* genes were not maternally deposited but were expressed zygotically in the basal keratinocytes, suggesting that type VII collagens encoded by the two genes may have similar function to that in humans.

Subsequently, I generated *col7a1* double knockout zebrafish using CRISPR/Cas9 system. Genotypically, the fish developed in this study were *col7a1* null to mimic the absence of *COL7A*1 in human. However, I observed no evidence of dystrophic epidermolysis bullosa phenotype. Transmission electron microscopy confirmed that there was no difference in the ultrastructure of the skin in the double knockout and wild type fish. This was surprising as loss of function of type VII collagen in human has been associated with blistering of the skin and patients die within a few days after birth(A. Christiano, Crollick, Pincus, & Uitto, 1999; A. M. Christiano, McGrath, Tan, & Uitto, 1996; J.-D. Fine et al., 2008; Shimizu, Suzumori, & Nishikawa, 1996).

In previous studies, it has also been demonstrated that a *col7a1* knockout mice developed blisters of the skin and mucous membrane of the oral cavity, erosions on

the feet, resulting in death within the first two weeks of life from complications of the disease (Heinonen et al., 1999). Specifically, no type VII collagen peptide could be detected by proteomics analysis using SWATH MS analysis at 30hpf and 5dpf. However, significant increase of three collagens namely, *col28a2*, *co6a2a* and *col14a1b* was detected. The findings presented here may also that upregulation of these collagens in double knockout fish may be compensating the function of type VII collagen and help maintain the structural integrity of the skin.

Collagen VI is ubiquitously expressed in connective tissue and important for structural integrity, cell adhesion and migration. In human and mouse, defects in Collagen VI causes a heterogeneous group of neuromuscular disorders (Bethlem & Wijngaarden, 1976; Merlini et al., 2008; Ullrich, 1930). Likewise, It has been shown that Col6a2 deficiency leads to muscle defect in zebrafish (Ramanoudjame et al., 2015). Collagen XIV null mice showed dysfunction fibrillogenesis in tendon and skin (Ansorge et al., 2009) in which the protein is involved as a regulator of fibrillogenesis. It has also been shown that *col14a1b* is expressed after 32hpf in zebrafish (H. L. Bader et al., 2013), but its spatio temporal expression and function is not yet explored. Little is known about Collagen XXVIII. This genetic compensation could help to identify the potential targets for therapeutic approaches against dystrophic epidermolysis bullosa.

On the other hand, we detected only one putative type VII collagen peptide using SWATH MS analysis in the adult double knockout fish. This could suggest that the presence of a transcription or translation start site after the site of mutation or exon skipping leading to a functional but N-terminally truncated type VII collagen. It

has been shown that alternative splicing through exon skipping, non-sense associated splicing or using cryptic splicing sites provides multicellular organisms with an extended proteome, the possibility of cell type and species specific protein isoforms without increasing the gene number, and the possibility of regulating the production of different proteins through specific signaling pathways (Anderson et al., 2017; Keren et al., 2010; Kornblihtt et al., 2013; Modrek & Lee, 2002). I am currently generating another double knockout to double confirm the status of type VII collagen targeting a more 3' exons to see if I can mimic DEB phenotype in zebrafish.

According to our proteomics analysis, we found upregulation of three collagens form the SWATH MS data namely, Col28a2, Col6a2a and Col14a1b, which might potentially be compensating the function of collagen VII. Further experiment could be performed to characterize or inhibit these upregulated collagens to understand their function in maintaining integrity of the skin. Generating epidermolysis bullosa zebrafish model will provide insights into molecular mechanism of heritable skin diseases and demonstrate zebrafish epidermis in modelling human diseases which can be used a fast drug screening platform for developing therapeutic targets. The drugs could alter expression of keratins, target unfolded keratin proteins and upregulate molecular chaperones responsible for directing protein folding and maintaining proper protein confirmation that could rescue structural defects of EB.

CHAPTER 6. REFERENCES

Aberdam, D., Gambaro, K., Rostagno, P., Aberdam, E., Divonne, S. d. l. F., & Rouleau, M. (2007). Key role of p63 in BMP-4-induced epidermal commitment of embryonic stem cells. *Cell cycle, 6*(3), 291-294.

Agarwal, P., Chhaperwal, M. K., Singh, A., Verma, A., Nijhawan, M., Singh, K., & Mathur, D. (2013). Pachyonychia congenita: A rare genodermatosis. *Indian dermatology online journal, 4*(3), 225.

Albers, K., & Fuchs, E. (1987). The expression of mutant epidermal keratin cDNAs transfected in simple epithelial and squamous cell carcinoma lines. *The Journal of cell biology, 105*(2), 791-806.

Albers, K., & Fuchs, E. (1989). Expression of mutant keratin cDNAs in epithelial cells reveals possible mechanisms for initiation and assembly of intermediate filaments. *The Journal of cell biology, 108*(4), 1477-1493.

Alberts, B., Johnson, A., Lewis, J., Raff, M., Roberts, K., & Walter, P. (2002). Cell junctions.

Alikhan, A., Farshidi, D., & Shwayder, T. (2009). Case of mistaken identity: bullous congenital ichthyosiform erythroderma mistaken as epidermolysis bullosa simplex. *Dermatology online journal, 15*(9).

Amsterdam, A., Burgess, S., Golling, G., Chen, W., Sun, Z., Townsend, K., . . . Hopkins, N. (1999). A large-scale insertional mutagenesis screen in zebrafish. *Genes & development, 13*(20), 2713-2724.

Anderson, J. L., Mulligan, T. S., Shen, M.-C., Wang, H., Scahill, C. M., Tan, F. J., . . . Farber, S. A. (2017). mRNA processing in mutant zebrafish lines generated by chemical and CRISPR-mediated mutagenesis produces unexpected transcripts that escape nonsense-mediated decay. *PLoS genetics, 13*(11), e1007105.

Ansorge, H. L., Meng, X., Zhang, G., Veit, G., Sun, M., Klement, J. F., . . . Birk, D. E. (2009). Type XIV collagen regulates fibrillogenesis: premature collagen fibril growth and tissue dysfunction in null mice. *Journal of Biological Chemistry*.

Anton-Lamprecht, I., & Schnyder, U. (1982). Epidermolysis bullosa herpetiformis Dowling-Meara. *Dermatology, 164*(4), 221-235.

Arin, M. J., & Roop, D. R. (2004). Inducible mouse models for inherited skin diseases: implications for skin gene therapy. *Cells Tissues Organs, 177*(3), 160-168.

Arnold, A. W., Bruckner-Tuderman, L., Züger, C., & Itin, P. H. (2009). Cetuximab therapy of metastasizing cutaneous squamous cell carcinoma in a patient with severe recessive dystrophic epidermolysis bullosa. *Dermatology, 219*(1), 80-83.

Atherton, D. J., & Denyer, J. (2003). Epidermolysis Bullosa: an outline for Professionals. *Adapted from the chapter Epidermolysis Bullosa written for Textbook of Paediatric Dermatology, edited by Harper JI, Oranje AP and Prose NS*.

Bader, B. L., Magin, T. M., Hatzfeld, M., & Franke, W. W. (1986). Amino acid sequence and gene organization of cytokeratin no. 19, an exceptional tail-less intermediate filament protein. *The EMBO journal, 5*(8), 1865-1875.

Bader, H. L., Lambert, E., Guiraud, A., Malbouyres, M., Driever, W., Koch, M., & Ruggiero, F. (2013). Zebrafish collagen XIV is transiently expressed in epithelia and is required for proper function of certain basement membranes. *Journal of Biological Chemistry*, jbc. M112. 430637.

Bakkers, J., Hild, M., Kramer, C., Furutani-Seiki, M., & Hammerschmidt, M. (2002). Zebrafish ΔNp63 is a direct target of Bmp signaling and encodes a transcriptional

repressor blocking neural specification in the ventral ectoderm. *Developmental cell, 2*(5), 617-627.

Banerjee, S., Wu, Q., Yu, P., Qi, M., & Li, C. (2014). In silico analysis of all point mutations on the 2B domain of K5/K14 causing epidermolysis bullosa simplex: a genotype–phenotype correlation. *Molecular Biosystems, 10*(10), 2567-2577.

Bär, J., Kumar, V., Roth, W., Schwarz, N., Richter, M., Leube, R. E., & Magin, T. M. (2014). Skin fragility and impaired desmosomal adhesion in mice lacking all keratins. *Journal of Investigative Dermatology, 134*(4), 1012-1022.

BARTEK, J., TAYLOR-PAPADIMITRIOU, J., MILLER, N., & MILLIS, R. (1985). Patterns of expression of keratin 19 as detected with monoclonal antibodies in human breast tissues and tumours. *International journal of cancer, 36*(3), 299-306.

Bazzoni, G., & Dejana, E. (2001). Pores in the sieve and channels in the wall: control of paracellular permeability by junctional proteins in endothelial cells. *Microcirculation, 8*(3), 143-152.

Bchetnia, M., Tremblay, M.-L., Leclerc, G., Dupérée, A., Powell, J., McCuaig, C., . . . Laprise, C. (2012). Expression signature of epidermolysis bullosa simplex. *Human genetics, 131*(3), 393-406.

Bethlem, J., & Wijngaarden, G. K. (1976). Benign myopathy, with autosomal dominant inheritance. A report on three pedigrees. *Brain: a journal of neurology, 99*(1), 91-100.

Birk, D. E., & Brückner, P. (2011). Collagens, suprastructures, and collagen fibril assembly *The extracellular matrix: an overview* (pp. 77-115): Springer.

Black, D. L. (2000). Protein diversity from alternative splicing: a challenge for bioinformatics and post-genome biology. *Cell, 103*(3), 367-370.

Blackburn, P. R., Campbell, J. M., Clark, K. J., & Ekker, S. C. (2013). The CRISPR system—keeping zebrafish gene targeting fresh: Mary Ann Liebert, Inc. 140 Huguenot Street, 3rd Floor New Rochelle, NY 10801 USA.

Blencowe, B. J. (2006). Alternative splicing: new insights from global analyses. *Cell, 126*(1), 37-47.

Boeira, V. L. S. Y., Souza, E. S., Rocha, B. d. O., Oliveira, P. D., Oliveira, M. d. F. S. P., Rêgo, V. R. P. d. A., & Follador, I. (2013). Inherited epidermolysis bullosa: clinical and therapeutic aspects. *Anais brasileiros de dermatologia, 88*(2), 185-198.

Bonifas, J., Rothman, A., & Epstein, E. (1991). Epidermolysis bullosa simplex: evidence in two families for keratin gene abnormalities. *Science, 254*(5035), 1202-1205.

Bowden, P. E., Haley, J. L., Kansky, A., Rothnagel, J. A., Jones, D. O., & Turner, R. J. (1995). Mutation of a type II keratin gene (K6a) in pachyonychia congenita. *Nature genetics, 10*(3), 363.

Bruckner-Tuderman, L. (2010). Dystrophic epidermolysis bullosa: pathogenesis and clinical features. *Dermatologic clinics, 28*(1), 107-114.

Bruckner-Tuderman, L., & Aimee, S. (2008). Epidermal and Epidermal–Dermal Adhesion.

Burgeson, R. E. (1993). Type VII collagen, anchoring fibrils, and epidermolysis bullosa. *Journal of Investigative Dermatology, 101*(3), 252-255.

Burgeson, R. E., & Christiano, A. M. (1997). The dermal—epidermal junction. *Current opinion in cell biology, 9*(5), 651-658.

Burgeson, R. E., Morris, N. P., Murray, L. W., Duncan, K. G., Keene, D. R., & Sakai, L. Y. (1985). The Structure of Type VII Collagen a. *Annals of the New York Academy of Sciences, 460*(1), 47-57.

Candi, E., Schmidt, R., & Melino, G. (2005). The cornified envelope: a model of cell death in the skin. *Nature reviews Molecular cell biology, 6*(4), 328.

Cao, T., Longley, M. A., Wang, X.-J., & Roop, D. R. (2001). An inducible mouse model for epidermolysis bullosa simplex: implications for gene therapy. *The Journal of cell biology, 152*(3), 651-656.

Carney, T. J., Feitosa, N. M., Sonntag, C., Slanchev, K., Kluger, J., Kiyozumi, D., . . . Sekiguchi, K. (2010). Genetic analysis of fin development in zebrafish identifies furin and hemicentin1 as potential novel fraser syndrome disease genes. *PLoS genetics, 6*(4), e1000907.

Carney, T. J., von der Hardt, S., Sonntag, C., Amsterdam, A., Topczewski, J., Hopkins, N., & Hammerschmidt, M. (2007). Inactivation of serine protease Matriptase1a by its inhibitor Hai1 is required for epithelial integrity of the zebrafish epidermis. *Development, 134*(19), 3461-3471.

Castiglia, D., & Zambruno, G. (2010). Molecular testing in epidermolysis bullosa. *Dermatologic clinics, 28*(2), 223-229.

Chamcheu, J. C., Lorié, E. P., Akgul, B., Bannbers, E., Virtanen, M., Gammon, L., . . . Törmä, H. (2009). Characterization of immortalized human epidermolysis bullosa simplex (KRT5) cell lines: trimethylamine N-oxide protects the keratin cytoskeleton against disruptive stress condition. *Journal of dermatological science, 53*(3), 198-206.

Chan, Y.-m., Anton-Lamprecht, I., Yu, Q.-C., Jäckel, A., Zabel, B., Ernst, J.-P., & Fuchs, E. (1994). A human keratin 14" knockout": the absence of K14 leads to severe epidermolysis bullosa simplex and a function for an intermediate filament protein. *Genes & development, 8*(21), 2574-2587.

Chen, M. A., Bonlfas, J. M., Matsumura, K., Blumenfeld, A., & Epstein Jr, E. H. (1993). A novel three-nucleotide deletion in the helix 2B region of keratin 14 in epidermolysis bullosa simples: δE375. *Human molecular genetics, 2*(11), 1971-1972.

Cheng, J., Syder, A. J., Yu, Q.-C., Letal, A., Paller, A. S., & Fuchs, E. (1992). The genetic basis of epidermolytic hyperkeratosis: a disorder of differentiation-specific epidermal keratin genes. *Cell, 70*(5), 811-819.

Cherdantseva, E. M., & Cherdantsev, V. G. (2003). Geometry and mechanics of teleost gastrulation and the formation of primary embryonic axes. *International Journal of Developmental Biology, 50*(2-3), 157-168.

Christiano, A., Crollick, J., Pincus, S., & Uitto, J. (1999). Squamous cell carcinoma in a family with dominant dystrophic epidermolysis bullosa: a molecular genetic study. *Experimental dermatology, 8*(2), 146-152.

Christiano, A. M., Hoffman, G. G., Chung-Honet, L. C., Lee, S., Cheng, W., Uitto, J., & Greenspan, D. S. (1994). Structural organization of the human type VII collagen gene (COL7A1), composed of more exons than any previously characterized gene. *Genomics, 21*(1), 169-179.

Christiano, A. M., McGrath, J. A., Tan, K. C., & Uitto, J. (1996). Glycine substitutions in the triple-helical region of type VII collagen result in a spectrum of dystrophic epidermolysis bullosa phenotypes and patterns of inheritance. *American journal of human genetics, 58*(4), 671.

Clark, P. W. (2003). Genetic Analysis of the Skin Disorder Weber-Cockayne Type Epidermolysis Simplex. *Senior Thesis Projects, 2003-2006*, 15.

Colombatti, A., Bonaldo, P., & Doliana, R. (1993). Type A modules: interacting domains found in several non-fibrillar collagens and in other extracellular matrix proteins. *Matrix, 13*(4), 297-306.

Concha, M. I., Molina, S. a., Oyarzún, C., Villanueva, J., & Amthauer, R. (2003). Local expression of apolipoprotein AI gene and a possible role for HDL in primary defence in the carp skin. *Fish & shellfish immunology, 14*(3), 259-273.

Conrad, M., Lemb, K., Schubert, T., & Markl, J. (1998). Biochemical identification and tissue-specific expression patterns of keratins in the zebrafish Danio rerio. *Cell and Tissue Research, 293*(2), 195-205.

Corden, L. D., & McLean, W. (1996). Human keratin diseases: hereditary fragility of specific epithelial tissues. *Experimental dermatology, 5*(6), 297-307.

Coulombe, M., Hao, L., Calcinaro, F., Gill, R., Eugui, E., Allison, A., & Lafferty, K. (1991). *Tolerance induction in adult animals: comparison of RS-61443 and anti-CD4 treatment.* Paper presented at the Transplantation proceedings.

Coulombe, P. A., Chan, Y. M., Albers, K., & Fuchs, E. (1990). Deletions in epidermal keratins leading to alterations in filament organization in vivo and in intermediate filament assembly in vitro. *The Journal of cell biology, 111*(6), 3049-3064.

Coulombe, P. A., Hutton, M. E., Letal, A., Hebert, A., Paller, A. S., & Fuchs, E. (1991). Point mutations in human keratin 14 genes of epidermolysis bullosa simplex patients: genetic and functional analyses. *Cell, 66*(6), 1301-1311.

Coulombe, P. A., Hutton, M. E., Vassar, R., & Fuchs, E. (1991). A function for keratins and a common thread among different types of epidermolysis bullosa simplex diseases. *The Journal of cell biology, 115*(6), 1661-1674.

Coulombe, P. A., Kerns, M. L., & Fuchs, E. (2009). Epidermolysis bullosa simplex: a paradigm for disorders of tissue fragility. *The Journal of clinical investigation, 119*(7), 1784-1793.

Coulombe, P. A., & Lee, C.-H. (2012). Defining keratin protein function in skin epithelia: epidermolysis bullosa simplex and its aftermath. *Journal of Investigative Dermatology, 132*(3), 763-775.

Coulombe, P. A., & Omary, M. B. (2002). 'Hard'and 'soft'principles defining the structure, function and regulation of keratin intermediate filaments. *Current opinion in cell biology, 14*(1), 110-122.

Coulombe, P. A., & Wong, P. (2004). Cytoplasmic intermediate filaments revealed as dynamic and multipurpose scaffolds. *Nature cell biology, 6*(8), 699.

Covello, S. (1998). Keratin 17 mutations cause either steatocystoma multiplex or pachyonyshia congenita type 2. *The Journal of investigative dermatology, 110*, 614.

D'Alessandro, M., Russell, D., Morley, S. M., Davies, A. M., & Lane, E. B. (2002). Keratin mutations of epidermolysis bullosa simplex alter the kinetics of stress response to osmotic shock. *Journal of cell science, 115*(22), 4341-4351.

Dooley, K., & Zon, L. I. (2000). Zebrafish: a model system for the study of human disease. *Current opinion in genetics & development, 10*(3), 252-256.

Eriksson, J. E., Dechat, T., Grin, B., Helfand, B., Mendez, M., Pallari, H.-M., & Goldman, R. D. (2009). Introducing intermediate filaments: from discovery to disease. *The Journal of clinical investigation, 119*(7), 1763-1771.

Fine, J.-D., Bruckner-Tuderman, L., Eady, R. A., Bauer, E. A., Bauer, J. W., Has, C., . . . Jonkman, M. F. (2014). Inherited epidermolysis bullosa: updated

recommendations on diagnosis and classification. *Journal of the American Academy of Dermatology, 70*(6), 1103-1126.

Fine, J.-D., Eady, R. A., Bauer, E. A., Bauer, J. W., Bruckner-Tuderman, L., Heagerty, A., . . . Leigh, I. (2008). The classification of inherited epidermolysis bullosa (EB): Report of the Third International Consensus Meeting on Diagnosis and Classification of EB. *Journal of the American Academy of Dermatology, 58*(6), 931-950.

Fine, J. D. (2010). Inherited epidermolysis bullosa: recent basic and clinical advances. *Current opinion in pediatrics, 22*(4), 453-458. doi: 10.1097/MOP.0b013e32833bb74f

Fine, J. D., Johnson, L., Weiner, M., & Suchindran, C. (2004). Assessment of mobility, activities and pain in different subtypes of epidermolysis bullosa. *Clinical and Experimental Dermatology: Clinical dermatology, 29*(2), 122-127.

Fishelson, L. (1984). A comparative study of ridge-mazes on surface epithelial cell-membranes of fish scales (Pisces, Teleostei). *Zoomorphology, 104*(4), 231-238.

Fritsch, A., Loeckermann, S., Kern, J. S., Braun, A., Bösl, M. R., Bley, T. A., . . . Erlacher, M. (2008). A hypomorphic mouse model of dystrophic epidermolysis bullosa reveals mechanisms of disease and response to fibroblast therapy. *The Journal of clinical investigation, 118*(5), 1669-1679.

Fuchs, E., & Green, H. (1980). Changes in keratin gene expression during terminal differentiation of the keratinocyte. *Cell, 19*(4), 1033-1042.

Fuchs, E., & Raghavan, S. (2002). Getting under the skin of epidermal morphogenesis. *Nature Reviews Genetics, 3*(3), 199.

Fuchs, E., & Weber, K. (1994). Intermediate filaments: structure, dynamics, function and disease. *Annual review of biochemistry, 63*(1), 345-382.

Furuse, M., Hata, M., Furuse, K., Yoshida, Y., Haratake, A., Sugitani, Y., . . . Tsukita, S. (2002). Claudin-based tight junctions are crucial for the mammalian epidermal barrier: a lesson from claudin-1–deficient mice. *The Journal of cell biology, 156*(6), 1099-1111.

Glover, C. N., Bucking, C., & Wood, C. M. (2013). The skin of fish as a transport epithelium: a review. *Journal of Comparative Physiology B, 183*(7), 877-891.

Gong, Z., Ju, B., Wang, X., He, J., Wan, H., Sudha, P. M., & Yan, T. (2002). Green fluorescent protein expression in germ-line transmitted transgenic zebrafish under a stratified epithelial promoter from Keratin8. *Developmental dynamics, 223*(2), 204-215.

González, Z. L. (2013). *Percutaneous absorption of UV filters contained in sunscreen cosmetic products: Development of analytical methods*: Springer Science & Business Media.

Grando, S. A., Grando, A. A., Glukhenky, B. T., Doguzovc, V., Nguyen, V. T., & Holubar, K. (2003). History and clinical significance of mechanical symptoms in blistering dermatoses: a reappraisal. *Journal of the American Academy of Dermatology, 48*(1), 86-92.

Graveley, B. R. (2001). Alternative splicing: increasing diversity in the proteomic world. *TRENDS in Genetics, 17*(2), 100-107.

Greenspan, D. S. (1993). The carboxyl-terminal half of type VII collagen, including the non-collagenous NC-2 domain and intron/exon organization of the corresponding region of the COL7A1 gene. *Human molecular genetics, 2*(3), 273-278.

Gurtner, G. C., Werner, S., Barrandon, Y., & Longaker, M. T. (2008). Wound repair and regeneration. *Nature, 453*(7193), 314.

Haake, A., Scott, G. A., & Holbrook, K. A. (2001). Structure and function of the skin: overview of the epidermis and dermis. *The biology of the skin, 2001*, 19-45.

Hamada, T., Fukuda, S., Ishii, N., Abe, T., Nagata, K., Koro, O., . . . Hashimoto, T. (2009). A Japanese family with dominant pretibial dystrophic epidermolysis bullosa: Identification of a new glycine substitution in the triple-helical collagenous domain of type VII collagen. *Journal of dermatological science, 54*(3), 212-214.

Haschek, W. M., Rousseaux, C. G., Wallig, M. A., Bolon, B., & Ochoa, R. (2013). *Haschek and Rousseaux's handbook of toxicologic pathology*: Academic Press.

Hawkes, J. W. (1974). The structure of fish skin. *Cell and Tissue Research, 149*(2), 147-158.

Heinonen, S., Mannikko, M., Klement, J. F., Whitaker-Menezes, D., Murphy, G. F., & Uitto, J. (1999). Targeted inactivation of the type VII collagen gene (Col7a1) in mice results in severe blistering phenotype: a model for recessive dystrophic epidermolysis bullosa. *J Cell Sci, 112*(21), 3641-3648.

Heisenberg, C.-P., & Tada, M. (2002). *Zebrafish gastrulation movements: bridging cell and developmental biology.* Paper presented at the Seminars in cell & developmental biology.

Herrmann, H., & Aebi, U. (2004). Intermediate filaments: molecular structure, assembly mechanism, and integration into functionally distinct intracellular scaffolds. *Annual review of biochemistry, 73*(1), 749-789.

Herrmann, H., Strelkov, S. V., Burkhard, P., & Aebi, U. (2009). Intermediate filaments: primary determinants of cell architecture and plasticity. *The Journal of clinical investigation, 119*(7), 1772-1783.

Hertl, M., Eming, R., & Veldman, C. (2006). T cell control in autoimmune bullous skin disorders. *The Journal of clinical investigation, 116*(5), 1159-1166.

Hesse, M., Zimek, A., Weber, K., & Magin, T. M. (2004). Comprehensive analysis of keratin gene clusters in humans and rodents. *European journal of cell biology, 83*(1), 19-26.

Hirsch, T., Rothoeft, T., Teig, N., Bauer, J. W., Pellegrini, G., De Rosa, L., . . . Kneisz, D. (2017). Regeneration of the entire human epidermis using transgenic stem cells. *Nature, 551*(7680), 327.

Hobbs, R. P., Jacob, J. T., & Coulombe, P. A. (2016). Keratins are going nuclear. *Developmental cell, 38*(3), 227-233.

Holmbeck, K., & Szabova, L. (2006). Aspects of extracellular matrix remodeling in development and disease. *Birth Defects Research Part C: Embryo Today: Reviews, 78*(1), 11-23.

Ishida-Yamamoto, A., McGrath, J. A., Chapman, S. J., Leigh, I. M., Lane, E. B., & Eady, R. A. (1991). Epidermolysis bullosa simplex (Dowling-Meara type) is a genetic disease characterized by an abnormal keratin-filament network involving keratins K5 and K14. *Journal of Investigative Dermatology, 97*(6), 959-968.

James, W., Berger, T., & Elston, D. (2006). Skin: basic structure and function. *Andrew's Diseases of the Skin-Clinical Dermatology, James WD, Berger TG, Elston DM (eds), 10a ed, Canada, Saunders Elsevier*, 18.

Jiang, C., Magnaldo, T., Ohtsuki, M., Freedberg, I., Bernerd, F., & Blumenberg, M. (1993). Epidermal growth factor and transforming growth factor alpha specifically induce the activation-and hyperproliferation-associated keratins 6 and 16. *Proceedings of the National Academy of Sciences, 90*(14), 6786-6790.

Jobard, F., Bouadjar, B., Caux, F., Hadj-Rabia, S., Has, C., Matsuda, F., . . . Fischer, J. (2003). Identification of mutations in a new gene encoding a FERM family protein with a

pleckstrin homology domain in Kindler syndrome. *Human molecular genetics, 12*(8), 925-935.

Jones, J. C., Hopkinson, S. B., & Goldfinger, L. E. (1998). Structure and assembly of hemidesmosomes. *Bioessays, 20*(6), 488-494.

Kanitakis, J. (2002). Anatomy, histology and immunohistochemistry of normal human skin. *European journal of dermatology: EJD, 12*(4), 390-399; quiz 400-391.

Kawakami, K. (2004). Transgenesis and gene trap methods in zebrafish by using the Tol2 transposable element *Methods in cell biology* (Vol. 77, pp. 201-222): Elsevier.

Kawakami, K., Takeda, H., Kawakami, N., Kobayashi, M., Matsuda, N., & Mishina, M. (2004). A transposon-mediated gene trap approach identifies developmentally regulated genes in zebrafish. *Dev Cell, 7*(1), 133-144. doi: 10.1016/j.devcel.2004.06.005

Keren, H., Lev-Maor, G., & Ast, G. (2010). Alternative splicing and evolution: diversification, exon definition and function. *Nature Reviews Genetics, 11*(5), 345.

Kierszenbaum, A. L., & Tres, L. (2015). *Histology and Cell Biology: An Introduction to Pathology E-Book*: Elsevier Health Sciences.

Kim, S. H., Choi, H. Y., So, J.-H., Kim, C.-H., Ho, S.-Y., Frank, M., . . . Uitto, J. (2010). Zebrafish type XVII collagen: gene structures, expression profiles, and morpholino "knock-down" phenotypes. *Matrix biology, 29*(7), 629-637.

Kimmel, C. B., Ballard, W. W., Kimmel, S. R., Ullmann, B., & Schilling, T. F. (1995). Stages of embryonic development of the zebrafish. *Developmental dynamics, 203*(3), 253-310.

Kimmel, C. B., Ballard, W. W., Kimmel, S. R., Ullmann, B., & Schilling, T. F. (1995). Stages of embryonic development of the zebrafish. *Dev Dyn, 203*(3), 253-310. doi: 10.1002/aja.1002030302

Kimmel, C. B., Warga, R. M., & Schilling, T. F. (1990). Origin and organization of the zebrafish fate map. *Development, 108*(4), 581-594.

Kornblihtt, A. R., Schor, I. E., Alló, M., Dujardin, G., Petrillo, E., & Muñoz, M. J. (2013). Alternative splicing: a pivotal step between eukaryotic transcription and translation. *Nature reviews Molecular cell biology, 14*(3), 153.

Kröger, C., Loschke, F., Schwarz, N., Windoffer, R., Leube, R. E., & Magin, T. M. (2013). Keratins control intercellular adhesion involving PKC-α–mediated desmoplakin phosphorylation. *J Cell Biol, 201*(5), 681-692.

Ku, N.-O., & Omary, M. B. (2006). A disease-and phosphorylation-related nonmechanical function for keratin 8. *The Journal of cell biology, 174*(1), 115-125.

Laale, H. W. (1977). The biology and use of zebrafish, Brachydanio rerio in fisheries research. A literature review. *Journal of Fish Biology, 10*(2), 121-173.

Lachnit, M., Kur, E., & Driever, W. (2008). Alterations of the cytoskeleton in all three embryonic lineages contribute to the epiboly defect of Pou5f1/Oct4 deficient MZspg zebrafish embryos. *Developmental biology, 315*(1), 1-17.

Lai-Cheong, J., Ussar, S., Arita, K., Hart, I., & McGrath, J. (2008). Colocalization of kindlin-1, kindlin-2, and migfilin at keratinocyte focal adhesion and relevance to the pathophysiology of Kindler syndrome. *Journal of Investigative Dermatology, 128*(9), 2156-2165.

Lane, E., Rugg, E., Navsaria, H., Leigh, I., Heagerty, A., Ishida-Yamamoto, A., & Eady, R. (1992). A mutation in the conserved helix termination peptide of keratin 5 in hereditary skin blistering. *Nature, 356*(6366), 244.

Langbein, L., Rogers, M. A., Praetzel, S., Winter, H., & Schweizer, J. (2003). K6irs1, K6irs2, K6irs3, and K6irs4 Represent the Inner-Root-Sheath-Specific Type II Epithelial Keratins of the Human Hair Follicle1. *The Journal of investigative dermatology, 120*(4), 512.

Langbein, L., Rogers, M. A., Winter, H., Praetzel, S., & Schweizer, J. (2001). The catalog of human hair keratins II. Expression of the six type II members in the hair follicle and the combined catalog of human type I and type II keratins. *Journal of Biological Chemistry*.

Le Guellec, D., Morvan-Dubois, G., & Sire, J.-Y. (2003). Skin development in bony fish with particular emphasis on collagen deposition in the dermis of the zebrafish (Danio rerio). *International Journal of Developmental Biology, 48*(2-3), 217-231.

Lee, H., & Kimelman, D. (2002). A dominant-negative form of p63 is required for epidermal proliferation in zebrafish. *Developmental cell, 2*(5), 607-616.

Lee, R. T., Asharani, P., & Carney, T. J. (2014). Basal keratinocytes contribute to all strata of the adult zebrafish epidermis. *PLoS One, 9*(1), e84858.

Lele, Z., & Krone, P. (1996). The zebrafish as a model system in developmental, toxicological and transgenic research. *Biotechnology advances, 14*(1), 57-72.

Leopold, P. L., Vincent, J., & Wang, H. (2012). *A comparison of epithelial-to-mesenchymal transition and re-epithelialization.* Paper presented at the Seminars in cancer biology.

Letunic, I., Doerks, T., & Bork, P. (2008). SMART 6: recent updates and new developments. *Nucleic acids research, 37*(suppl_1), D229-D232.

Li, Q., Sadowski, S., Frank, M., Chai, C., Váradi, A., Ho, S.-Y., . . . Thisse, B. (2010). The abcc6a gene expression is required for normal zebrafish development. *Journal of Investigative Dermatology, 130*(11), 2561-2568.

Li, Q., & Uitto, J. (2014). Zebrafish as a model system to study skin biology and pathology. *The Journal of investigative dermatology, 134*(6), 1-6. doi: 10.1038/jid.2014.182

Liao, E. C., Paw, B. H., Peters, L. L., Zapata, A., Pratt, S. J., Do, C. P., . . . Zon, L. I. (2000). Hereditary spherocytosis in zebrafish riesling illustrates evolution of erythroid beta-spectrin structure, and function in red cell morphogenesis and membrane stability. *Development, 127*(23), 5123-5132.

Lieschke, G. J., & Currie, P. D. (2007). Animal models of human disease: zebrafish swim into view. *Nature Reviews Genetics, 8*(5), 353.

Liovic, M., D'alessandro, M., Tomic-Canic, M., Bolshakov, V. N., Coats, S. E., & Lane, E. B. (2009). Severe keratin 5 and 14 mutations induce down-regulation of junction proteins in keratinocytes. *Experimental cell research, 315*(17), 2995-3003.

Litjens, S. H., de Pereda, J. M., & Sonnenberg, A. (2006). Current insights into the formation and breakdown of hemidesmosomes. *Trends in cell biology, 16*(7), 376-383.

Little, S. C., & Mullins, M. C. (2006). Extracellular modulation of BMP activity in patterning the dorsoventral axis. *Birth Defects Research Part C: Embryo Today: Reviews, 78*(3), 224-242.

Lunstrum, G., Sakai, L., Keene, D., Morris, N., & Burgeson, R. (1986). Large complex globular domains of type VII procollagen contribute to the structure of anchoring fibrils. *Journal of Biological Chemistry, 261*(19), 9042-9048.

Lupas, A. (1996). Coiled coils: new structures and new functions. *Trends in biochemical sciences, 21*(10), 375-382.

M'Boneko, V., & Merker, H.-J. (1988). Development and morphology of the periderm of mouse embryos (days 9–12 of gestation). *Cells Tissues Organs, 133*(4), 325-336.

Maestrini, E., Monaco, A. P., McGrath, J. A., Ishida-Yamamoto, A., Camisa, C., Hovnanian, A., . . . Christiano, A. M. (1996). A molecular defect in loricrin, the major component of the cornified cell envelope, underlies Vohwinkel's syndrome. *Nature genetics, 13*(1), 70.

Markl, J., Winter, S., & Franke, W. (1989). The catalog and the expression complexity of cytokeratins in a lower vertebrate: biochemical identification of cytokeratins in a teleost fish, the rainbow trout. *European journal of cell biology, 50*(1), 1-16.

Marks, J. G., & Miller, J. J. (2017). *Lookingbill and Marks' Principles of Dermatology E-Book*: Elsevier Health Sciences.

Martin, P. (1997). Wound healing--aiming for perfect skin regeneration. *Science, 276*(5309), 75-81.

Matter, K., & Balda, M. S. (2003). Signalling to and from tight junctions. *Nature reviews Molecular cell biology, 4*(3), 225.

McGrath, J., Eady, R., & Pope, F. (2004). Anatomy and organization of human skin. *Rook's textbook of dermatology, 3*, 1-15.

McGrath, J. A., Duijf, P. H., Doetsch, V., Irvine, A. D., Waal, R. d., Vanmolkot, K. R., . . . Griffiths, W. A. D. (2001). Hay–Wells syndrome is caused by heterozygous missense mutations in the SAM domain of p63. *Human molecular genetics, 10*(3), 221-230.

McGregor, L., Makela, V., Darling, S. M., Vrontou, S., Chalepakis, G., Roberts, C., . . . Hopkins, J. (2003). Fraser syndrome and mouse blebbed phenotype caused by mutations in FRAS1/Fras1 encoding a putative extracellular matrix protein. *Nature genetics, 34*(2), 203.

McMillan, J. R., Akiyama, M., & Shimizu, H. (2003). Epidermal basement membrane zone components: ultrastructural distribution and molecular interactions. *Journal of dermatological science, 31*(3), 169-177.

Merlini, L., Martoni, E., Grumati, P., Sabatelli, P., Squarzoni, S., Urciuolo, A., . . . Bonaldo, P. (2008). Autosomal recessive myosclerosis myopathy is a collagen VI disorder. *Neurology, 71*(16), 1245-1253.

Metcalfe, A. D., & Ferguson, M. W. (2007). Tissue engineering of replacement skin: the crossroads of biomaterials, wound healing, embryonic development, stem cells and regeneration. *Journal of the Royal Society Interface, 4*(14), 413-437.

Modrek, B., & Lee, C. (2002). A genomic view of alternative splicing. *Nature genetics, 30*(1), 13.

Moll, R., Löwe, A., Laufer, J., & Franke, W. (1992). Cytokeratin 20 in human carcinomas. A new histodiagnostic marker detected by monoclonal antibodies. *The American journal of pathology, 140*(2), 427.

Morley, S., D'alessandro, M., Sexton, C., Rugg, E., Navsaria, H., Shemanko, C., . . . Leigh, I. (2003). Generation and characterization of epidermolysis bullosa simplex cell lines: scratch assays show faster migration with disruptive keratin mutations. *British Journal of Dermatology, 149*(1), 46-58.

Müller, F. B., Küster, W., Wodecki, K., Almeida Jr, H., Bruckner-Tuderman, L., Krieg, T., . . . Arin, M. J. (2006). Novel and recurrent mutations in keratin KRT5 and KRT14 genes in epidermolysis bullosa simplex: implications for disease phenotype and keratin filament assembly. *Human mutation, 27*(7), 719-720.

North, A. C., Steinert, P. M., & Parry, D. A. (1994). Coiled-coil stutter and link segments in keratin and other intermediate filament molecules: a computer modeling study. *Proteins: Structure, Function, and Bioinformatics, 20*(2), 174-184.

Odorisio, T., Di Salvio, M., Orecchia, A., Di Zenzo, G., Piccinni, E., Cianfarani, F., . . . Conti, A. (2014). Monozygotic twins discordant for recessive dystrophic epidermolysis bullosa phenotype highlight the role of TGF-β signalling in modifying disease severity. *Human molecular genetics, 23*(15), 3907-3922.

Ołdak, M., Kowalewski, C., Maksym, R. B., Woźniak, K., Pollak, A., Podgórska, M., . . . Płoski, R. (2010). Novel keratin 14 hotspot mutation in Dowling-Meara type of epidermolysis bullosa simplex: Strategy to avoid KRT14 pseudogene amplification by a simple approach. *Journal of dermatological science, 57*(1), 69-70.

Owens, D. W., & Lane, E. B. (2003). The quest for the function of simple epithelial keratins. *Bioessays, 25*(8), 748-758.

Padhi, B. K., Akimenko, M.-A., & Ekker, M. (2006). Independent expansion of the keratin gene family in teleostean fish and mammals: an insight from phylogenetic analysis and radiation hybrid mapping of keratin genes in zebrafish. *Gene, 368*, 37-45.

Pallari, H.-M., & Eriksson, J. E. (2006). Intermediate filaments as signaling platforms. *Science Signaling, 2006*(366), pe53-pe53.

Pan, X., Hobbs, R. P., & Coulombe, P. A. (2013). The expanding significance of keratin intermediate filaments in normal and diseased epithelia. *Current opinion in cell biology, 25*(1), 47-56.

Pan, Y., Zheng, W., Moyer, A. E., O'Connor, J. K., Wang, M., Zheng, X., . . . Schweitzer, M. H. (2016). Molecular evidence of keratin and melanosomes in feathers of the Early Cretaceous bird Eoconfuciusornis. *Proceedings of the National Academy of Sciences, 113*(49), E7900-E7907.

Pastar, I., Stojadinovic, O., Yin, N. C., Ramirez, H., Nusbaum, A. G., Sawaya, A., . . . Tomic-Canic, M. (2014). Epithelialization in wound healing: a comprehensive review. *Advances in wound care, 3*(7), 445-464.

Paulsson, M. (1992). Basement membrane proteins: structure, assembly, and cellular interactions. *Critical reviews in biochemistry and molecular biology, 27*(1-2), 93-127.

Perez-Moreno, M., Jamora, C., & Fuchs, E. (2003). Sticky business: orchestrating cellular signals at adherens junctions. *Cell, 112*(4), 535-548.

Petersen, T. E., Thøgersen, H. C., Skorstengaard, K., Vibe-Pedersen, K., Sahl, P., Sottrup-Jensen, L., & Magnusson, S. (1983). Partial primary structure of bovine plasma fibronectin: three types of internal homology. *Proceedings of the National Academy of Sciences, 80*(1), 137-141.

Pfeiffer, W. (1977). The distribution of fright reaction and alarm substance cells in fishes. *Copeia*, 653-665.

Pfendner, E. G., Sadowski, S. G., & Uitto, J. (2005). Epidermolysis bullosa simplex: recurrent and de novo mutations in the KRT5 and KRT14 genes, phenotype/genotype correlations, and implications for genetic counseling and prenatal diagnosis. *Journal of General Internal Medicine, 20*(5), 239-243.

Pohla-Gubo, G., Cepeda-Valdes, R., & Hintner, H. (2010). Immunofluorescence mapping for the diagnosis of epidermolysis bullosa. *Dermatologic clinics, 28*(2), 201-210.

Postel, R., Margadant, C., Fischer, B., Kreft, M., Janssen, H., Secades, P., . . . Sonnenberg, A. (2013). Kindlin-1 mutant zebrafish as an in vivo model system to study

adhesion mechanisms in the epidermis. *Journal of Investigative Dermatology, 133*(9), 2180-2190.

Proksch, E., Brandner, J. M., & Jensen, J. M. (2008). The skin: an indispensable barrier. *Experimental dermatology, 17*(12), 1063-1072.

Pulkkinen, L., & Uitto, J. (1999). Mutation analysis and molecular genetics of epidermolysis bullosa. *Matrix biology, 18*(1), 29-42.

Quilhac, A., & Sire, J. Y. (1999). Spreading, proliferation, and differentiation of the epidermis after wounding a cichlid fish, Hemichromis bimaculatus. *The Anatomical Record: An Official Publication of the American Association of Anatomists, 254*(3), 435-451.

Ramanoudjame, L., Rocancourt, C., Lainé, J., Klein, A., Joassard, L., Gartioux, C., . . . Ciura, S. (2015). Two novel COLVI long chains in zebrafish that are essential for muscle development. *Human molecular genetics, 24*(23), 6624-6639.

Reis, A., Hennies, H.-C., Langbein, L., Digweed, M., Mischke, D., Drechsler, M., . . . Sperling, K. (1994). Keratin 9 gene mutations in epidermolytic palmoplantar keratoderma (EPPK). *Nature genetics, 6*(2), 174.

Richard, G., De Laurenzi, V., Didona, B., Bale, S. J., & Compton, J. G. (1995). Keratin 13 point mutation underlies the hereditary mucosal epithelia disorder white sponge nevus. *Nature genetics, 11*(4), 453.

Ridley, A. J., Schwartz, M. A., Burridge, K., Firtel, R. A., Ginsberg, M. H., Borisy, G., . . . Horwitz, A. R. (2003). Cell migration: integrating signals from front to back. *Science, 302*(5651), 1704-1709.

Rothnagel, J. A., Traupe, H., Wojcik, S., Huber, M., Hohl, D., Pittelkow, M. R., . . . Roop, D. R. (1994). Mutations in the rod domain of keratin 2e in patients with ichthyosis bullosa of Siemens. *Nature genetics, 7*(4), 485.

Rugg, E., McLean, W., Allison, W., Lunny, D., Macleod, R., Felix, D., . . . Munro, C. (1995). A mutation in the mucosal keratin K4 is associated with oral white sponge nevus. *Nature genetics, 11*(4), 450.

Rugg, E. L., Horn, H. M., Smith, F. J., Wilson, N. J., Hill, A. J., Magee, G. J., . . . Lane, E. B. (2007). Epidermolysis bullosa simplex in Scotland caused by a spectrum of keratin mutations. *Journal of Investigative Dermatology, 127*(3), 574-580.

Ryynänen, M., Knowlton, R. G., Parente, M. G., Chung, L. C., Chu, M.-L., & Uitto, J. (1991). Human type VII collagen: genetic linkage of the gene (COL7A1) on chromosome 3 to dominant dystrophic epidermolysis bullosa. *American journal of human genetics, 49*(4), 797.

Sabel, J. L., d'Alençon, C., O'Brien, E. K., Van Otterloo, E., Lutz, K., Cuykendall, T. N., . . . Cornell, R. A. (2009). Maternal Interferon Regulatory Factor 6 is required for the differentiation of primary superficial epithelia in Danio and Xenopus embryos. *Developmental biology, 325*(1), 249-262.

Sakai, L. Y., Keene, D. R., Morris, N. P., & Burgeson, R. E. (1986). Type VII collagen is a major structural component of anchoring fibrils. *The Journal of cell biology, 103*(4), 1577-1586.

Sawamura, D., Nakano, H., & Matsuzaki, Y. (2010). Overview of epidermolysis bullosa. *The Journal of dermatology, 37*(3), 214-219.

Scholz, S., Fischer, S., Gündel, U., Küster, E., Luckenbach, T., & Voelker, D. (2008). The zebrafish embryo model in environmental risk assessment—applications beyond acute toxicity testing. *Environmental Science and Pollution Research, 15*(5), 394-404.

Schultz, J., Milpetz, F., Bork, P., & Ponting, C. P. (1998). SMART, a simple modular architecture research tool: identification of signaling domains. *Proceedings of the National Academy of Sciences, 95*(11), 5857-5864.

Schweizer, J., Bowden, P. E., Coulombe, P. A., Langbein, L., Lane, E. B., Magin, T. M., . . . Rogers, M. A. (2006). New consensus nomenclature for mammalian keratins. *J Cell Biol, 174*(2), 169-174.

Seltmann, K., Roth, W., Kröger, C., Loschke, F., Lederer, M., Hüttelmaier, S., & Magin, T. M. (2013). Keratins mediate localization of hemidesmosomes and repress cell motility. *Journal of Investigative Dermatology, 133*(1), 181-190.

Shimizu, H., Suzumori, K., & Nishikawa, T. (1996). Heterogeneous reactivity with LH7. 2 and the first prenatal diagnosis of generalized recessive dystrophic epidermolysis bullosa among Japanese patients. *Dermatology, 192*(3), 203-207.

Shinkuma, S. (2015). Dystrophic epidermolysis bullosa: a review. *Clinical, cosmetic and investigational dermatology, 8*, 275.

Simpson, C. L., Patel, D. M., & Green, K. J. (2011). Deconstructing the skin: cytoarchitectural determinants of epidermal morphogenesis. *Nature reviews Molecular cell biology, 12*(9), 565.

Sire, J. Y. (1989). Scales in young Polypterus senegalus are elasmoid: new phylogenetic implications. *American Journal of Anatomy, 186*(3), 315-323.

Slanchev, K., Carney, T. J., Stemmler, M. P., Koschorz, B., Amsterdam, A., Schwarz, H., & Hammerschmidt, M. (2009). The epithelial cell adhesion molecule EpCAM is required for epithelial morphogenesis and integrity during zebrafish epiboly and skin development. *PLoS genetics, 5*(7), e1000563.

Smith, F. J., Porter, R. M., Corden, L. D., Lunny, D. P., Lane, E. B., & McLean, W. I. (2002). Cloning of human, murine, and marsupial keratin 7 and a survey of K7 expression in the mouse. *Biochemical and biophysical research communications, 297*(4), 818-827.

Sonawane, M., Carpio, Y., Geisler, R., Schwarz, H., Maischein, H.-M., & Nuesslein-Volhard, C. (2005). Zebrafish penner/lethal giant larvae 2 functions in hemidesmosome formation, maintenance of cellular morphology and growth regulation in the developing basal epidermis. *Development, 132*(14), 3255-3265.

Stahl, F. (1985). George Streisinger (December 27, 1927-August 11, 1984). *Genetics, 109*(1), 1-2.

Steed, E., Balda, M. S., & Matter, K. (2010). Dynamics and functions of tight junctions. *Trends in cell biology, 20*(3), 142-149.

Sun, T.-T., Eichner, R., NELsoN, W. G., Tseng, C. S., WEIss, R. A., JARvINEN, M., & Woodcock-Mitchell, J. (1983). Keratin classes: molecular markers for different types of epithelial differentiation. *Journal of Investigative Dermatology, 81*(1), S109-S115.

Szeverenyi, I., Cassidy, A. J., Chung, C. W., Lee, B. T., Common, J. E., Ogg, S. C., . . . Ng, K. W. (2008). The Human Intermediate Filament Database: comprehensive information on a gene family involved in many human diseases. *Human mutation, 29*(3), 351-360.

Takeichi, M. (1988). The cadherins: cell-cell adhesion molecules controlling animal morphogenesis. *Development, 102*(4), 639-655.

Thisse, C., & Thisse, B. (2008). High-resolution in situ hybridization to whole-mount zebrafish embryos. *Nature protocols, 3*(1), 59.

Titeux, M., Mejía, J. E., Mejlumian, L., Bourthoumieu, S., Mirval, S., Tonasso, L., . . . Hovnanian, A. (2006). Recessive dystrophic epidermolysis bullosa caused by COL7A1 hemizygosity and a missense mutation with complex effects on splicing. *Human mutation, 27*(3), 291-292.

Toivola, D., Strnad, P., Habtezion, A., & Omary, M. (2010). Intermediate filaments take the heat as stress proteins. *Trends in cell biology, 20*(2), 79-91.

Toivola, D. M., Tao, G.-Z., Habtezion, A., Liao, J., & Omary, M. B. (2005). Cellular integrity plus: organelle-related and protein-targeting functions of intermediate filaments. *Trends in cell biology, 15*(11), 608-617.

Tsuruta, D., Sowa, J., Tateishi, C., Obase, Y., Tsubura, A., Fukumoto, T., . . . Hashimoto, T. (2011). Atypical epidermolysis bullosa simplex with a missense keratin 14 mutation p. Arg125Cys. *The Journal of dermatology, 38*(12), 1177-1179.

Uitto, J. (2012). Molecular therapeutics for heritable skin diseases. *The Journal of investigative dermatology, 132*, E29.

Uitto, J., & Richard, G. (2004). *Progress in epidermolysis bullosa: genetic classification and clinical implications.* Paper presented at the American Journal of Medical Genetics Part C: Seminars in Medical Genetics.

Uitto, J., Richard, G., & McGrath, J. A. (2007). Diseases of epidermal keratins and their linker proteins. *Experimental cell research, 313*(10), 1995-2009.

Ullrich, O. (1930). Kongenitale, atonisch-sklerotische Muskeldystrophie, ein weiterer Typus der heredodegenerativen Erkrankungen des neuromuskulaeren Systems. *Zeitschrift für die gesamte Neurologie und Psychiatrie, 126*(1), 171-201.

Ussar, S., Moser, M., Widmaier, M., Rognoni, E., Harrer, C., Genzel-Boroviczeny, O., & Fässler, R. (2008). Loss of Kindlin-1 causes skin atrophy and lethal neonatal intestinal epithelial dysfunction. *PLoS genetics, 4*(12), e1000289.

Uttam, J., Hutton, E., Coulombe, P. A., Anton-Lamprecht, I., Yu, Q.-C., Gedde-Dahl, T., . . . Fuchs, E. (1996). The genetic basis of epidermolysis bullosa simplex with mottled pigmentation. *Proceedings of the National Academy of Sciences, 93*(17), 9079-9084.

Van Eeden, F., Granato, M., Schach, U., Brand, M., Furutani-Seiki, M., Haffter, P., . . . Kane, D. A. (1996). Genetic analysis of fin formation in the zebrafish, Danio rerio. *Development, 123*(1), 255-262.

Varki, R., Sadowski, S., Uitto, J., & Pfendner, E. (2007). Epidermolysis bullosa. II. Type VII collagen mutations and phenotype–genotype correlations in the dystrophic subtypes. *Journal of medical genetics, 44*(3), 181-192.

Vasioukhin, V., & Fuchs, E. (2001). Actin dynamics and cell–cell adhesion in epithelia. *Current opinion in cell biology, 13*(1), 76-84.

Vilella, A. J., Severin, J., Ureta-Vidal, A., Durbin, R., Heng, L., & Birney, E. (2008). EnsemblCompara GeneTrees: Analysis of complete, duplication aware phylogenetic trees in vertebrates. *Genome research*, gr. 073585.073107.

Villone, D., Fritsch, A., Koch, M., Bruckner-Tuderman, L., Hansen, U., & Bruckner, P. (2008). Supramolecular interactions in the dermo-epidermal junction zone: anchoring fibril-collagen VII tightly binds to banded collagen fibrils. *Journal of Biological Chemistry*.

Virtanen, M., Gedde-Dahl Jr, T., Mork, N.-J., Leigh, I., Bowden, P. E., & Vahlquist, A. (2001). Phenotypic/genotypic correlations in patients with epidermolytic hyperkeratosis and the effects of retinoid therapy on keratin expression. *ACTA DERMATOVENEREOLOGICA-STOCKHOLM-, 81*(3), 163-170.

Walko, G., Castañón, M. J., & Wiche, G. (2015). Molecular architecture and function of the hemidesmosome. *Cell and Tissue Research, 360*(3), 529-544.

Webber, B. R., T O'Connor, K., McElmurry, R. T., Durgin, E. N., Eide, C. R., Lees, C. J., . . . Kluth, M. A. (2017). Rapid generation of Col7a1−/− mouse model of recessive dystrophic epidermolysis bullosa and partial rescue via immunosuppressive dermal mesenchymal stem cells. *Laboratory Investigation, 97*(10), 1218.

Weber, K., Plessmann, U., Dodemont, H., & Kossmagk-Stephan, K. (1988). Amino acid sequences and homopolymer-forming ability of the intermediate filament proteins from an invertebrate epithelium. *The EMBO journal, 7*(10), 2995-3001.

Weiss, R. A., Eichner, R., & Sun, T.-T. (1984). Monoclonal antibody analysis of keratin expression in epidermal diseases: a 48-and 56-kdalton keratin as molecular markers for hyperproliferative keratinocytes. *The Journal of cell biology, 98*(4), 1397-1406.

Wertheim-Tysarowska, K., Sobczyńska-Tomaszewska, A., Kowalewski, C., Skroński, M., Święćkowski, G., Kutkowska-Kaźmierczak, A., . . . Bal, J. (2012). The COL7A1 mutation database. *Human mutation, 33*(2), 327-331.

Westerfield, M. (1995). *The zebrafish book: a guide for the laboratory use of zebrafish (Brachydanio rerio)*: University of Oregon press.

Whitear, M. (1986). Epidermis *Biology of the Integument* (pp. 8-38): Springer.

Wozniak, M. A., Modzelewska, K., Kwong, L., & Keely, P. J. (2004). Focal adhesion regulation of cell behavior. *Biochimica et Biophysica Acta (BBA)-Molecular Cell Research, 1692*(2-3), 103-119.

Yonemura, S., Itoh, M., Nagafuchi, A., & Tsukita, S. (1995). Cell-to-cell adherens junction formation and actin filament organization: similarities and differences between non-polarized fibroblasts and polarized epithelial cells. *Journal of cell science, 108*(1), 127-142.

ANNEXES

Annex 1: Proteomics data of upregulated and down regulated proteins of *col7a1* double knockout fish at 30hpf.

Gene names	Protein names	Gene ontology (biological process)	Fold Change Col7a1 vs WT	log2 Fold change	p-value	No. peptides
sptbn1	Spectrin beta chain	actin filament capping	2.29	1.19	0.0343	9
akap12b	A kinase (PRKA) anchor protein 12b	animal organ morphogenesis ; bleb assembly ; cell morphogenesis ; convergent extension involved in axis elongation ; muscle cell development ; negative regulation of Rho protein signal transduction ; positive regulation of protein kinase A signaling ; protein targeting ; regulation of protein kinase C signaling ; signal transduction ; slow muscle cell migration	1.82	0.87	0.2470	10
zgc:171967	Zgc:171967	carbohydrate metabolic process	1.51	0.60	0.3565	7
gnb1b gnb1l	Gnb1l protein (Guanine nucleotide binding protein (G protein), beta polypeptide 1, like) (Guanine nucleotide-binding protein (G protein), beta polypeptide 1b)	posterior lateral line neuromast primordium migration ; signal transduction	0.68	-0.56	0.3285	6
atp1a1a.1 atp1a1	Sodium/potassium-transporting ATPase subunit alpha (EC 3.6.3.-)	bract development ; brain development ; brain morphogenesis ; cardiocyte differentiation ; cell migration involved in heart formation ; determination of left/right symmetry ; embryonic	0.60	-0.74	0.4797	10

		body morphogenesis ; embryonic heart tube development ; embryonic heart tube morphogenesis ; extracellular matrix organization ; heart development ; midbrain-hindbrain boundary development ; otic vesicle development ; otic vesicle formation ; otolith development ; ventricular system development				
api5	Apoptosis inhibitor 5		0.54	-0.88	0.1389	6
si:ch73-244f7.4	Si:ch73-244f7.4		0.54	-0.88	0.06601	6

Genes highlighted in light orange are upregulated and those heighted in light green are down regulated genes, p-value is set at 5% and fold change cut value is 1.5

Annex 2: Proteomics data of upregulated and down regulated proteins of *col7a1* double knockout fish at 5dpf

Gene names	Protein names	Gene ontology (biological process)	Fold Change Col7a1vsWT	log2 fold change	p-value	No. of peptides
col14a1b	Collagen, type XIV, alpha 1b		16.29	4.03	0.0708	2
tpd52l2a	Tumor protein D52-like 2a		15.36	3.94	0.0040	
si:ch211-202f3.3 im:7154842	Si:ch211-202f3.3 (Fragment)		14.03	3.81	0.9999	
pgls	6-phosphogluconolactonase		13.52	3.76	0.0200	
pon2 zgc:77556	Paraoxonase 2 (Zgc:77556)		11.17	3.48	0.0157	
ube2h	Ube2h protein (Ubiquitin-conjugating enzyme E2H (UBC8 homolog, yeast))		11.14	3.48	0.1442	
col28a2a	Collagen, type XXVIII, alpha 2a		10.93	3.45	0.1013	2

col6a2	Collagen, type VI, alpha 2		10.40	3.38	0.8075	1
coch	Coagulation factor C homolog, cochlin (Limulus polyphemus)		10.27	3.36	0.0027	
	Uncharacterized protein		7.96	2.99	0.1724	
acads	Acyl-CoA dehydrogenase, C-2 to C-3 short chain (Acyl-Coenzyme A dehydrogenase, C-2 to C-3 short chain)		7.16	2.84	0.0152	
hsd17b12a	Very-long-chain 3-oxoacyl-CoA reductase-A		6.93	2.79	0.1062	
dpp9	Dipeptidyl-peptidase 9		6.61	2.72	0.8140	
tnni2b.1	Troponin I type 2b (skeletal, fast), tandem duplicate 1		4.75	2.25	0.0293	
crabp1b	Cellular retinoic acid binding protein 1b (Cellular retinoic acid-binding protein 1b) (Cellular retinoic acid-binding protein type I)		4.00	2.00	0.2613	
trnau1apb trnau1apl	tRNA selenocysteine 1-associated protein 1b		3.55	1.83	0.0171	
eea1	Early endosome antigen 1		2.23	1.16	0.0900	
surf4l	Surf4l protein (Surfeit gene 4, like) (Surfeit gene 4,-like)		2.17	1.12	0.0486	
slc27a2a slc27a2	Solute carrier family 27 (fatty acid transporter), member 2a		2.08	1.06	0.0156	
myl6	Myosin, light chain 6, alkali, smooth muscle and non-muscle		2.08	1.06	0.0789	
zgc:114181	Zgc:114181		1.95	0.96	0.1055	2
vtg3	Vitellogenin 3, phosvitinless		1.90	0.93	0.0151	8
vtg6 si:rp71-	Vitellogenin 6 (Fragment)		1.88	0.91	0.1487	2

23d18.1						
phb2b	Prohibitin 2b		1.64	0.71	0.1773	
vtg1	Vitellogenin 1		1.55	0.63	0.6706	2
crygn2	Crystallin, gamma N2 (Fragment)		0.66	-0.59	0.0031	3
si:dkey-261m9.19	Histone H2B		0.66	-0.60	0.0137	
adh5	S-(hydroxymethyl)glutathione dehydrogenase (EC 1.1.1.284)	ethanol oxidation	0.65	-0.62	0.0688	2
ahcy AHCY	Adenosylhomocysteinase (EC 3.3.1.1)		0.65	-0.63	0.0533	6
tfa	Serotransferrin	hemoglobin biosynthetic process ; iron ion homeostasis ; iron ion transport ; response to bacterium	0.63	-0.68	0.3036	5
hsp90aa1.2 hsp90a.2	Heat shock protein 90, alpha (cytosolic), class A member 1, tandem duplicate 2 (Heat shock protein 90-alpha 2)		0.57	-0.81	0.0853	
pvalb2 pvalb pvalbl	Parvalbumin-2 (Parvalbumin beta)		0.50	-1.00	0.4071	3
crygm2d15	Crystallin, gamma M2d15		0.47	-1.09	0.0073	
zgc:153405	Zgc:153405		0.44	-1.20	0.1841	
pvalb3	Parvalbumin 3 (Parvalbumin isoform 1b) (Pvalb3 protein)		0.35	-1.50	0.0331	
cbx1b	Chromobox homolog 1b (HP1 beta homolog Drosophila)		0.32	-1.65	0.0367	2
si:dkey-65b12.6	Si:dkey-65b12.6		0.30	-1.74	0.0016	2
rpl19 zgc:77733	60S ribosomal protein L19		0.28	-1.84	0.0985	

epcam	Epithelial cell adhesion molecule	epiboly involved in gastrulation with mouth forming second ; liver development ; morphogenesis of an epithelium ; single organismal cell-cell adhesion	0.27	-1.92	0.0057	2
pvalb8	Parvalbumin 8 (Pvalb8 protein)		0.16	-2.64	0.0007	
nol10	Nucleolar protein 10		0.14	-2.83	0.4097	
c3a.2	Complement component c3a, duplicate 2 (Fragment)		0.11	-3.13	0.0220	
ppa2	Pyrophosphatase (inorganic) 2		0.10	-3.28	0.7372	
decr2 si:ch211-153c20.5 zgc:85626	Peroxisomal 2,4-dienoyl-CoA reductase (EC 1.3.1.34) (2,4-dienoyl-CoA reductase 2)		0.09	-3.55	0.0086	

Genes highlighted in light orange are upregulated and those heighted in light green are down regulated genes, p-value is set at 5% and fold change cut value is 1.5

Annex 3: Proteomics data of upregulated and down regulated proteins of *col7a1* double knockout of adult fish

Gene names	Protein names	Gene ontology (biological process)	Fold change Col7a1 vs WT	log2 fold change	p-value	No of peptides
acat2	Acetyl-CoA acetyltransferase 2	fatty acid beta-oxidation	2.74	1.46	0.0039	
zgc:92161	Zgc:92161		2.32	1.21	0.0004	
itih3a	Inter-alpha-trypsin inhibitor heavy chain 3a	hyaluronan metabolic process	2.25	1.17	0.0292	
aldh1l1	10-formyltetrahydrofolate dehydrogenase (EC 1.5.1.6)	10-formyltetrahydrofolate catabolic process ; biosynthetic process ; embryonic viscerocranium morphogenesis ; gastrulation ; heart development ; neural crest cell migration ; neuromast deposition ;	2.25	1.17	0.0059	

		one-carbon metabolic process				
padi2	Peptidyl arginine deiminase, type II	histone citrullination	2.23	1.16	0.0414	
papss2a	3'-phosphoadenosine 5'-phosphosulfate synthase 2a	3'-phosphoadenosine 5'-phosphosulfate biosynthetic process ; sulfate assimilation	2.07	1.05	0.0270	
fasn	Fatty acid synthase	biosynthetic process	1.96	0.97	0.0019	
aclya	ATP-citrate synthase (EC 2.3.3.8) (ATP-citrate (pro-S-)-lyase) (Citrate cleavage enzyme)	acetyl-CoA biosynthetic process ; citrate metabolic process ; fatty acid biosynthetic process	1.93	0.95	0.0219	
bpnt1	Bisphosphate nucleotidase 1	phosphatidylinositol phosphorylation	1.89	0.92	0.0066	
zgc:152945	Zgc:152945		1.88	0.91	0.0037	
paics	Phosphoribosylaminoimidazole carboxylase, phosphoribosylaminoimidazole succinocarboxamide synthetase	de novo' IMP biosynthetic process ; camera-type eye development ; chordate embryonic development ; pigmentation ; retina development in camera-type eye	1.72	0.78	0.0286	
itih2	Inter-alpha-trypsin inhibitor heavy chain 2	hyaluronan metabolic process	1.71	0.77	0.0051	
xrn2	5'-3' exoribonuclease 2		1.60	0.68	0.0175	
bhmt	Betaine--homocysteine S-methyltransferase 1	methionine biosynthetic process	1.55	0.63	0.0382	
mdh1aa MDH1 mdh1a mdhA	Malate dehydrogenase (EC 1.1.1.37)	carbohydrate metabolic process ; malate metabolic process ; NADH metabolic process ; oxaloacetate metabolic process ; tricarboxylic acid cycle	1.53	0.62	0.0076	
uba7	Ubiquitin-like modifier-activating enzyme 7	cellular response to DNA damage stimulus ; ubiquitin-dependent protein catabolic process	0.70	-0.52	0.0190	
wu:fj29h11	Wu:fj29h11		0.70	-0.52	0.0493	
serpinh1a zgc:171630	Serpin peptidase inhibitor, clade H (heat shock protein	collagen fibril organization	0.67	-0.57	0.0329	

	47), member 1a (Zgc:171630 protein)					
LOC795887	Uncharacterized protein		0.59	-0.76	0.0361	
pcna	Proliferating cell nuclear antigen (PCNA)	leading strand elongation ; mismatch repair ; regulation of DNA replication ; response to activity ; response to bacterium ; translesion synthesis	0.59	-0.77	0.0253	
fetub	Fetuin B		0.55	-0.85	0.0096	
leg1a zgc:172246	Protein leg1a (Leg1-A) (Liver-enriched gene protein 1-A)	digestive system development ; embryonic liver development ; liver development	0.54	-0.88	0.0004	
apobb.2 si:dkeyp-88f5.1	Apolipoprotein Bb, tandem duplicate 2		0.50	-1.01	0.0046	
mxb	Interferon-induced GTP-binding protein MxB		0.48	-1.06	0.0213	
wu:fc34e06	Wu:fc34e06		0.43	-1.21	0.0049	
apoa1 apoa zgc:103718	Apolipoprotein A-I (Apo-AI) (ApoA-I) (Apolipoprotein A1) [Cleaved into: Proapolipoprotein A-I (ProapoA-I)]	cholesterol biosynthetic process ; cholesterol efflux ; cholesterol homeostasis ; high-density lipoprotein particle assembly ; lipoprotein metabolic process ; neuron projection regeneration ; phosphatidylcholine metabolic process ; phospholipid efflux ; positive regulation of cholesterol esterification ; positive regulation of fatty acid biosynthetic process ; positive regulation of lipoprotein lipase activity ; positive regulation of triglyceride catabolic process ; regulation of intestinal cholesterol absorption ; reverse cholesterol transport ; triglyceride catabolic process ; triglyceride homeostasis ; very-low-density lipoprotein particle remodeling	0.41	-1.27	0.0273	
si:dkeyp-9d4.2	Si:dkeyp-9d4.2		0.41	-1.30	0.0043	

apobb.1 apobl	Apolipoprotein Bb, tandem duplicate 1	cellular response to xenobiotic stimulus	0.40	-1.32	0.0123	
hsp90aa1.2 hsp90a.2	Heat shock protein 90, alpha (cytosolic), class A member 1, tandem duplicate 2 (Heat shock protein 90-alpha 2)	protein folding ; response to antibiotic ; response to cold ; response to heat	0.39	-1.35	0.0128	
zgc:153654	Zgc:153654		0.37	-1.43	0.0225	
gstm.2 zgc:173994	Glutathione S-transferase mu tandem duplicate 2 (Zgc:173994 protein)	metabolic process	0.31	-1.71	0.0241	
anxa1c	Annexin		0.27	-1.89	0.0429	
isg15 si:rp71-1c23.2	ISG15 ubiquitin-like modifier		0.20	-2.35	0.0052	
serpinh1b hsp47	Serpin peptidase inhibitor, clade H (heat shock protein 47), member 1b	collagen fibril organization ; fin regeneration	0.18	-2.49	0.0078	

Genes highlighted in light orange are upregulated and those heighted in light green are down regulated genes, p-value is set at 5% and fold change cut value is 1.5